HOSTED BY

ELSEVIER

GEOSCIENCE FRONTIERS

Research paper

# Cambrian–early Ordovician volcanism across the South Armorican and Occitan domains of the Variscan Belt in France: Continental break-up and rifting of the northern Gondwana margin

André Pouclet [a,*], J. Javier Álvaro [b], Jacques-Marie Bardintzeff [c], Andrés Gil Imaz [d], Eric Monceret [e], Daniel Vizcaïno [f]

[a] 3 rue des Foulques, 85560 Longeville-sur-mer, France
[b] Instituto de Geociencias (CSIC-UCM), c/José Antonio Novais 12, 28040 Madrid, Spain
[c] Volcanology and Planetology, UMR CNRS 8148 GEOPS, University of Paris-Saclay, 91405 Orsay, France
[d] Departamento Ciencias de la Tierra, Universidad de Zaragoza, 50009 Zaragoza, Spain
[e] 18 rue des Pins, 11570 Cazilhac, France
[f] 7 Jean-Baptiste Chardin, Maquens, 11090 Carcassonne, France

## ABSTRACT

The Cambrian–lower Ordovician volcanic units of the South Armorican and Occitan domains are analysed in a tectonostratigraphic survey of the French Variscan Belt. The South Armorican lavas consist of continental tholeiites in middle Cambrian–Furongian sequences related to continental break-up. A significant volcanic activity occurred in the Tremadocian, dominated by crustal melted rhyolitic lavas and initial rifting tholeiites. The Occitan lavas are distributed into five volcanic phases: (1) basal Cambrian rhyolites, (2) upper lower Cambrian Mg-rich tholeiites close to N-MORBs but crustal contaminated, (3) upper lower–middle Cambrian continental tholeiites, (4) Tremadocian rhyolites, and (5) upper lower Ordovician initial rift tholeiites. A rifting event linked to asthenosphere upwelling took place in the late early Cambrian but did not evolve. It renewed in the Tremadocian with abundant crustal melting due to underplating of mixed asthenospheric and lithospheric magmas. This main tectono-magmatic continental rift is termed the "Tremadocian Tectonic Belt" underlined by a chain of rhyolitic volcanoes from Occitan and South Armorican domains to Central Iberia. It evolved with the setting of syn-rift coarse siliciclastic deposits overlain by post-rift deep water shales in a suite of sedimentary basins that forecasted the South Armorican–Medio-European Ocean as a part of the Palaeotethys Ocean.

© 2016, China University of Geosciences (Beijing) and Peking University. Production and hosting by Elsevier B.V. This is an open access article under the CC BY-NC-ND license (http://creativecommons.org/licenses/by-nc-nd/4.0/).

## 1. Introduction

In SW Europe, the Variscan Ibero-Armorican Arc of the Gondwana margin comprises two branches (Fig. 1). The NE branch includes (1) the Armorican Massif, (2) the northern Massif Central, (3) the South Armorican Domain (southwestern Bretagne and Vendée), (4) the Occitan Domain (Albigeois, Montagne Noire, Mouthoumet, and Cévennes parts of the southern Massif-Central), and its lateral prolongation into Corsica and Sardinia, and (5) the Pyrenean Domain. The SW branch is completed with the Variscan zones of the Iberian Peninsula (Quesada, 1991; Martínez Catalán et al., 2009).

A common Cambrian–early Ordovician geodynamic framework is recognized throughout both branches (Ballèvre et al., 2014). After the post-Cadomian Ediacaran tectonic and magmatic events, a Cambrian transgression was linked to a long-term continental extensional process that led to the rifting of the Rheic Ocean in the mid Cambrian and its drifting in the early Ordovician, with the separation of Neoproterozoic arc terranes from the northern continental margin of Gondwana, such as Avalonia, Ganderia, Carolina and Meguma (Nance et al., 2008, 2010). Separation

* Corresponding author.
E-mail addresses: andre.pouclet@sfr.fr (A. Pouclet), jj.alvaro@csic.es (J.J. Álvaro), jacques-marie.bardintzeff@u-psud.fr (J.-M. Bardintzeff), agil@unizar.es (A.G. Imaz), eric.monceret@orange.fr (E. Monceret), daniel.vizcaino@wanadoo.fr (D. Vizcaïno).
Peer-review under responsibility of China University of Geosciences (Beijing).
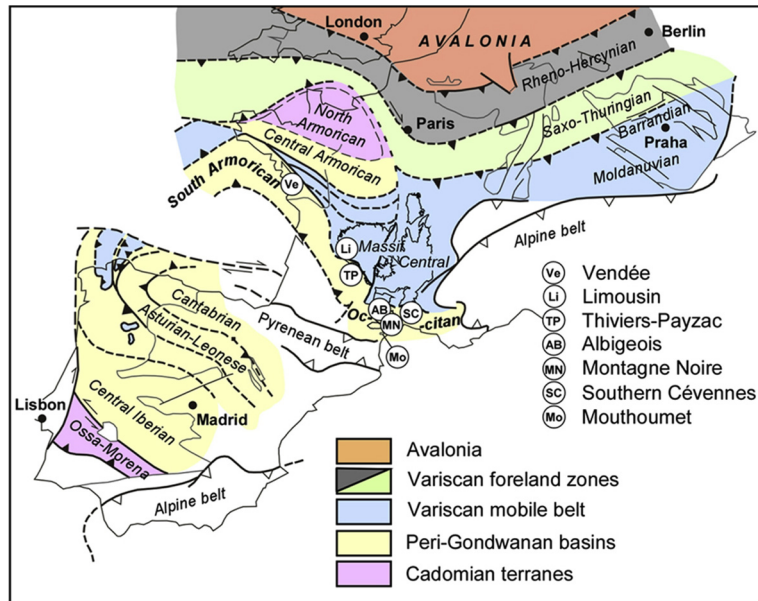
**Figure 1.** Geological sketch of the Ibero-Armorican Arc; modified from Ballèvre et al. (2009). Location of the studied areas in the South Armorican and Occitan domains.

occurred along the line of former Neoproterozoic sutures following the onset of subduction in the outboard Iapetus Ocean (Murphy et al., 2006). Opening of the Rheic Ocean propagated from southwest to northeast, in relationships with intra-continental rifting announcing the opening of the Palaeotethys oceanic Domain (Linnemann et al., 2008; Stampfli et al., 2013; Von Raumer et al., 2013, 2015). This Cambrian–early Ordovician tectono-magmatic history is incompletely understood in the South Armorican and Occitan domains, hereafter named SAOD, due to partial studies of disconnected volcanic exposures, the lack of well-constrained geochemical data, including incompatible elements useful for geodynamic interpretations, and the necessity of thorough stratigraphic revisions particularly of the volcanic units and their host formations.

The aim of this paper is to review the tectonostratigraphic pattern of the SAOD and to decipher the magmatic activities contemporaneous with the Cambrian–lower Ordovician sedimentary succession. Our targets are to understand the magmatic signatures of this activity and the tectonic significances of magma products in the geodynamic history of the northwestern Gondwanan margin. For this purpose, petrographical and geochemical investigations have been performed, using a new set of geochemical analyses and selected data from the literature.

## 2. Geological background and stratigraphic framework

The stratigraphic successions of the SAOD display numerous episodes of effusive and explosive events that are not necessarily correlatable throughout neighbouring Variscan tectonostratigraphic units bearing Cambrian–lower Ordovician exposures. We investigated the Vendean area and the southern Massif Central from Albigeois to Mouthoumet regions. The lithostratigraphic nomenclature for the Vendée (southern Armorican Domain) has been revised and a new structural scheme is proposed. For the Montagne Noire and Albigeois Mountains (Occitan Domain), we followed the recent nomenclature of their tectonostratigraphic units by Álvaro et al. (2014a). Published available lithostratigraphic patterns are retained for the other areas: southern Cévennes (Verraes, 1979; Alabouvette, 1984; Ortenzi, 1986), and Mouthoumet Massif (Bessière et al., 1989; Berger et al., 1997).

### 2.1. South Armorican Domain

The South Armorican Domain including the Vendée area (Fig. 2) is limited with the Central Armorican Domain by the Nort-sur-Erde Fault (NEF), a former suture zone of a basin between the Gondwanan margin and the Middle Armorican terrane (Faure et al., 1997, 2008). Based on structural arguments (Cartier et al., 2001; Cartier and Faure, 2004; Faure et al., 2005, 2008; Ballèvre et al., 2009), it is suspected that an oceanic crust subducted to the north beneath Armorica. After ocean closure, collision of the margins evolved to dextral wrenching and northward backthrusting of the South Armorican northern area above Central Brittany between about 335 and 305 Ma (Gumiaux et al., 2004a).

South of the so-called suture zone area, we divide the South Armorican Domain into four structural areas or zones bounded by major NW–SE trending faults: (1) the Northern Area between the NEF system and a southern branch of the South Armorican shear-zone that is the Montaigu-Secondigny Shear Zone in Vendée (MSSZ); (2) the Central Structural Zone between the MSSZ and the Chantonnay Fault (ChaF) continued with the Mervent Shear Zone (MSZ); (3) the Intermediate Structural Zone between the ChaF-MSZ, the Sainte-Pazanne-Mervant tectonic line (SPTL) and the Saint-Martin-des-Noyers tectonic line (SMTL); and (4) the Western or Littoral Structural Zone between SMTL and the Atlantic coast.

The structural nomenclature of South-Armorican pre-Variscan units is defined according to the autochthonous-allochthonous scheme of Ballèvre et al. (2014), with modifications based on the present study in Table 1. A synthetic cross section (Fig. 2b) illustrates the relationships between the allochthonous units or complexes in the Vendean area.

#### 2.1.1. Northern structural area

The Ligerian region or domain located between the northern and southern branches of the South Armorican Shear-Zone is divided into two subdomains by the NEF: the northern subdomain including the Saint-Georges-sur-Loire Basin Unit and the southern subdomain that is defined as the northern structural area of the South Armorican Domain. This area consists of the Champtoceaux Complex thrust over the Neoproterozoic Mauves parautochthonous basement, the allochthonous Neoproterozoic Mauges Unit and its
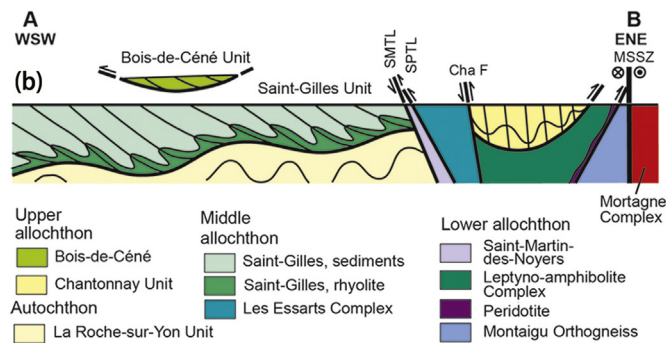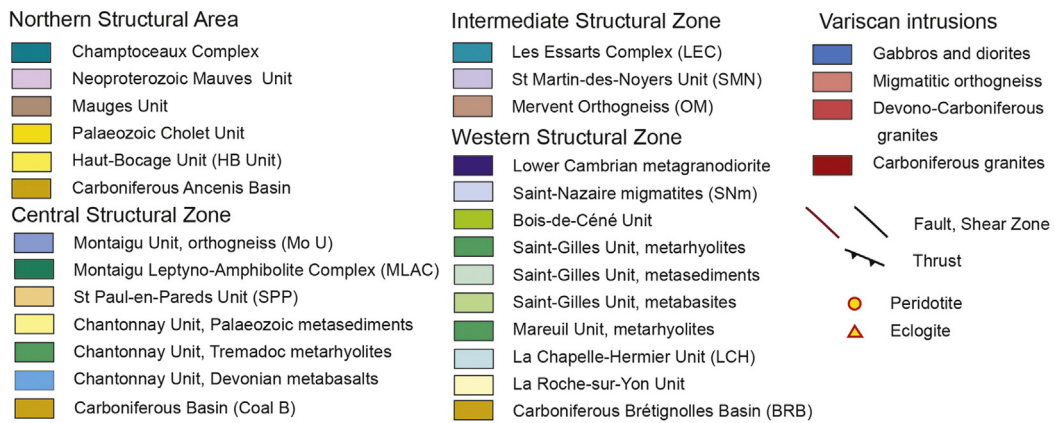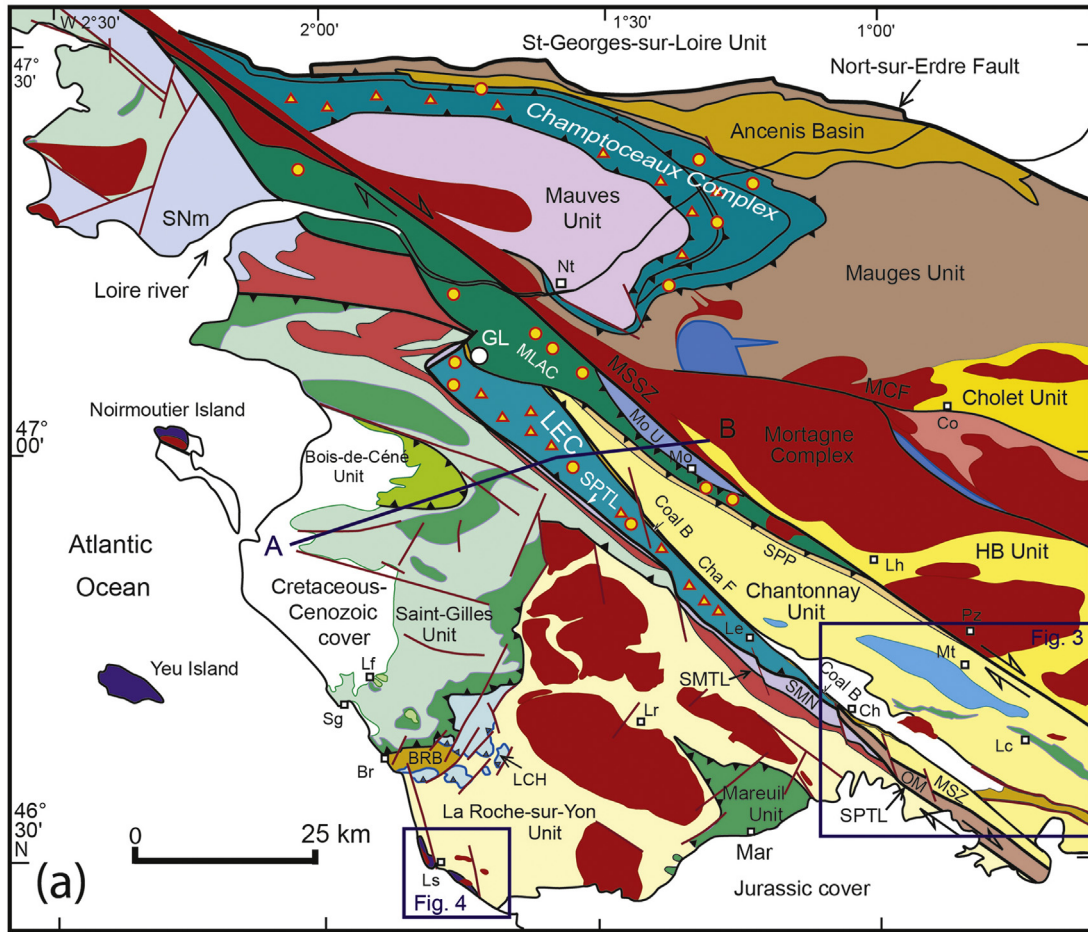
**Figure 2.** Structural sketch of the Southern Armorican Domain in the Vendean area. (a) Geological map after removing the Quaternary deposits. ChaF: Chantonnay Fault; MCF: Mortagne-Cholet Fault; MSZ: Mervent Shear Zone; MSSZ: Montaigu-Secondigny Shear Zone; SMTL: St Martin-des-Noyers Tectonic Line; SPTL: Sainte-Pazanne-Mervent tectonic Line. Sites: Br: Brétignolles; Ch: Chantonnay; Co: Cholet; GL: Grand-Lieu Lake; Le: Les Essarts; Lf: Le Fenouiller; Lh: Les Herbiers; LR: La Roche-sur-Yon; Ls: Les Sables-d'Olonne; MAR: Mareuil-sur-Lay; Mo: Montaigu; Mt: La Meilleraie; Nt: Nantes; Pz: Pouzauges; Sg: Saint-Gilles. AB, cross section. (b) A—B, synthetic cross-section of the Vendean area.

**Table 1**
Structural nomenclature of the South-Armorican pre-Variscan units.

| | Northern structural zone | Central structural zone | Intermediate structural zone | Littoral structural zone | | Tectonic setting of the Gondwana multi-rifted platform |
|---|---|---|---|---|---|---|
| Upper Allochthon | Mauges | | | | | Basement |
| | Cholet | Chantonnay | | | Northeastern marginal basins | Sediments and volcanics |
| Middle Allochthon | Haut-Bocage | St-Paul-en-Pareds | | | | |
| | | | Les Essarts Complex paragneiss | Bois-de-Céné Saint-Gilles metasediments | Oceanic basin | Basin wedge Sedimentary pile |
| | | | Les Essarts Complex orthogneiss | Saint-Gilles - La Sauzaie-Mareuil metarhyolites | | Pre-rifting Tremadocian magmatism |
| | Champtoceaux-Drain, Folies-Siffait | | Les Essarts Complex eclogite lenses | | | Ridge |
| Lower Allochthon | Champtoceaux-Cellier | Montaigu LAC Montaigu orthogneiss | St-Martin-des-Noyers Mervent orthogneiss | | | Volcanic passive margin Pre-rifting Tremadocian magmatism |
| | Mauves | | | | | Basement |
| Parautochthon Autochthon | | | | La Chapelle-Hermier La Roche-sur-Yon | Southwestern marginal basin | Tremadocian magmatism sedimentary pile |

limited Palaeozoic cover, the allochthonous Palaeozoic Cholet and Haut-Bocage units, and the Ancenis Basin (Cartier and Faure, 2004; Ballèvre et al., 2009; Ducassou et al., 2011).

The Northern Structural Area is limited to the south by the left-lateral Montfaucon-Cholet Fault (MCF) along which Variscan granites and gabbros were intruded and mylonitized. Between the MCF and the MSSZ, a large granitic arch was emplaced during late Devonian to late mid-Carboniferous times, represented by the Les Herbiers migmatites ($368 \pm 7$ Ma; Cocherie and Albarède, 2001), the Pouzauges monzogranite massif ($347 \pm 4$ Ma; Poncet and Bouton, 2010), and the Mortagne leucogranitic batholith ($313 \pm 15$ Ma; Guineberteau, 1986).

The lower Palaeozoic volcanic rock-bearing formations are distributed into two units, the Cholet and the Haut-Bocage units.

The *Cholet Unit* includes a basal detrital formation that unconformably overlies the Neoproterozoic Mauges Group basement and is overlain by a thick acidic volcanic series, the Choletais rhyolites (Thiéblemont et al., 1987a, 2001; Thiéblemont, 1988). The basal detrital formation comprises, in ascending order, conglomerates, sandstones, and shales dated by trilobites as mid Cambrian (Cavet et al., 1966). The overlying volcanic series is divided into two units by an intermediate detrital formation of conglomerates and sandstones. Both the lower and upper volcanic units mainly consist of lava and pyroclastic flows of rhyolites, associated dykes of rhyolites and microgranites, and subordinate extrusive and intrusive bodies of mafic and intermediate volcano-plutonic rocks. Although the upper unit was formerly dated around 440 Ma by Rb/Sr method (Le Métour and Bernard-Griffiths, 1979), a zircon dating of the Thouars microgranite gives $519 + 14/-10$ Ma (Thiéblemont et al., 2001). In spite of a large error, this dating implies a mid Cambrian age for the magmatic activity, though more recent acidic intrusive events are not excluded. More accurate age dating is requested.

The *Haut-Bocage Unit* is located between the Mortagne batholith and the Bressuire and Moncoutant granitic and dioritic massifs. It is limited to the southwest by the Montaigu-Secondigny Shear Zone and is invaded by the Tournaisian Pouzauges granite ($374 \pm 4$ Ma, Poncet and Bouton, 2010). Two groups of sedimentary formations are preserved southeast and north of the Pouzauges granite. To the southeast, the Montournais Formation consists of turbiditic interbedded shales and greywackes with few small sills of metabasites (Poncet and Bouton, 2010). To the north, three members are distributed from south to north: a first sandstone pile at the contact of the Pouzauges granite, a shaly sequence transformed to schists and micaschists, and a second sandstone pile at the contact of the metatexites wrapping the Mortagne batholith (Rolin et al., 2000). No stratigraphic order can be evidenced.

### 2.1.2. Central Structural Zone

The Central Structural Zone includes the Montaigu Gneiss Unit, the Montaigu Leptyno-Amphibolite Complex, the Saint-Paul-en-Pareds Unit, the lower Palaeozoic Chantonnay Basin, and the Carboniferous coal-bearing basin.

The *Montaigu Gneiss Unit* is a migmatized and orthogneissified metagranite extended along the southwest of the MSSZ in the Montaigu area. It is dated at $488 \pm 12$ Ma (Godard et al., 2010). The planar fabric trending NW–SE and 50° southwest dipping shows a stretching lineation gently dipping to the southeast and consistent with the right-lateral motion of the MSSZ.

The *Montaigu Leptyno-Amphibolite Complex* (MLAC) consists of thick piles of ortho-amphibolites alternating with leucocratic gneisses that may represent former acidic magmatic rocks or sediments. The complex extends on the southwest margin of the Montaigu orthogneiss and the MSSZ, from Les Herbiers to the northwestern Loire valley. The rocks display a mineral foliation trending NW–SE and dipping 30° to 50° to the southwest. The tectonic contact with the orthogneiss is underlined by an elongated slice of serpentinized peridotite indicative of a crustal-scale main fault. This fault is underlined with a suite of SE–NW elongated and brecciated bodies of peridotites parallel to the MSSZ (Fig. 2). This salient tectonic feature is termed the "MLAC Peridotite Line". The MLAC was thrust to the northeast above the Montaigu orthogneiss and wrenched along the MSSZ. It is assigned to the lower Allochthon (Table 1). Based on the lack of dating, Godard et al. (2010) allotted the MLAC to the basement of the Chantonnay Basin, and assumed that its magmatic activity was related to the Cambro–Ordovician history.

The *Saint-Paul-en-Pareds Unit* (SPP), made of shales and sandstones, extends along the southwestern margin of the MSSZ and the MLAC from Pouzauges to northwest of Montaigu. The rocks are foliated NW–SE with a 50 to 80° dip to the southwest. The contact with the MLAC is characterized by a tectonic mélange of metasediment, amphibolite and leptynite slices. In addition, lenses of metasediments are enclosed in the complex, implying that the MLAC was thrust by the SPP in a number of slices. To the southwest, the contact of the SPP and the Chantonnay Basin is faulted. On both fault sides, sedimentary features, structural patterns and metamorphism are similar. Thus, we consider that the Saint-Paul-en-Pareds Unit belongs to the eastern lower part of the Chantonnay Basin.
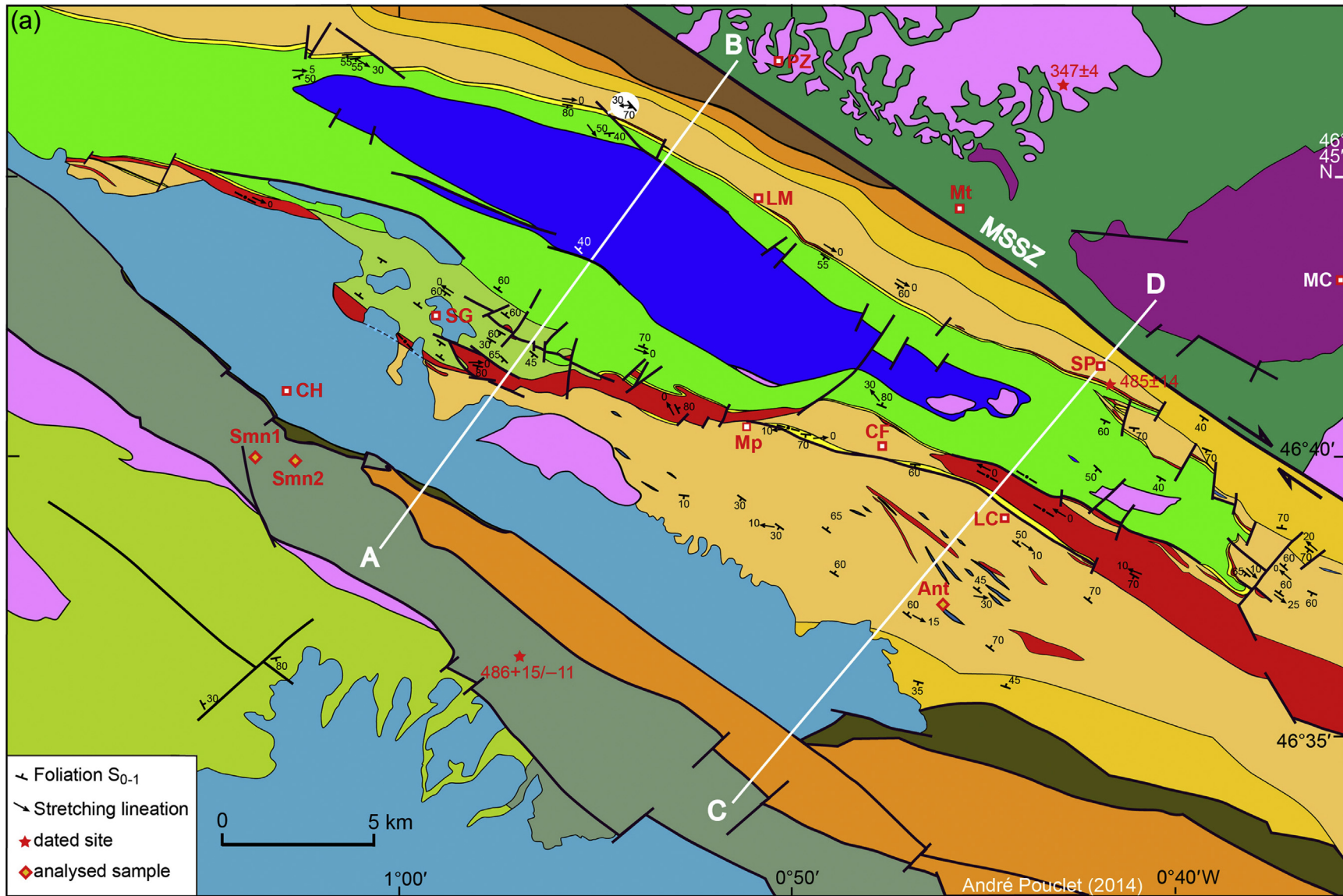
**Figure 3.** Geological map of the Chantonnay Basin. (a) Map; (b) cross sections. Ant: Antigny; CF: Cheffois; CH: Chantonnay; LC: La Châtaigneraie; MC: Moncoutant; Mp: Mouilleron-en-Pareds; Mt: Montournais; PZ: Pouzauges; SG: Sigournais; SP: St-Pierre-du-Chemin; MSSZ: Montaigu-Secondigny Shear Zone. A-B, C-D, cross sections. U-Pb age dating: 486 Ma, orthogneiss of Mervent (Diot et al., 2007); 485 Ma, metarhyolite (blaviérite) of St-Pierre-du-Chemin, La Châtaigneraie Volcanic Formation (Bouton and Branger, 2007); 347 Ma, granite of Pouzauges (Poncet and Bouton, 2010). Ant, Smn1, Smn2: analysed samples.

The *Chantonnay Unit* is a basinal piling of Cambrian to middle—upper Devonian sedimentary formations including several interbedded mafic and acidic volcanic lavas. The basin is elongated NW—SE from the east of the Grand-Lieu Lake to Saint-Maixent-l'école, with a lenticular shape, an overall length of 140 km and a maximum width of 25 km. It is limited to the northeast by the Montaigu Leptyno-Amphibolite Complex, the Saint-Paul-en-Pareds Unit, and the Montaigu-Secondigny Shear Zone (MSSZ) that obliquely cuts the sedimentary formations, and to the southwest by the Chantonnay Fault, the Mervent Shear Zone, and the Jurassic limestones that partly cover the eastern tectonic basin boundary until the Parthenay shear zone (Rolin and Colchen, 2001a,b). The southern area is crosscut by the southeastern extension of the Carboniferous coal basin. Considering that the Saint-Paul-en-Pareds Unit constitutes the base of the Chantonnay Basin, this basin is thrust above the Montaigu Leptyno-Amphibolite Complex and is assigned to the Upper Allochthon (Table 1). The geological map and structural pattern are illustrated in Fig. 3 and the lithostratigraphy summarized in Table 2. The lowermost formations of lower to middle Cambrian age are dominated by basinal turbiditic sequences (Ménardière, Roc-Cervelle). The overlying middle Cambrian formations consist, in the lower part, of black shales (Gerbaudières) and interbedded sandstones that predominate in the southeastern

side of the basin (Marillet-Puy Hardy), and in the upper part, of turbiditic sequences that hosted sills of metabasites and rhyolites (Bourgneuf). Sedimentation is interrupted by the flowing of a rhyolitic activity, the La Châtaigneraie Volvanic Formation, dated to Tremadocian by two samples: $470 \pm 11$ and $485 \pm 14$ Ma (Fig. 3a) (Cocherie in Bouton and Branger, 2007; Poncet and Bouton, 2010). The sedimentation renewed with a coarse detrital deposition of conglomerates, sandstones and siltstones that attest for a major tectonic event related to a syn-rift stage and erosion of rift shoulders (Cheffois, Sigournais). Then, a major change occurs with a deep-water post-rift deposition of black shales interbedded with Silurian phtanites in the lower part and Devonian limestones in the upper part (Réaumur). The basin history ended with the flowing of sub-water basaltic lavas (La Meilleraie).

The last tectonostratigraphic unit, the *Carboniferous Coal Basin*, is superimposed at the southwestern edge of the Central Structural Zone, along the Chantonnay Fault. It consists of an elongated NW—SE narrow trough extended from the Grand-Lieu Lake to the southeast of Chantonnay, and of two pull-apart troughs emplaced in the southern part of the Chantonnay Basin suggesting an N—S extensional strain. These basins are filled with conglomerates, sandstones, shales, and coal lenses. Their palaeoflora indicates a Namurian to Stephanian age.
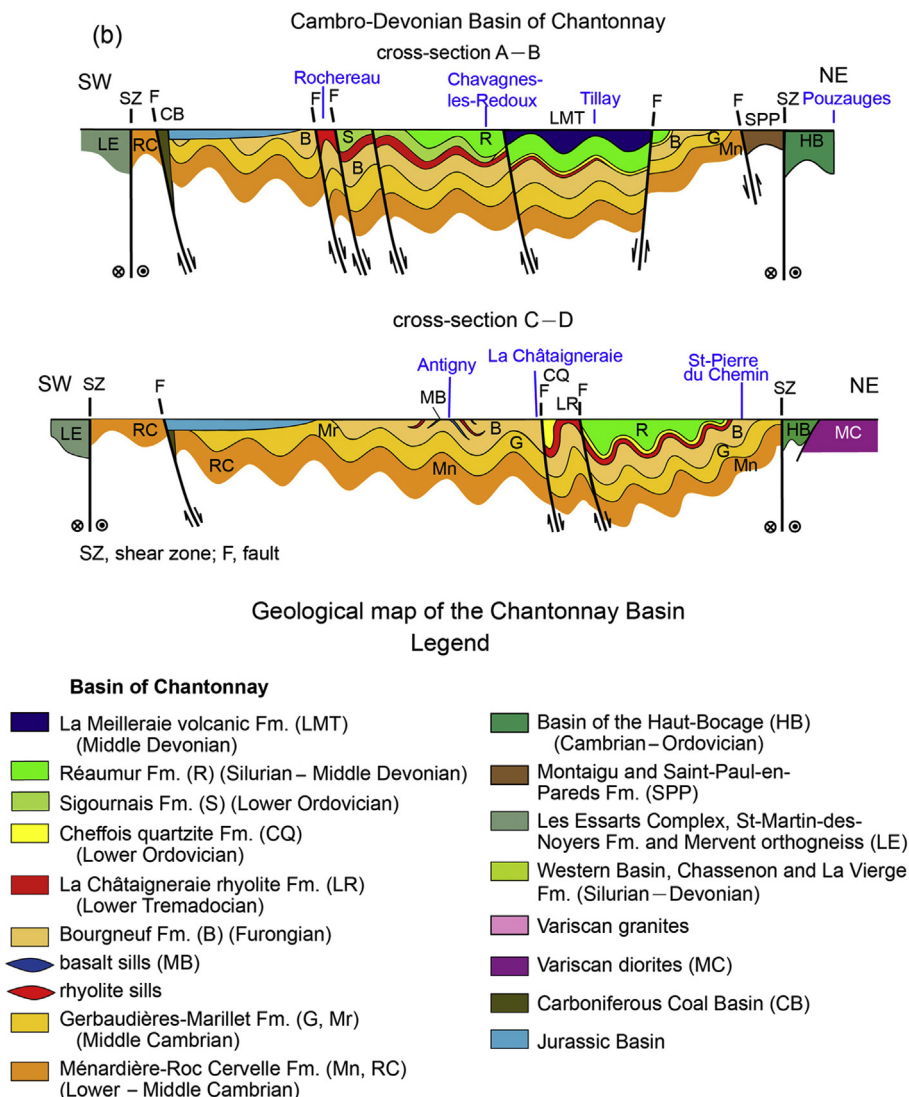


**Figure 3.** (continued).

**Table 2**
Lithostratigraphy of the Chantonnay and La Roche-sur-Yon basins.

| Chantonnay basin | | | | La Roche-sur-Yon basin | | Age |
|---|---|---|---|---|---|---|
| *Upper part* | | | | *Formations* | *Lithology* | |
| *Formations* | | *Lithology* | | | | |
| La Meilleraie | | Lava flows of basalts | | | | Mid Devonian |
| | | | | Chassenon | Shales | |
| | | | | La Vierge | Siltstones | Siluro-Devonian |
| Réaumur | | Black shales, phtanites and rare limestones | | Nieul-le-Dolent | Black shales and phtanites | Silurian |
| | | | | Le Girouard | Shales | Mid Ordovician |
| Sigournais | | Conglomerates, sandstones and siltstones | | Grosbreuil | Siltstones and sandstones | Floian |
| Cheffois | | Conglomerates and sandstones | | | | Floian |
| La Châtaigneraie | | Lava and pyroclastite flows of rhyolite | | Les Sables-d'Olonne | Shales, rare dolostones, sills of metabasites and rhyolites | Tremadocian |
| Bourgneuf | | Turbidites, sills of metabasites and metarhyolites | | Payré | Sandstones | Furongian |
| *Lower part* | | | | | | |
| Northwestern side | | Southeastern side | | | | |
| *Formations* | *Lithology* | *Formations* | *Lithology* | | | |
| Gerbaudières | Black shales | Marillet - Puyhardy | Shales and sandstones | | | Furongian |
| Ménardière | Turbidites | Roc-Cervelle | Turbidites | | | Mid Cambrian |

### 2.1.3. Intermediate Structural Zone

The Intermediate Structural Zone is made of the Les Essarts Complex, the Saint-Martin-des-Noyers Unit, and the Mervent orthogneiss. These units are considered as NW—SE tectonic slices (Godard, 2001a).

The *Les Essarts Complex* (LEC) is an 80 km-long slice from the Grand-Lieu Lake to Chantonnay town. It is limited to the northeast by the fault system of the Carboniferous coal basin, and to the southwest, by the SPTL. It is made of polycyclic gneisses and amphibolites including metre- to kilometre-sized lenses of eclogites and peridotites stretched and boudinaged within the gneisses (Godard, 1981, 1983, 1988, 2001a,b, 2010). The gneisses are both ortho- and paragneisses showing relics of two consecutive high-*T* and high-*P* parageneses (Godard, 2001a). An orthogneiss is dated at 483 ± 4 Ma (U-Pb zircon; Lahondère et al., 2009). The eclogites, derived from metagabbros, recorded a high-pressure metamorphic event and then retrograded in the amphibolite facies. The LEC is supposed to be a tectonic mélange of a partly subducted oceanic crust (eclogites) and a pre-Variscan continental crust (paragneisses) intruded by granite plutons (orthogneisses) (Godard, 2001a, 2010). In its northwestern and main part, the LEC is thrust to the southwest above the Saint-Martin-des-Noyers Unit and is thrust by the Chantonnay Unit (Godard, 2001a). It is therefore assigned to the middle Allochthon (Table 1).

The *Saint-Martin-des-Noyers Unit* (SMN) is elongated from the Grand-Lieu Lake to the south of Mervent with a total length of 100 km. It is thrust against the Les Essarts Complex and the Mervent Orthogneiss along the SPTL and suspected to belong to the lower Allochthon. It is limited to the southwest by a shear-zone fringed by a mylonitized linear pluton, the L'Angle metagranite that metamorphosed the basin sediments of the Western Zone but not the SMN (Lahondère et al., 2009). The metamorphosed sediments of the Western Zone are dated to Ordovician and Silurian. It means that the metagranite postdating these sediments is Variscan and that the SMN unaffected by the metagranite was tectonically jointed with the pluton. Consequently, we locate the western boundary of the Intermediate Zone at the southwestern margin of the SMN along a newly defined tectonic line, the SMTL. The SMN consists of amphibolites and amphibole-rich gneisses belonging to the epidote-amphibolite facies of medium-grade metamorphism. The syn-metamorphic foliation is transposed along a dextral shear foliation trending NNW—SSE and highly dipping toward the southwest. The amphibolites display few relics of doleritic textures

and derived from volcanic rocks (Thiéblemont et al., 1987b). The gneisses range from gneissic amphibolites to amphibole-bearing gneisses. They may be either evolved magmatic rocks or volcano-sedimentary formations, in the lack of magmatic or sedimentary remnant features.

The *Mervent Orthogneiss* is a 60 km stretched body from west of Chantonnay to southeast of Mervent, between the MSZ and the SPTL. Mylonitization planes are vertical with a subhorizontal stretching lineation and a right-lateral motion. The granite crystallization is dated at 486 + 15/−11 Ma (Diot et al., 2007).

### 2.1.4. Western Structural Zone

The Western Structural Zone is made of four lithological groups, in chronological order: (1) lower Cambrian igneous bodies of orthogneissified metagranodiorites constituting the Yeu island and the Les Sables-d'Olonne coast; (2) Furongian to middle Carboniferous metasedimentary and metavolcanic formations including five units, from base to top (structurally): the La Roche-sur-Yon, La Chapelle-Hermier, Brétignolles Basin, Saint-Gilles and Mareuil-sur-Lay, and Bois-de-Céné Units; (3) the middle Carboniferous migmatitic formations of Saint-Nazaire, also occurring in the metagranodiorite of Les Sables-d'Olonne; and (4) the Carboniferous granites (not studied here).

The *Cambrian granitic massif* constitutes the Yeu Island. It is dated to 530 ± 8 Ma (U-Pb zircon; Diot et al., 2015). The massif represents a tectonic pile of increasing metamorphic conditions from protomylonitic granite to kyanite- and sillimanite-bearing orthogneisses. Its foliation dips gently to the north and bears an N—S stretching lineation. Kinematic features attest a top-to-the south thrust (Sassier et al., 2006; Diot et al., 2015). Though less severely deformed, the metagranite north of the Noirmoutier Island resembles that of the Yeu island. It is intruded by late granitic apophyses (Fig. 2).

At the seashore, from northwest to southeast of Les Sables-d'Olonne, a comparable granodioritic orthogneiss is exposed. Its N—S stretching lineation is clearly expressed, but it is overprinted by an E—W stretching lineation (Iglesias and Brun, 1976; Cannat and Bouchez, 1986; Goujou et al., 1994; Cagnard et al., 2004). This orthogneiss body was migmatized and thrust into the basal sequences of the La Roche-sur-Yon Basin as illustrated in Fig. 4, and exhibits a high-grade metamorphic foliation trending WSW—ENE and dipping 35° to the north. It can be assumed that the crystallization age of the original granite is contemporaneous with that of
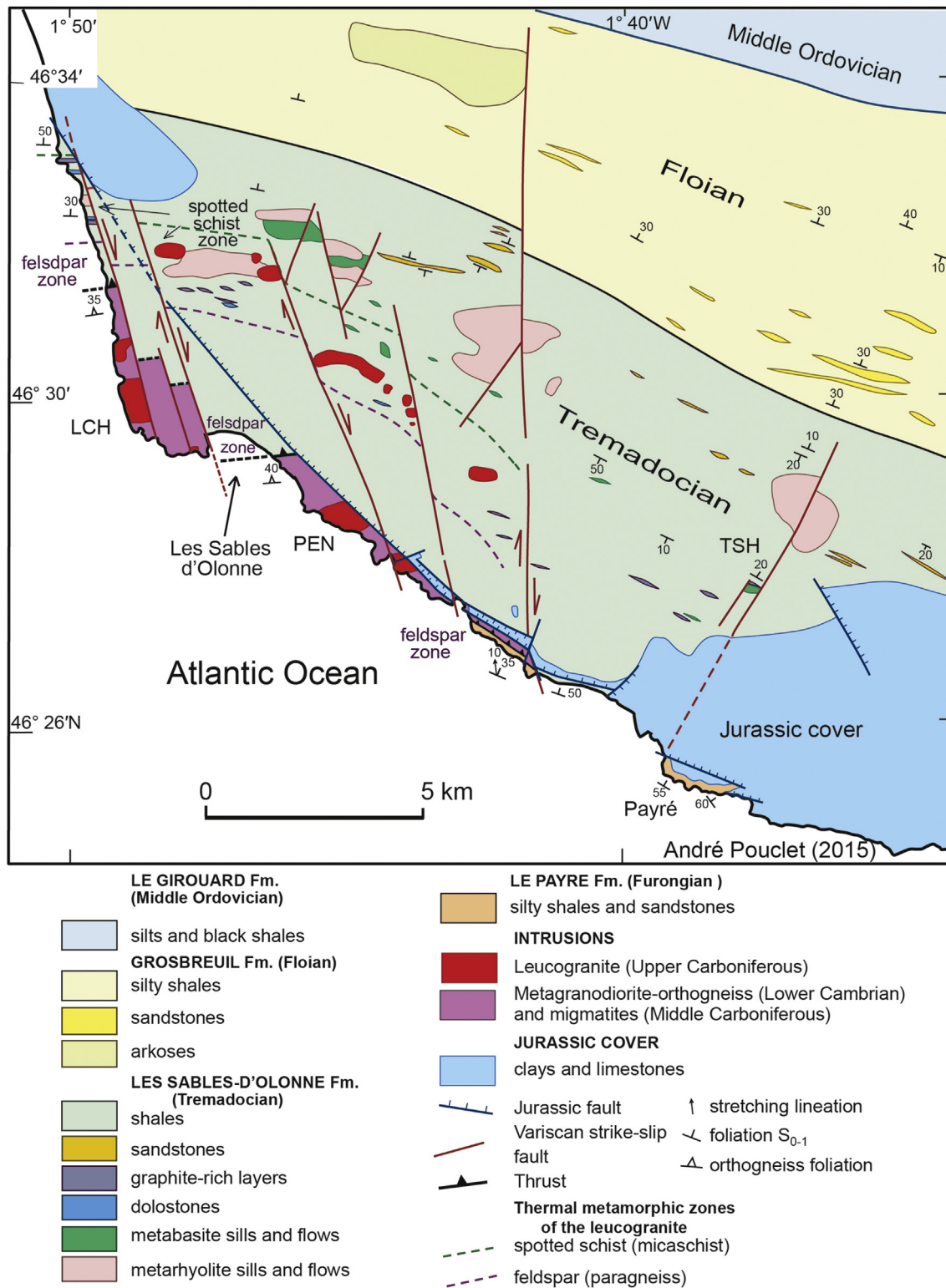
**Figure 4.** Geological map of the Les Sables-d'Olonne area; western part of the La Roche-sur-Yon Basin. LCH: La Chaume and PEN, Puits d'Enfer, main apophyses of the late Variscan granite; TSH: Talmont-St-Hilaire, location of the analysed metabasite sill.

the Yeu Island, i.e. 530 Ma. The migmatites are dated between 328 and 320 Ma (monazite U-Th/Pb chemical dating; Turillot, 2010; Turillot et al., 2011; Augier et al., 2015). A late granitic pluton intruded both the La Roche-sur-Yon Basin sediments and the migmatized orthogneiss, and provided numerous apophyses and dykes of pegmatite and aplite, inducing thermal metamorphism (Fig. 4).

This pluton could be contemporaneous with the neighbouring Avrillé granite, 25 km east of Les Sables-d'Olonne, dated to 313 ± 3 Ma (Cocherie, 2008 in Béchennec et al., 2010).

The *La Roche-sur-Yon Unit* emplaced in the largest basin of the Vendean area and extends from the Saint-Martin-des-Noyers tectonic line (SMTL) to the Atlantic coast (Fig. 2). The sedimentary infill
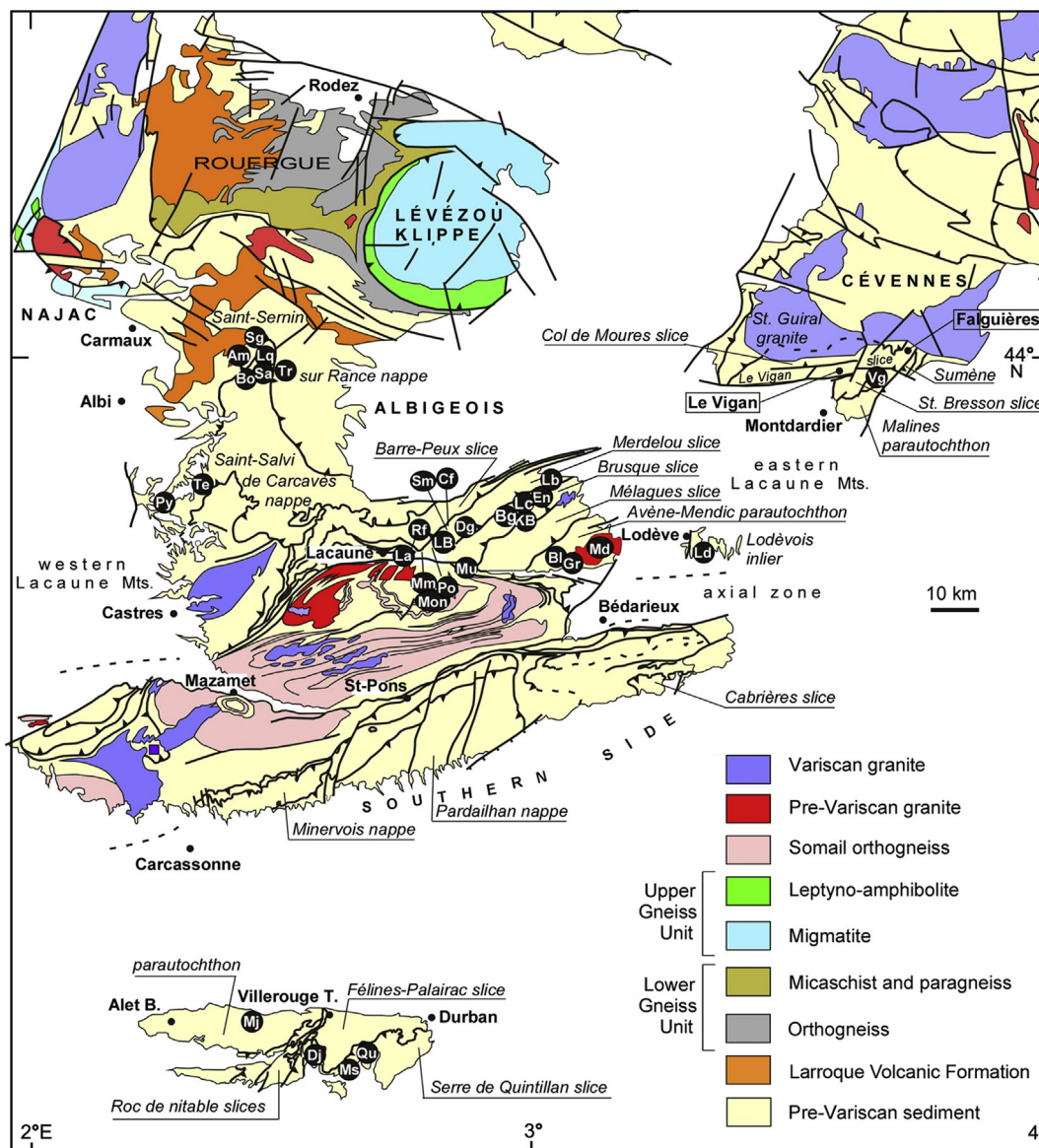
**Figure 5.** Geological map of the tectonostratigraphic units in Albigeois, Montagne Noire, Cévennes and Mouthoumet regions with location of sampled rocks. Abbreviations: Montagne Noire and Albigeois: Am, Larroque hamlet; Bg, Belougos; Bl, Layrac summit; Bo, Bonneval; Cf, Couffouleux; Dg, Degoutal; En, Ensèges; Gr, Graissessac; KB, Kbeta; La, Lacaune; Lb, Le Blanc; LB, Les Bayles; Lc, Lacan; Ld, Grandmont abbey; Lq, La Roque; Md, Mendic; MM, Masnau-Massuguès; Mm, Moulin-Mage; Mon, east of Moulin-Mage; Ms, Massals; Mu, Murat-sur-Brève; Po, Plos; Py, Peyrebrune; Sm, Saint-Méen; Rf, Raffanel; Sa, Saint-André; Sg, Saint-Géraud; Te, Teillet; Tr, Trébas-Mercadial. Mouthoumet-Cévennes: Dj, Davejean; Ms, Maisons; Mj, Mtj, Montjoi; Qu, Quintillan; Vg, Saint-Bresson.

resembles that of the Chantonnay Basin with a piling of Cambrian to Siluro—Devonian detrital formations and interbedded mafic and acidic volcanic lavas. The lithostratigraphy is summarized in Table 2. The geological map of the westernmost and lower part of the basin is illustrated in Fig. 4. The structural pattern of the basin is controlled by the anatectic domes of Les Sables-d'Olonne and La Roche-sur-Yon. The lower and oldest sediments crop out at the southern sea shore and are dominated by sandstones (Payré). The overlying formations consist of shales (Les Sables d'Olonne) inter-bedded with sandstones and rare dolostones and intruded by sills of basalts and rhyolites, a sequence of shales with interbedded sandstones and arkoses (Grosbreuil), and a shale-dominated sequence (Le Girouard). These last formations are suspected to date to lower and middle Ordovician owing to rare palaeontological remnants (Deflandre and Ters, 1966) and assuming a correlation of the rhyolitic activity with the Tremadocian one of the Chantonnay Basin. The overlying pile is made of black shales rich in phtanite

beds dated to Silurian by fossils (Deflandre and Ters, 1970; Ters, 1970; Ters and Viaud, 1987) (Nieul-le-Dolent), and of undated up-per siltstones and shales (La Vierge, Chassenon).

The *La Chapelle-Hermier Unit* is located to the northwestern side of the La Roche-sur-Yon Basin. It consists of slices of rhyolitic lava and pyroclastic flows southward thrust above the Ordovician—Silurian basin formations, along a reverse fault system dipping to the north. The northwestern limit of the unit is the basal thrust plane of the Saint-Gilles-sur-Vie nappe, and, in its west side, the Dinantian Brétignolles Basin. The rhyolite flows are charac-terised by a magmatic planar fabric 30° dipping to the north and a magmatic prismation normal to the planar fabric. The slices resulted from basal décollement of thick and massive lava flows in the La Roche-sur-Yon sedimentary basin during a north-to-south compressive event. The La Chapelle-Hermier Unit rhyolites are dated to Tremadocian by Béchennec et al. (2008) (U-Pb zircon): $486 \pm 4$ Ma (Chie-loup), $483 \pm 10$ Ma (Coex), and $478 \pm 14$ Ma (La
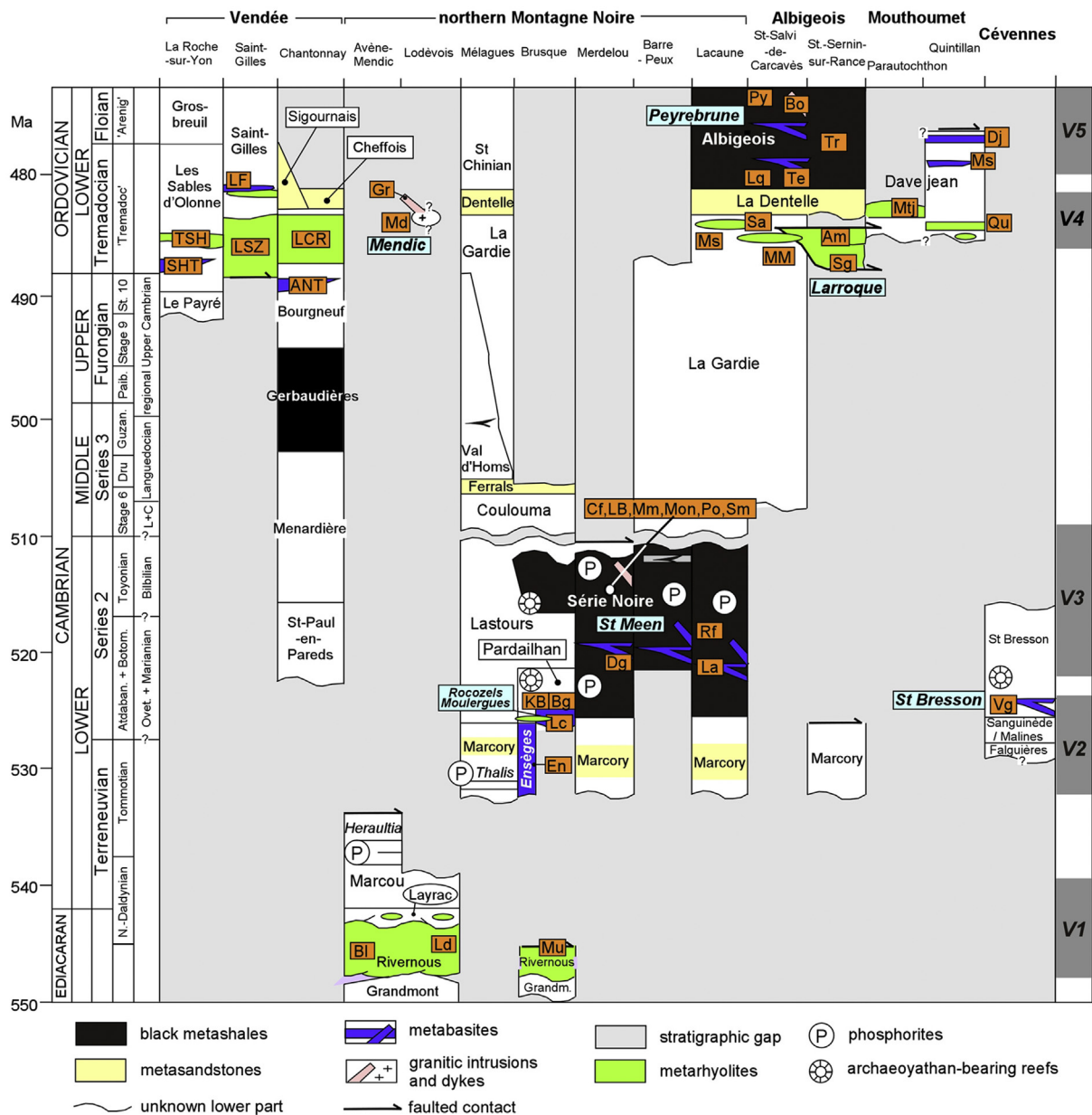
**Figure 6.** Correlation chart of the uppermost Ediacaran–lower Ordovician stratigraphic units from the South Armorican and Occitan domains. Setting of volcanic complexes after Álvaro et al. (2010, 2014a) and this work. Abbreviations, Vendée: ANT, Antigny metabasites; LCR, La Châtaigneraie metarhyolites; LF, Le Fenouiller metabasite; LSZ, Saint-Gilles and Mareuil-sur-Lay metarhyolites; SHT, Saint-Hilaire-de-Talmont metabasite; TSH, Talmont-Saint-Hilaire and Les Sables-d'Olonne metarhyolites. Albigeois, Montagne Noire, Cévennes and Mouthoumet abbreviations, see Fig. 5.

Chapelle-Hermier) and by Ballèvre et al. (2012): 486 ± 4 Ma (Chieloup) and 472 ± 4 Ma (Bréthomé).

*The Brétignolles Basin Unit* consists of lower Carboniferous sediments filling a tectonic trough located east of Brétignolles, E–W trending and averaging 20 km in length (Comble et al., 1985; Colchen and Poncet, 1989). This basin is thrust at its northern side by the metarhyolite of the Saint-Gilles Unit nappe and is thrust to the south above the southernmost La Chapelle-Hermier slices. The whole basin sediments are folded in E–W trending and northward dipping reverse folds.

The *Saint-Gilles-sur-Vie* and *Mareuil-sur-Lay Units* (reduced to "Saint-Gilles" and "Mareuil") are located to northwest and southeast of the La Roche-sur-Yon Basin, respectively (Fig. 2). They were related to a former single nappe overlying the La Roche-sur-Yon Basin. The tectonic pattern of the nappe is evidenced by

subhorizontal mylonitic foliation and shear planes gently dipping to the east and bearing an E–W stretching lineation indicating a westward transport. The basal thrust is reworked by NNW-dipping reverse faults along the northwestern edge of the La Roche-sur-Yon Basin. The nappe extends to the northwest until the St-Gildas cape, south of the Loire estuary, and is correlatable with the La Vilaine and Belle-île nappe (Audren et al., 1975). To the northeast, the nappe is limited by a metagranite that intruded and metamorphosed the nappe sediments (Lahondère et al., 2009), indicating that the granitic intrusion post-dated the nappe setting. This northeastern border is parallel to the SPTL and recorded the strong dextral shearing with highly dipping to the southwest foliation and subhorizontal stretching lineation.

The base of the nappe is a stack of rhyolitic lavas and pyroclastics dated to Tremadocian by five U-Pb zircon ages from Saint-Gilles

**Table 3**
Geographical and tectonostratigraphic location of the selected samples for petrographical and chemical analyses.

| Structural site | Volcanic formation | Sample nb | Rock type | Latitude | Longitude |
|---|---|---|---|---|---|
| **Chantonnay Basin** | **Bourgneuf Fm** | | | | |
| | Antigny sill | Ant 1-3 | Metabasalt | N46°36′ 38.16″ | W00°46′ 50.10″ |
| **St-Martin-des-Noyers Unit** | **Saint-Martin-des-Noyers Fm** | | | | |
| | Le Moulin neuf | Smn 1 | Ortho-amphibolite | N46°39′ 29.28″ | W01°03′ 51.78″ |
| | Pont-Charron | Smn 2 | Ortho-amphibolite | N46°39′ 24.06″ | W01°02′ 38.52″ |
| **La Roche-sur-Yon Basin** | **Les Sables-d'Olonne Fm** | | | | |
| | Talmont-Saint-Hilaire sill | Tsh 1-2-3 | Metabasalt | N46°27′ 36.57″ | W01°37′ 52.11″ |
| **Saint-Gilles nappe** | **Saint-Gilles Fm** | | | | |
| | Le Fenouiller | Lfr 2 | Metabasite | N46°43′ 08.42″ | W01°53′ 49.56″ |
| **Avène-Mendic parautochthon** | **Rivernous Rhyolitic Complex** | | | | |
| | Grandmont Abbey | Lod | Metarhyolite | N43°43′ 54.05″ | E03°21′ 51.64″ |
| | Layrac summit | Bl 1-2 | Metarhyolite | N43°41′ 40.64″ | E03°03′ 09.40″ |
| | Murat-sur-Brève | Murat | Metarhyolite | N43°41′ 12.78″ | E02°50′ 58.73″ |
| **Brusque slice** | **Ensèges Volcanic Complex** | | | | |
| | Ensèges flow | Ens 1-2-3 | Metabasalt | N43°48′ 06.83″ | E03°01′ 12.01″ |
| **Brusque slice** | **Moulergues Volcanic Complex** | | | | |
| | Lacan flow | Lacan 1-2-3 | Metabasalt | N43°47′ 33.87″ | E02°59′ 42.59″ |
| | Bélougos | Bel 1-2 | Meta-epiclastite | N43°47′ 28.05″ | E02°58′ 52.09″ |
| | Kbeta | Kb 2-7 | Meta-albitophyre | N43°47′ 30.00″ | E02°59′ 34.84″ |
| | Kbeta | Kb 4-6 | Metarhyolite | N43°47′ 32.01″ | E02°59′ 59.58″ |
| **Merdelou slice** | **Saint-Méen Volcanic Complex** | | | | |
| | Dégoutal | Degout 1-2 | Metapyroclastite | N43°46′ 44.04″ | E02°56′ 13.64″ |
| | Couffouleux | Couf 3 | Metabasalt | N43°46′ 26.46″ | E02°52′ 38.76″ |
| | Saint-Méen sill | Meen | Metadolerite | N43°45′ 17.47″ | E02°51′ 43.72″ |
| | Plos | Plos-R | Metapyroclastite | N43°42′ 54.84″ | E02°50′ 14.10″ |
| | Le Blanc | Blanc 1-2 | Metapyroclastite | N43°44′ 24.42″ | E02°53′ 10.74″ |
| | Moulin-Mage (Cantoul) | Mom 3 | Meta-epiclastite | N43°43′ 55.03″ | E02°49′ 12.17″ |
| | Moulin-Mage (Gabande) | Mom 4 | Meta-epiclastite | N43°43′ 38.63″ | E02°51′ 09.85″ |
| | Les Bayles dyke | Bay 1 | Dolerite | N43°48′ 55.38″ | E03°03′ 15.96″ |
| | Les Bayles | Bay 2 | Meta-epiclastite | N43°48′ 55.38″ | E03°03′ 15.96″ |
| | Moulin-Mage | Mom 1-2 | Meta-epiclastite | N43°42′ 36.27″ | E02°47′ 35.62″ |
| | close to Moulin-Mage | Mon | Meta-pyroclastite | N43°42′ 36.70″ | E02°49′ 02.62″ |
| **Lacaune slice** | Raffanel sill | Raff | Metadolerite | N43°43′ 15.95″ | E02°44′ 16.10″ |
| | Lacaune sill | Lac 1 | Metadolerite | N43°43′ 06.37″ | E02°43′ 28.32″ |
| | Lacaune | Lac 2-3 | Meta-epiclastite | N43°42′ 25.81″ | E02°45′ 58.06″ |
| **St-Sernin-sur-Rance nappe** | **Larroque Metarhyolites** | | | | |
| | Larroque hamlet | Amb 1-2 | Metarhyolite | N43°56′ 41.14″ | E02°18′ 10.41″ |
| | St Géraud | Stg | Metarhyolite | N44°02′ 00.81″ | E02°19′ 12.20″ |
| **St-Salvi-de-Carcavès nappe** | St André castle | Sta | Metarhyolite | N43°55′ 57.17″ | E02°27′ 44.77″ |
| **Avène-Mendic autochthon** | **Mendic Granite massif** | | | | |
| | Mendic | Men 1-2 | Granite | N43°43′ 36.41″ | E03°07′ 35.05″ |
| | Graissessac dyke | Gra 2 | Microgranite | N43°41′ 06.22″ | E03°05′ 25.83″ |
| **St-Salvi-de-Carcavès nappe** | **Peyrebrune Volcanic Complex** | | | | |
| | Trebas flow-sill | Tb 1-2 | Metabasalt | N43°57′ 12.67″ | E02°26′ 59.30″ |
| | Bonneval sill | Bon 1-2-3 | Metadolerite | N43°55′ 56.42″ | E02°23′ 54.30″ |
| | La Roque sill | Lrq | Metadolerite | N43°57′ 08.92″ | E02°25′ 01.51″ |
| | Teillet sill | Tei 1a-1b | Metadolerite | N43°49′ 13.75″ | E02°20′ 58.43″ |
| | Teillet | Tei 2-4 | Meta-epiclastite | N43°49′ 23.20″ | E02°21′ 7.95″ |
| | Peyrebrune flow-sill | Pey 5-6 | Metabasalt | N43°45′ 44.52″ | E02°14′ 36.37″ |
| **Southern Cévennes** | **Saint-Bresson Volcanic Complex** | | | | |
| | Saint-Bresson flow | Vg 2-6 | Metabasalt | N43°57′ 21.8″ | E03°38′ 30.0″ |
| **Mouthoumet Massif** | | | | | |
| Parautochthon | Montjoi | Mtj1 | Metarhyodacite | N43°00′ 12.04″ | E02°29′ 32.80″ |
| Serre de Quintillan nappe | Quintillan | Qu | Metarhyolite | N42°57′ 02.7″ | E02°42′ 10.6″ |
| | **Davejean Volcanic Complex** | | | | |
| Serre de Quintillan nappe | Davejean flow | Dj 1-2 | metabasalt | N42°57′ 07.09″ | E02°36′ 38.30″ |
| Serre de Quintillan nappe | Maisons flow | Ms 1-2 | metaspilite | N42°55′ 25.1″ | E02°39′ 06.8″ |

(491 ± 12, 481 ± 14, and 477 ± 7 Ma) and Mareuil (479 ± 4 and 478 ± 2 Ma), and two U-Th/Pb monazite ages from Mareuil (486 ± 6 and 483 ± 4 Ma) (Béchennec et al., 2008, 2010; Ballèvre et al., 2012). This stack averages 500 m in thickness and is termed the "La Sauzaie Volcanic Formation".

The overlying sedimentary deposition is made of a lower transitional part made of rhyolitic pyroclastites and volcanosediments, and an upper part with fining upward sandstones and interbedded shales ("Saint-Gilles Formation"). In this sedimentary pile, a second volcanic sequence is recorded and termed the "Le Fenouiller Member". It consists of two kilometre-scale rhyolitic lenses overlain by metabasites and located east of Saint-Gilles-sur-Vie (Lf, Fig. 2).

The *Bois-de-Céné Unit* is a 12 km-scale klippe emplaced above the Saint-Gilles Formation in the middle area of the Saint-Gilles nappe. The rocks consist of shales and interbedded sandstones transformed to micaschists with abundant metre- to hectometre-sized lenses of metabasites and serpentinites, strongly foliated and folded with axial planes trending WNW–ESE. The paragenesis indicates a high-pressure metamorphism in the blueschist facies (Ters and Viaud, 1983; Guiraud et al., 1987). There is a synmetamorphic shear contact separating the Bois-de-Céné and the underlying Saint-Gilles formations. These were folded together during the deformation events that postdated the nappe thrusting and are only distinguished according to their different metamorphic patterns.

**Table 4**

Chemical analyses of magmatic rocks. ICP and ICP-MS methods at ACME-LABS in Canada and at the "Service d'Analyse des Roches et des Minéraux du Centre de Recherches en Pétrographie et Géochimie" of Nancy, France. -: no analytical data.

| Sample# | Ant 1 | Ant 3 | Smn 1 | Smn 2 | Tsh 1 | Tsh 2 | Tsh 3 | Lfr2 | Bl 1 | Bl 2 | Murat | Ens 1 | Ens 2 | Lacan 1 | Lacan 3 | Bel 2 | Kb 2 | Kb 7 | Kb 4 | Degout | Couf 3 | Meen | Plos-R | Blanc 1 | Mom 3 | Mom 4 | Mon | Bay 1 | Bay 2 | Raff | Lac 1 | Lac 2 | Am 1 | Am 2 | Stg | Sta | Men 1 | Men 2 | Gra 2 | Tb 1 | Tb 2 | Bon 1 | Bon 3 | Lrq | Tei 1b | Tei 2 | Pey 5 | Vg 2 | Vg 6 | Mtj 1 | Qu | Dj 1 | Dj 2 | Ms 1 | Ms 2 |
|---|---|---|---|---|---|---|---|---|---|---|---|---|---|---|---|---|---|---|---|---|---|---|---|---|---|---|---|---|---|---|---|---|---|---|---|---|---|---|---|---|---|---|---|---|---|---|---|---|---|---|---|---|---|---|---|
| **Major elements (wt.%)** | | | | | | | | | | | | | | | | | | | | | | | | | | | | | | | | | | | | | | | | | | | | | | | | | | | | | | | |
| SiO2 | 44.89 | 46.11 | 52.48 | 51.13 | 46.30 | 49.27 | 52.82 | 55.62 | 68.73 | 75.15 | 76.99 | 44.27 | 44.57 | 44.63 | 43.50 | 62.62 | 59.44 | 54.53 | 74.50 | 49.26 | 54.79 | 49.99 | 49.40 | 59.23 | 60.11 | 67.69 | 64.14 | 38.39 | 59.39 | 49.30 | 49.98 | 59.92 | 68.48 | 68.97 | 66.72 | 74.95 | 74.52 | 74.86 | 73.89 | 48.46 | 45.69 | 47.84 | 50.22 | 51.35 | 55.52 | 68.13 | 52.07 | 47.18 | 47.98 | 44.18 | 69.35 | 75.66 | 57.13 | 58.93 | 63.73 |
| TiO2 | 1.06 | 1.10 | 1.25 | 1.82 | 2.14 | 2.29 | 2.12 | 1.21 | 0.15 | 0.17 | 0.09 | 0.90 | 0.82 | 0.83 | 0.88 | 0.50 | 0.57 | 0.63 | 0.35 | 0.44 | 1.02 | 0.94 | 0.47 | 0.58 | 0.79 | 0.31 | 0.46 | 2.89 | 0.45 | 0.85 | 0.76 | 0.55 | 0.26 | 0.30 | 0.57 | 0.16 | 0.35 | 0.31 | 0.38 | 2.39 | 4.38 | 3.13 | 1.96 | 3.85 | 2.18 | 0.44 | 3.12 | 1.99 | 0.84 | 0.89 | 0.42 | 0.14 | 0.74 | 0.86 | 0.52 |
| Al2O3 | 14.54 | 15.19 | 14.96 | 13.23 | 14.92 | 14.27 | 15.01 | 14.52 | 18.49 | 13.50 | 12.14 | 16.76 | 17.99 | 18.26 | 19.29 | 15.50 | 18.81 | 20.02 | 13.37 | 17.98 | 18.60 | 17.05 | 21.12 | 19.36 | 19.24 | 19.24 | 12.36 | 13.38 | 19.00 | 15.99 | 16.54 | 19.10 | 15.85 | 15.49 | 16.36 | 12.97 | 13.53 | 12.68 | 12.70 | 13.33 | 13.85 | 15.21 | 14.68 | 14.62 | 13.50 | 15.50 | 13.35 | 14.14 | 17.62 | 19.41 | 16.55 | 14.83 | 15.24 | 17.04 | 17.33 |
| Fe2O3 | 9.90 | 9.45 | 14.46 | 16.06 | 11.54 | 11.75 | 10.24 | 1.94 | 1.69 | 1.59 | 10.11 | 10.19 | 10.82 | 9.72 | 7.18 | 5.96 | 6.93 | 1.99 | 7.10 | 6.84 | 8.40 | 6.58 | 3.75 | 5.93 | 1.89 | 4.01 | 11.68 | 6.73 | 6.98 | 7.56 | 5.12 | 2.37 | 2.46 | 4.37 | 2.18 | 2.49 | 2.43 | 2.50 | 13.54 | 16.26 | 13.79 | 12.05 | 16.19 | 13.30 | 4.58 | 13.91 | 12.40 | 9.61 | 10.75 | 3.31 | 0.73 | 6.34 | 7.25 | 4.64 | 4.56 |
| MnO | 0.17 | 0.15 | 0.28 | 0.24 | 0.18 | 0.14 | 0.14 | 0.19 | 0.02 | 0.03 | 0.01 | 0.17 | 0.15 | 0.17 | 0.14 | 0.10 | 0.06 | 0.11 | 0.00 | 0.09 | 0.09 | 0.11 | 0.09 | 0.05 | 0.01 | 0.05 | 0.07 | 0.21 | 0.08 | 0.13 | 0.14 | 0.10 | 0.01 | 0.02 | 0.08 | 0.00 | 0.02 | 0.03 | 0.01 | 0.19 | 0.22 | 0.24 | 0.17 | 0.19 | 0.19 | 0.04 | 0.19 | 0.05 | 0.08 | 0.04 | 0.02 | 0.11 | 0.09 | 0.07 | 0.07 |
| MgO | 7.13 | 7.64 | 4.06 | 3.40 | 3.74 | 3.01 | 5.49 | 0.44 | 0.22 | 0.40 | 14.63 | 12.91 | 11.61 | 12.88 | 3.34 | 3.89 | 4.44 | 1.34 | 7.06 | 7.64 | 8.56 | 5.15 | 4.52 | 2.98 | 1.07 | 4.89 | 7.83 | 2.14 | 7.83 | 8.79 | 2.37 | 0.70 | 0.93 | 1.31 | 1.84 | 0.30 | 0.20 | 0.12 | 6.02 | 4.90 | 6.03 | 6.08 | 3.41 | 2.46 | 1.53 | 4.31 | 7.41 | 12.62 | 12.26 | 0.53 | 0.27 | 4.58 | 3.89 | 2.35 | 2.28 |
| CaO | 9.24 | 9.09 | 6.06 | 7.42 | 7.61 | 5.48 | 4.60 | 3.39 | 0.22 | 0.56 | 0.28 | 4.12 | 3.42 | 1.98 | 1.55 | 1.76 | 0.33 | 2.59 | 0.46 | 4.05 | 0.36 | 6.54 | 7.51 | 0.48 | 0.16 | 0.02 | 8.43 | 12.76 | 0.42 | 11.06 | 7.65 | 2.89 | 0.22 | 0.26 | 0.09 | 0.06 | 0.43 | 0.25 | 0.14 | 9.52 | 6.35 | 4.54 | 6.07 | 1.06 | 2.69 | 0.41 | 5.59 | 10.16 | 0.20 | 0.20 | 0.28 | 0.12 | 3.07 | 0.73 | 0.53 | 0.45 |
| Na2O | 1.91 | 2.51 | 4.30 | 5.28 | 3.97 | 4.16 | 4.69 | 5.00 | 0.63 | 1.04 | 2.79 | 1.86 | 3.53 | 2.73 | 3.75 | 4.38 | 8.00 | 7.00 | 6.69 | 6.50 | 5.49 | 4.07 | 4.57 | 8.31 | 2.30 | 0.09 | 0.65 | 1.67 | 8.05 | 2.63 | 4.11 | 5.87 | 0.84 | 1.34 | 1.63 | 0.61 | 5.79 | 2.98 | 1.59 | 1.37 | 3.94 | 4.49 | 3.95 | 2.74 | 4.44 | 4.25 | 4.59 | 2.60 | 3.41 | 0.05 | 2.12 | 3.68 | 5.42 | 5.89 | 6.35 | 6.52 |
| K2O | 0.89 | 0.70 | 0.11 | 0.18 | 0.35 | 0.15 | 0.34 | 1.11 | 5.27 | 5.95 | 4.08 | 0.80 | 0.34 | 2.62 | 0.59 | 1.53 | 0.08 | 0.37 | 0.11 | 0.11 | 0.33 | 0.31 | 0.75 | 0.28 | 3.50 | 5.15 | 0.05 | 0.81 | 0.88 | 0.38 | 0.55 | 0.53 | 5.31 | 7.91 | 5.35 | 3.96 | 1.41 | 4.97 | 7.02 | 0.28 | 0.14 | 0.26 | 0.65 | 0.62 | 1.59 | 1.72 | 0.12 | 0.07 | 0.91 | 4.89 | 3.82 | 2.36 | 0.75 | 0.53 | 1.50 | 1.28 |
| P2O5 | 0.10 | 0.09 | 0.08 | 0.12 | 0.23 | 0.23 | 0.35 | 0.15 | 0.51 | 0.48 | 0.16 | 0.05 | 0.05 | 0.06 | 0.05 | 0.14 | 0.12 | 0.07 | 0.05 | 0.06 | 0.15 | 0.11 | 0.08 | 0.12 | 0.22 | 0.06 | 0.07 | 0.95 | 0.12 | 0.10 | 0.09 | 0.09 | 0.16 | 0.15 | 0.13 | 0.05 | 0.12 | 0.10 | 0.11 | 0.22 | 0.32 | 0.39 | 0.29 | 0.62 | 0.90 | 0.09 | 0.42 | 0.15 | 0.12 | 0.14 | 0.23 | 0.09 | 0.22 | 0.23 | 0.21 |
| Cr2O3 | 0.04 | 0.04 | 0.00 | 0.00 | 0.00 | 0.00 | 0.00 | 0.02 | 0.00 | 0.00 | 0.00 | 0.04 | 0.03 | 0.04 | 0.04 | 0.01 | 0.00 | 0.03 | 0.01 | 0.01 | 0.02 | 0.05 | 0.05 | 0.01 | 0.00 | 0.00 | 0.09 | 0.06 | 0.01 | 0.04 | 0.04 | 0.00 | 0.00 | 0.00 | 0.00 | 0.00 | 0.00 | 0.00 | 0.00 | 0.01 | 0.00 | 0.00 | 0.01 | 0.03 | 0.00 | 0.00 | 0.03 | 0.04 | 0.00 | 0.00 | 0.00 | 0.00 | 0.03 | 0.00 | 0.00 | 0.00 |
| LOI | 10.22 | 6.96 | 1.70 | 1.53 | 9.20 | 8.30 | 6.50 | 2.92 | 3.77 | 1.93 | 1.40 | 6.00 | 5.70 | 5.90 | 7.30 | 2.80 | 2.60 | 3.10 | 1.10 | 7.10 | 4.20 | 3.60 | 4.10 | 3.20 | 4.60 | 4.30 | 4.70 | 8.10 | 2.60 | 4.50 | 3.50 | 3.30 | 1.60 | 2.00 | 3.20 | 3.10 | 1.00 | 1.10 | 1.40 | 4.40 | 3.70 | 3.80 | 3.60 | 5.10 | 3.00 | 3.10 | 2.10 | 3.40 | 6.30 | 6.80 | 3.20 | 2.00 | 6.10 | 4.30 | 2.50 | 2.70 |
| Total | 100.09 | 99.03 | 99.72 | 99.15 | 99.84 | 99.78 | 99.82 | 99.89 | 100.16 | 100.72 | 99.93 | 99.71 | 99.70 | 99.65 | 99.69 | 99.86 | 99.86 | 99.82 | 99.97 | 99.76 | 99.53 | 99.73 | 99.83 | 99.88 | 99.85 | 99.87 | 99.92 | 98.73 | 99.87 | 99.79 | 99.71 | 99.84 | 99.80 | 99.83 | 99.81 | 99.88 | 99.96 | 99.91 | 99.86 | 99.73 | 99.75 | 99.73 | 99.75 | 99.75 | 99.77 | 99.79 | 99.79 | 99.79 | 99.69 | 99.85 | 99.90 | 99.73 | 99.78 | 99.76 | 99.85 | |
| **Minor elements (ppm)** | | | | | | | | | | | | | | | | | | | | | | | | | | | | | | | | | | | | | | | | | | | | | | | | | | | | | | | |
| Sc | 36.08 | 38.29 | 47.71 | 43.29 | 26 | 32 | 27 | 31.99 | 5 | 3 | 2 | 38 | 33 | 31 | 38 | 14 | 13 | 24 | 9 | 24 | 28 | 29 | 23 | 14 | 17 | 8 | 14 | 30 | 17 | 29 | 29 | 18 | 4 | 4 | 9 | 12 | 7 | 5 | 6 | 40 | 45 | 40 | 37 | 41 | 23 | 14 | 38 | 45 | 39 | 44 | 3 | 6 | 22 | 22 | 12 | 12 |
| V | 195.7 | 208.8 | 298.3 | 435.9 | 287 | 332 | 170 | 232.1 | - | 11 | 38 | 174 | 161 | 164 | 167 | 67 | 61 | 65 | <8.0 | 122 | 169 | 151 | 147 | 121 | 109 | 26 | 75 | 256 | 81 | 169 | 143 | 107 | <8 | 11 | 54 | <8 | 18 | <8 | 16 | 365 | 527 | 320 | 230 | 278 | 77 | 18 | 323 | 345 | 183 | 52 | <8 | 16 | 144 | 164 | 104 | 112 |
| Co | 38.88 | 40.12 | 29.98 | 38.86 | 33.3 | 42.8 | 26.1 | 30.97 | - | - | 1.6 | 45.5 | 47 | 50.5 | 45.2 | 17.8 | 16.9 | 23.9 | 7.3 | 26.5 | 11.2 | 36.6 | 23.2 | 15.5 | 8.5 | 4.5 | 22.8 | 67.8 | 26.1 | 33.4 | 33.2 | 19.2 | 3 | 3.4 | 7.1 | 1.3 | 2.7 | 7.2 | 3.3 | 43.9 | 37 | 45 | 39 | 30.5 | 17.5 | 5.8 | 28.7 | 43.3 | 38.8 | 49.4 | 2.8 | 1 | 23.1 | 24.3 | 11 | 10.7 |
| Ni | 59.36 | 55.07 | 6.651 | 14.06 | 6 | 6.8 | 1.8 | 50.08 | - | - | 1.1 | 130.3 | 151.7 | 181.5 | 171 | 32.9 | 22 | 76.8 | 15.5 | 19.9 | 50.2 | 99.1 | 13.5 | 14.5 | 23.5 | 16.2 | 155.3 | 367.2 | 17 | 97.5 | 99.3 | 17.4 | 3.2 | 3.8 | 10.8 | 2 | 3.7 | 2.7 | 6.4 | 28.4 | 9.8 | 38.3 | 41.1 | 1.7 | 0.4 | 9.5 | 2.5 | 40.7 | 80.4 | 57.4 | 2.7 | 0.7 | 74.7 | 92.9 | 12.6 | 16.3 |
| Cu | 39.58 | 94.35 | <L.D. | 41.35 | 16.7 | 71.8 | 19 | 35.68 | - | - | 3.1 | 65.8 | 57.2 | 42.2 | 54 | 4.6 | 101.2 | 3.6 | 9.1 | 3.4 | 24.6 | 21 | 2.7 | 8.1 | 35.8 | 15.2 | 11.1 | 2259.3 | 5.5 | 37.6 | 43.6 | 40.8 | 9 | 17 | 9.8 | 3.6 | 2.9 | 104.3 | 6.1 | 69.8 | 12.8 | 64.6 | 44.4 | 20.1 | 3.9 | 9.6 | 14 | 100.4 | 8.6 | 1.3 | 3.1 | 8.4 | 45.1 | 47.1 | 20.7 | 38.1 |
| Zn | 109.3 | 85.42 | 120.3 | 139.3 | 83 | 90 | 93 | 110.1 | - | - | 10 | 42 | 50 | 52 | 50 | 64 | 50 | 58 | 21 | 54 | 447 | 59 | 42 | 20 | 52 | 31 | 23 | 129 | 67 | 34 | 43 | 39 | 27 | 34 | 35 | 91 | 7 | 9 | 42 | 81 | 115 | 121 | 55 | 142 | 142 | 35 | 104 | 66 | 60 | 28 | 123 | 77 | 69 | 99 | 64 | 73 |
| Ga | 16.15 | 16.27 | 16.99 | 20.39 | 20.8 | 18.7 | 21.4 | 18.15 | 30 | 19 | 17.5 | 13.1 | 13.2 | 15.1 | 13.3 | 16.5 | 17.4 | 14 | 7.4 | 13 | 17.8 | 15.3 | 16.7 | 14.2 | 19.3 | 21 | 15 | 19.4 | 16.2 | 14.4 | 12.7 | 14.7 | 20.3 | 18.6 | 22.4 | 19.9 | 19.9 | 15.7 | 18.2 | 20.5 | 24.1 | 21.4 | 19.1 | 26.3 | 27.7 | 24.1 | 22.6 | 18.9 | 13 | 15.9 | 24.6 | 15.3 | 16 | 17.7 | 18.3 | 18.9 |
| Rb | 32.81 | 30.41 | 3.122 | 3.84 | 9.9 | 3 | 10.2 | 22.71 | 298 | 303 | 168 | 23.8 | 10.3 | 43 | 17.2 | 32.8 | 0.6 | 11.4 | 1.8 | 1.7 | 9.6 | 4.6 | 13.7 | 5.2 | 119.1 | 160.5 | 1.1 | 93.8 | 41.1 | 5 | 19.5 | 12 | 189 | 169.2 | 213.7 | 113.1 | 56.8 | 143.2 | 129.4 | 8.2 | 7.3 | 6.9 | 18.3 | 16 | 128.9 | 63.2 | 2.7 | 1.8 | 15.6 | 137.9 | 153 | 74.9 | 27.9 | 20.8 | 39.1 | 36.2 |
| Sr | 209.8 | 336.1 | 97.4 | 99.15 | 313.2 | 192.4 | 178.2 | 87.61 | 18 | 145 | 80.2 | 123 | 160.5 | 158.1 | 129 | 265.9 | 95.8 | 464 | 140.5 | 664.8 | 794.6 | 490.4 | 599.3 | 361.5 | 165.1 | 44.7 | 21.5 | 627.5 | 128.4 | 350.4 | 713.4 | 755.1 | 84 | 79.1 | 31.6 | 18.9 | 80 | 84.6 | 442 | 368.2 | 338.8 | 205.9 | 415 | 114.7 | 179.5 | 71.4 | 196.7 | 406.8 | 26 | 3 | 67.6 | 134.7 | 448.4 | 428.2 | 346.4 | 359.2 |
| Y | 17.65 | 19.24 | 21.66 | 44.52 | 29.6 | 27.6 | 42.3 | 36.54 | 30.6 | 38.8 | 11.4 | 20.5 | 18.8 | 17.6 | 15.3 | 16.7 | 12.6 | 21.5 | 12.1 | 7.6 | 18.8 | 17.5 | 10.8 | 14.4 | 29.4 | 45.4 | 22.9 | 28.7 | 13.3 | 17.9 | 15.1 | 14.7 | 31.1 | 31.8 | 33.4 | 32.9 | 38.7 | 34.6 | 24 | 33.3 | 37.9 | 35.1 | 25.9 | 61.4 | 62.4 | 48.2 | 47.7 | 28.3 | 15 | 16.3 | 23.5 | 20.6 | 19.6 | 24.3 | 19.6 | 16 |
| Zr | 67.13 | 74.17 | 38.28 | 96.87 | 131.9 | 150.9 | 203 | 131.9 | 130 | 111 | 48.1 | 56.5 | 51.4 | 48.7 | 46.3 | 127.7 | 153.8 | 137.1 | 144.9 | 40.1 | 120.4 | 80.8 | 61.1 | 107.2 | 157.9 | 118.5 | 70.5 | 328.2 | 108.4 | 83.3 | 65.3 | 105.4 | 147.3 | 166.8 | 300.8 | 160 | 205.8 | 178.2 | 233.6 | 141.8 | 212.1 | 210.8 | 148.8 | 329.7 | 467.2 | 402 | 319.8 | 111.9 | 63.1 | 64.8 | 274.8 | 122.9 | 128.2 | 148.7 | 158.3 | 156.9 |
| Nb | 2.23 | 2.08 | 0.48 | 0.43 | 11.5 | 12.6 | 18.4 | 4.17 | 13.6 | 11.3 | 7.6 | 0.2 | 0.2 | 0.1 | 0.2 | 1.8 | 1.5 | 2.3 | 2.6 | 0.6 | 2.3 | 2.3 | 0.8 | 1.4 | 9.1 | 10.9 | 1.7 | 150.9 | 3.8 | 0.7 | 0.6 | 1.4 | 10.6 | 11.1 | 19.1 | 14.3 | 10.7 | 10.6 | 12.6 | 11.5 | 21.1 | 23.3 | 14.6 | 34.9 | 48.5 | 50.8 | 28.6 | 7.6 | 2.1 | 1.9 | 17.8 | 28.3 | 10.2 | 11.8 | 14.9 | 15.7 |
| Mo | - | - | - | - | 0.5 | 0.5 | 0.5 | - | <2 | <2 | 4.2 | <0.1 | <0.1 | <0.1 | <0.1 | <0.1 | <0.1 | 0.1 | 0.1 | <0.1 | 0.1 | 0.1 | <0.1 | 0.4 | 0.6 | 0.1 | 0.3 | 2.4 | <0.1 | 0.2 | 0.2 | 0.3 | 0.3 | 0.4 | 0.2 | 0.1 | 1.4 | 0.7 | 1.1 | 0.4 | 0.5 | 0.5 | 0.6 | 1.8 | 2.7 | 0.9 | 0.5 | <0.1 | <0.1 | 0.2 | 0.2 | 0.5 | 0.8 | 0.5 | 0.3 | |
| Sb | 1.06 | 1.57 | 0.27 | 0.40 | 0.2 | <0.1 | 0.52 | 2.9 | 1.9 | - | <0.1 | <0.1 | <0.1 | 0.3 | <0.1 | 0.6 | <0.2 | <0.1 | 0.1 | <0.1 | 0.3 | 1.4 | 0.3 | 0.1 | 49.2 | 1.2 | 0.1 | <0.1 | 0.2 | 0.5 | 2.3 | 0.5 | 0.1 | 0.2 | 0.5 | 1.9 | 1.2 | 1.8 | 0.7 | 0.5 | <0.1 | 0.3 | 0.2 | 0.3 | 0.4 | 0.5 | 0.5 | 0.6 | 1.8 | 2.7 | 0.5 | <0.1 | 0.2 | 0.2 | 0.2 | 0.3 |
| Cs | 4.33 | 4.20 | 1.02 | 1.59 | 2.3 | 0.5 | 2.8 | 1.70 | 7.2 | 7.4 | 4.3 | 4.2 | 2 | 2.3 | 1.4 | 1.6 | 0.4 | 1.6 | 0.3 | 0.5 | 0.7 | 0.8 | 0.5 | 0.6 | 4.7 | 8.1 | <0.1 | 137.5 | 6.8 | 1.1 | 1.8 | 1.2 | 4.4 | 5.2 | 5 | 5.7 | 4.5 | 8.9 | 1 | - | 5 | 2.4 | 1.5 | 0.8 | 4.1 | - | 0.1 | 1.6 | 7.4 | 7.3 | 1 | 1 | 0.6 | 3.1 | 1.8 | |
| Ba | 245 | 153.70 | 27.11 | 24.65 | 46 | 24 | 41 | 345.9 | 154 | 156 | 137 | 48 | 48 | 502 | 59 | 509 | 15 | 44 | 23 | 45 | 731 | 141 | 205 | 202 | 652 | 948 | 18 | 4525 | 164 | 297 | 102 | 369 | 1090 | 1368 | 861 | 520 | 113 | 511 | 672 | 77 | 161 | 209 | 269 | 180 | 398 | 585 | 190 | 84 | 46 | 120 | 657 | 400 | 284 | 270 | 507 | 347 |
| Hf | 1.88 | 1.95 | 1.26 | 2.93 | 3.20 | 3.40 | 5.00 | 3.99 | 4.40 | 3.50 | 1.7 | 1.7 | 1.3 | 1.4 | 1.5 | 3.3 | 4.5 | 4.1 | 4.1 | 1.5 | 2.8 | 1.9 | 1.5 | 2.8 | 4.6 | 4.5 | 2.5 | 7.3 | 2.9 | 1.6 | 1.8 | 3.4 | 4.2 | 4.6 | 8.1 | 5.6 | 6.3 | 5.7 | 6.5 | 4.3 | 5.2 | 4.7 | 4 | 8.8 | 11.6 | 10.2 | 7.6 | 2.8 | 1.4 | 1.7 | 7.9 | 3.6 | 3.5 | 4 | 3.8 | 3.9 |
| Ta | 0.17 | 0.18 | 0.05 | 0.05 | 0.70 | 0.70 | 1.10 | 0.36 | 1.36 | 1.11 | 1.1 | 0.09 | 0.1 | 0.09 | 0.09 | 0.1 | 0.2 | 0.2 | 0.15 | 0.2 | 0.2 | 0.1 | 0.1 | 0.2 | 0.7 | 1 | 0.2 | 9.3 | 0.3 | 0.15 | 0.2 | 0.1 | 1 | 0.9 | 1.8 | 1.1 | 1 | 0.9 | 1.1 | 0.8 | 1.5 | 1.6 | 0.9 | 2.1 | 3 | 3.3 | 1.6 | 0.4 | 0.2 | 0.1 | 1.2 | 1.5 | 0.6 | 0.7 | 0.9 | 0.9 |
| Pb | 4.54 | 7.49 | 2.18 | 2.51 | 2.8 | 4.8 | 5.3 | 1062 | 19 | 2.7 | 0.09 | 2.3 | 1.7 | 0.6 | 2.3 | 0.9 | 4.7 | 2.4 | 0.9 | 1.2 | 3.2 | 5.6 | 5.5 | 3.6 | - | 2.3 | 2.7 | 2.1 | 2.9 | 21.8 | 34.1 | 5.7 | 1.5 | 1.3 | 2.8 | 2.8 | 2.2 | 4.1 | 14.7 | 2 | 1.7 | 2.3 | 9.3 | 8.5 | 1.1 | 2.8 | 0.8 | 5.3 | 10.6 | 9.2 | 21.3 | 2.7 | 5.2 | | | |
| Bi | 0.10 | - | - | <0.1 | <0.1 | <0.1 | - | 0.8 | 0.2 | - | <0.1 | <0.1 | <0.1 | 0.3 | 0.15 | 0.2 | 0.1 | 0.2 | <0.1 | <0.1 | <0.1 | <0.1 | 0.1 | 0.7 | - | 5 | 2.4 | 1.5 | 0.8 | 4.1 | - | 0.1 | 1.6 | | | | | | | | | | | | | | | | | | | | | | | |
| Th | 0.34 | 0.43 | 0.75 | 0.25 | 1.80 | 1.90 | 2.30 | 2.75 | 10.30 | 6.52 | 1.6 | 0.15 | 0.15 | 0.3 | 0.15 | 3.2 | 4.2 | 4 | 4.3 | 0.4 | 1 | 1.2 | 1 | 2.5 | 8 | 12.1 | 3.7 | 9.6 | 3.1 | 0.8 | 0.6 | 3 | 17.5 | 18.3 | 20.2 | 17.3 | 20.9 | 3.1 | 2.7 | 2.5 | 4.9 | 0.4 | 1.1 | 1.3 | 0.6 | 1.6 | 2.3 | 5.1 | 1.4 | <0.1 | 1.6 | 13.9 | 6.3 | 7.5 | 8.7 | 8.4 |
| U | 0.24 | 0.15 | 0.31 | 0.19 | 0.6 | 1.4 | 4.9 | 1.01 | 2.1 | 6.4 | 1.9 | 0.08 | 0.06 | 0.08 | 0.08 | 0.7 | 0.8 | 0.6 | 0.7 | 0.09 | 0.3 | 0.3 | 0.2 | 1 | 2.9 | 3 | 1.1 | 2.2 | 0.8 | 0.2 | 0.1 | 0.7 | 3.2 | 3.4 | 10.9 | 3.1 | 2.7 | 2.5 | 4.9 | 0.4 | 1.1 | 1.3 | 0.6 | 6.2 | 8 | 22 | 0.6 | 1 | 1.1 | 1.3 | 0.6 | 2.3 | 5.1 | 1.4 | 2.4 | 2.5 |
| **Rare earth elements (ppm)** | | | | | | | | | | | | | | | | | | | | | | | | | | | | | | | | | | | | | | | | | | | | | | | | | | | | | | | |
| La | 3.22 | 3.54 | 3.23 | 2.73 | 12.70 | 15.00 | 22.50 | 11.07 | 18.90 | 14.50 | 4.70 | 1.50 | 1.50 | 1.90 | 1.20 | 9.20 | 5.40 | 5.80 | 4.30 | 4.80 | 6.90 | 5.60 | 4.60 | 3.70 | 8.60 | 33.20 | 42.00 | 45.60 | 45.20 | 35.50 | 36.90 | 11.80 | 39.60 | 7.90 | 5.00 | 63.00 | 59.30 | 27.60 | 29.80 | 41.50 | 28.50 | 20.00 | 11.40 | 14.90 | 126.80 | 112.80 | 55.60 | 83.00 | 58.20 | | | | | | | |
| Ce | 8.68 | 9.49 | 7.92 | 9.48 | 31.50 | 34.40 | 52.60 | 25.78 | 44.70 | 33.10 | 10.50 | 6.60 | 5.40 | 5.80 | 4.30 | 20.50 | 10.50 | 24.60 | 14.00 | 5.50 | 12.30 | 15.70 | 11.80 | 10.90 | 34.30 | 60.60 | 35.20 | 134.70 | 14.60 | 11.50 | 9.70 | 23.10 | 69.90 | 94.90 | 89.70 | 94.80 | 71.30 | 77.10 | 28.00 | 31.20 | 57.00 | 48.30 | 34.70 | 79.70 | 112.70 | 140.60 | 86.60 | 20.00 | 11.40 | 14.90 | 126.80 | 112.80 | 55.60 | 83.00 | 58.20 | |
| Pr | 1.30 | 1.48 | 1.22 | 1.80 | 3.71 | 4.13 | 6.27 | 3.53 | 5.19 | 4.08 | 1.20 | 1.10 | 0.95 | 1.10 | 0.77 | 2.81 | 1.42 | 3.20 | 1.94 | 0.82 | 1.84 | 2.02 | 1.59 | 1.97 | 5.09 | 7.99 | 4.07 | 15.26 | 1.93 | 1.78 | 1.44 | 2.91 | 8.12 | 9.69 | 10.20 | 10.87 | 8.14 | 8.55 | 3.39 | 4.52 | 7.00 | 6.72 | 4.72 | 10.70 | 14.75 | 15.52 | 10.98 | 2.86 | 1.69 | 2.23 | 15.03 | 13.92 | 6.42 | 6.72 | 8.48 | 6.13 |
| Nd | 6.31 | 7.32 | 6.38 | 10.77 | 16.30 | 18.60 | 29.30 | 15.65 | 21.20 | 18.90 | 5.20 | 6.40 | 5.40 | 5.20 | 5.10 | 11.70 | 5.70 | 15.10 | 9.00 | 3.50 | 9.10 | 9.00 | 7.30 | 9.10 | 20.60 | 32.20 | 18.10 | 56.70 | 9.80 | 8.60 | 7.30 | 11.00 | 29.00 | 32.30 | 38.40 | 40.70 | 28.30 | 29.50 | 12.60 | 19.30 | 31.70 | 25.80 | 21.20 | 46.60 | 63.90 | 57.80 | 45.40 | 14.50 | 7.80 | 8.30 | 56.20 | 36.20 | 25.60 | 25.70 | 30.80 | 21.80 |
| Sm | 2.08 | 2.39 | 2.15 | 4.19 | 4.20 | 4.60 | 6.81 | 4.44 | 5.24 | 5.30 | 1.26 | 2.06 | 1.97 | 1.92 | 1.38 | 2.65 | 1.55 | 3.26 | 2.00 | 1.00 | 2.60 | 2.56 | 1.57 | 2.31 | 4.63 | 7.22 | 3.29 | 9.74 | 2.88 | 2.28 | 1.85 | 2.85 | 5.97 | 6.69 | 7.70 | 7.87 | 6.29 | 5.95 | 3.12 | 5.29 | 7.46 | 6.95 | 5.34 | 11.83 | 14.48 | 10.89 | 10.36 | 4.16 | 1.91 | 3.06 | 10.81 | 5.53 | 5.21 | 5.70 | 4.89 | 3.89 |
| Eu | 0.69 | 0.91 | 0.85 | 1.45 | 1.49 | 1.52 | 2.37 | 1.30 | 0.38 | 0.73 | 0.18 | 0.72 | 0.71 | 0.82 | 0.61 | 0.77 | 0.40 | 1.06 | 0.42 | 0.36 | 0.99 | 0.62 | 0.73 | 0.85 | 0.78 | 0.98 | 2.95 | 0.49 | 0.67 | 0.74 | 0.82 | 1.00 | 1.12 | 1.14 | 0.70 | 0.52 | 0.51 | 0.34 | 1.77 | 2.66 | 2.27 | 1.88 | 4.02 | 3.82 | 1.81 | 3.06 | 1.59 | 0.42 | 0.93 | 1.33 | 1.11 | 1.21 | 1.38 | 1.39 | 1.03 | |
| Gd | 2.50 | 2.74 | 2.69 | 5.51 | 5.03 | 5.20 | 7.82 | 4.92 | 4.53 | 5.79 | 2.38 | 2.95 | 2.74 | 2.55 | 2.15 | 2.80 | 1.60 | 3.69 | 1.78 | 1.10 | 2.98 | 2.76 | 1.92 | 2.61 | 4.48 | 7.40 | 3.70 | 8.55 | 2.23 | 2.79 | 2.42 | 2.84 | 6.25 | 6.49 | 7.01 | 6.61 | 6.18 | 5.83 | 3.76 | 6.38 | 8.57 | 7.30 | 5.53 | 12.47 | 14.92 | 9.87 | 11.10 | 5.61 | 1.77 | 2.60 | 8.70 | 6.83 | 4.76 | 4.60 | 3.30 | |
| Tb | 0.46 | 0.50 | 0.50 | 1.04 | 0.93 | 0.97 | 1.42 | 0.87 | 0.89 | 1.09 | 0.34 | 0.54 | 0.48 | 0.48 | 0.39 | 0.46 | 0.28 | 0.66 | 0.34 | 0.21 | 0.56 | 0.53 | 0.33 | 0.44 | 0.82 | 1.32 | 0.62 | 1.23 | 0.36 | 0.51 | 0.41 | 0.46 | 0.99 | 1.01 | 1.23 | 1.10 | 1.04 | 0.95 | 0.66 | 1.03 | 1.29 | 1.29 | 0.97 | 2.14 | 2.50 | 1.74 | 1.72 | 0.87 | 0.35 | 0.45 | 1.16 | 0.69 | 0.61 | 0.71 | 0.66 | 0.56 |
| Dy | 3.23 | 3.38 | 3.49 | 7.37 | 5.11 | 5.17 | 7.77 | 5.97 | 5.54 | 6.69 | 2.27 | 3.32 | 3.21 | 3.09 | 2.68 | 2.76 | 2.00 | 4.10 | 2.47 | 1.20 | 3.36 | 3.02 | 1.76 | 2.59 | 4.78 | 8.23 | 3.79 | 6.07 | 2.05 | 3.25 | 2.56 | 3.16 | 6.07 | 5.77 | 6.52 | 6.56 | 5.71 | 6.01 | 4.03 | 6.01 | 7.56 | 6.58 | 5.41 | 12.55 | 12.90 | 9.35 | 9.70 | 5.35 | 2.52 | 3.04 | 5.33 | 3.70 | 3.48 | 4.23 | 3.65 | 3.20 |
| Ho | 0.72 | 0.75 | 0.83 | 1.69 | 1.22 | 1.17 | 1.85 | 1.36 | 1.06 | 1.27 | 0.43 | 0.76 | 0.69 | 0.66 | 0.63 | 0.56 | 0.45 | 0.82 | 0.46 | 0.31 | 0.81 | 0.65 | 0.42 | 0.55 | 1.01 | 1.75 | 0.85 | 1.07 | 0.54 | 0.66 | 0.58 | 0.55 | 1.16 | 1.29 | 1.43 | 1.25 | 1.40 | 1.21 | 0.89 | 1.39 | 1.47 | 1.43 | 1.01 | 2.44 | 2.75 | 1.99 | 1.92 | 1.14 | 0.58 | 0.68 | 0.88 | 0.83 | 0.71 | 0.87 | 0.64 | 0.58 |
| Er | 1.96 | 2.01 | 2.32 | 4.68 | 3.04 | 3.09 | 5.22 | 3.82 | 2.90 | 3.30 | 1.19 | 2.35 | 2.30 | 2.10 | 1.90 | 1.96 | 1.81 | 2.75 | 1.92 | 0.89 | 2.46 | 1.88 | 1.29 | 1.82 | 3.04 | 5.01 | 2.36 | 3.14 | 1.62 | 1.97 | 1.57 | 1.65 | 3.49 | 3.56 | 4.08 | 4.05 | 3.85 | 3.54 | 2.80 | 3.35 | 4.29 | 3.86 | 2.96 | 6.37 | 7.83 | 5.40 | 5.07 | 3.13 | 1.81 | 2.06 | 1.99 | 2.05 | 2.00 | 2.66 | 2.03 | 1.78 |
| Tm | 0.29 | 0.30 | 0.35 | 0.70 | 0.46 | 0.48 | 0.78 | 0.56 | 0.39 | 0.43 | 0.17 | 0.34 | 0.31 | 0.29 | 0.27 | 0.28 | 0.30 | 0.42 | 0.31 | 0.13 | 0.37 | 0.31 | 0.18 | 0.28 | 0.43 | 0.78 | 0.36 | 0.40 | 0.23 | 0.28 | 0.24 | 0.22 | 0.49 | 0.50 | 0.61 | 0.60 | 0.62 | 0.53 | 0.39 | 0.50 | 0.63 | 0.55 | 0.41 | 0.96 | 1.03 | 0.83 | 0.80 | 0.45 | 0.26 | 0.30 | 0.34 | 0.28 | 0.30 | | | |
| Yb | 1.95 | 2.02 | 2.42 | 4.74 | 2.99 | 3.01 | 4.61 | 3.90 | 2.20 | 2.35 | 1.01 | 2.42 | 1.98 | 1.89 | 1.94 | 2.01 | 2.23 | 2.63 | 2.45 | 0.72 | 2.49 | 2.02 | 1.18 | 1.86 | 2.43 | 4.76 | 2.39 | 2.40 | 1.61 | 2.03 | 1.57 | 1.64 | 2.91 | 2.89 | 3.72 | 4.02 | 3.74 | 3.35 | 2.56 | 3.00 | 3.54 | 3.00 | 2.32 | 6.14 | 6.22 | 5.01 | 5.00 | 2.42 | 1.82 | 2.17 | 1.66 | 2.09 | 1.77 | 2.43 | 1.95 | 1.86 |
| Lu | 0.30 | 0.31 | 0.39 | 0.74 | 0.43 | 0.47 | 0.72 | 0.62 | 0.28 | 0.29 | 0.16 | 0.37 | 0.31 | 0.30 | 0.27 | 0.34 | 0.36 | 0.46 | 0.38 | 0.11 | 0.42 | 0.28 | 0.18 | 0.28 | 0.41 | 0.76 | 0.33 | 0.35 | 0.25 | 0.29 | 0.25 | 0.30 | 0.46 | 0.42 | 0.54 | 0.64 | 0.53 | 0.47 | 0.40 | 0.41 | 0.54 | 0.46 | 0.35 | 0.88 | 0.95 | 0.81 | 0.74 | 0.44 | 0.26 | 0.33 | 0.22 | 0.38 | 0.27 | 0.36 | 0.31 | 0.32 |

## 2.2. Limousin and Occitan domains

To the southeast of the South Armorican Domain, and beyond a Mesozoic cover (the so-called "Seuil du Poitou") Cambro–Ordovician sedimentary and volcanic formations are distributed along the western to southern Massif Central. There, a major Variscan structural contact allows differentiation between the northern and southern Massif Central domains. The former domain is dominated by the lower and upper Gneiss Allochthonous Units, but includes some low-grade sedimentary basins in the Limousin area. The latter domain, here named Occitan Domain, comprises the Variscan tectonostratigraphic units of the Thiviers-Payzac, Rouergue-Albigeois, Montagne Noire, Southern Cévennes and Mouthoumet massifs (Fig. 1). The Occitan Domain represents a proximal early Palaeozoic Gondwana margin that linked to the NW with the South Armorican Domain, as shown by the seuil du Poitou structural map of Rolin and Colchen (2001a), and to the SE with Corsica and Sardinia. The domain is limited to the south by the North Pyrenean frontal thrust.

### 2.2.1. Limousin

Lower Palaeozoic low-grade sedimentary series, the Bas-Limousin Group, are preserved in the western and southwestern margins of the high-grade metamorphic Limousin Massif. From north to south, these series are the La Gartempe, Saint-Salvadour and Mazerolles Units (Santallier and Floc'h, 1989; Floc'h et al., 1993), the Thiviers-Payzac and Génis Units (Guillot et al., 1977; Roig et al., 1996), and the Leyme Unit (Guillot et al., 1989, 1992). The more complete sequence is recorded in the Thiviers-Payzac and Genis area and shows: (1) lower Cambrian sandstones, (2) a metadolerite and metagabbro stack, (3) middle Cambrian–Furongian shales and sandstones, (4) a lower Ordovician metarhyolitic pile, (5) lower Ordovician sandstones, and (6) Ordovician to upper Silurian shales and ampelites. All these formations were metamorphosed in the greenschist facies, folded and displaced along a shear corridor.

### 2.2.2. Albigeois and northern Montagne Noire

Thick lower Palaeozoic sedimentary and volcanic formations occur in the Albigeois nappes, namely the Saint-Sernin-sur-Rance and Saint-Salvi-de-Carcavès nappes. These nappes southward overthrust the Lacaune Mountains (northern Montagne Noire), which consist of a succession of imbricated slices named Lacaune, Barre-Peux, Merdelou, Brusque, and Mélagues. All these units are closely related to the Avène-Mendic parautochthon and its eastern prolongation, the Lodevois inlier (Guérangé-Lozes and Burg, 1990; Álvaro et al., 2014a). The geological map of this region and location of the study area are illustrated in Fig. 5.

To the south, the northern Montagne Noire is separated by the metamorphic Axial Zone forming an elongated dome of migmatized orthogneiss (Somail orthogneiss) and micaschists tectonically overlain by lower Palaeozoic schists and marbles. Dating of orthogneiss has been revised to Ordovician (460–450 Ma; Roger et al., 2004). The southern Montagne Noire is made of south-facing nappes including a complete and fossiliferous Cambrian–Carboniferous succession (Vizcaïno and Álvaro, 2001, 2003).

The lithostratigraphy of the northern Montagne Noire and Albigeois has been updated by Álvaro et al. (2014a) based on recent discovery and re-study of significant fossiliferous sites and on stratigraphic re-setting of volcanosedimentary units (Álvaro et al., 1998; Álvaro and Vizcaïno, 1999; Devaere et al., 2013). This region recorded a basinal stratigraphy with an uppermost Ediacaran–lower Ordovician continuous sedimentation. A noticeable volcanic activity is widespread in many of the sedimentary sequences. The lithostratigraphic succession followed in this study, focused on latest Ediacaran–early Ordovician times, is given in Fig. 6. From base to top, eleven units are distinguished: exposures of (1) the Grandmont Formation and (2) its overlying Rivernous Rhyolitic Complex are limited to the southeastern parautochthon sites; they are dated to latest Ediacaran, and the Ediacaran–Cambrian boundary interval, assuming a correlation with the "Schistes X" of the Axial Zone (Fournier-Vinas and Débat, 1970) dated at $545 \pm 15$ Ma by Pb isotope single zircon method (Lescuyer and Cocherie, 1992); they are overlain by the volcanosedimentary Layrac Formation; (3) the carbonate- and shale-bearing Marcou Formation has been recently dated to Terreneuvian (Devaere et al., 2013); (4) the siliciclastic Marcory Formation is widespread in the northern and southern Montagne Noire where it is dated at the Tommotian–Atdabanian interval (Álvaro et al., 1998; Álvaro and Vizcaïno, 1999), and includes thick basaltic flows known as the Ensèges Volcanic Complex; (5) the Pardailhan, Série Noire, and Lastours formations consist of carbonates and black shales dated from Atdabanian to Toyonian (Thoral, 1935; Courtessole, 1973; Donnot and Guérangé, 1978; Debrenne and Courjault-Radé, 1986); in the lower part, abundant volcanic units of mafic and acidic pyroclastic flows and deposits are distributed into two areas of the Brusque slice, namely the Moulergues-Lacan and Rocozels-Soubras volcanics; in the upper part, another basaltic activity is embedded, namely the Saint-Méen Volcanic Complex; (6) the siliciclastic Coulouma and Ferrals formations are dated to lower middle Cambrian (Bogdanoff et al., 1984; Tormo, 2002, 2003); (7) the thick pile of shales of the La Gardie Formation deposited during mid Cambrian times (Thoral, 1935; Tormo, 2003; Cohen and Tormo, 2006); (8) the Larroque Volcanic Formation is a thick (500–1000 m) and widespread package of porphyroclastic metarhyolites exposed from Albigeois to Rouergue (allochthonous in the former and parautochthonous in the latter; Fig. 5); this volcanic activity emplaced above the Furongian and the so-called "série schisto-gréseuse verte" (*sensu* Guérangé-Lozes et al., 1996; Guérangé-Lozes and Alabouvette, 1999) in the uppermost part of La Gardie Formation; (9) the Mendic metagranite intruded the Grandmont Formation and is suspected to be contemporaneous with the Larroque Volcanic Formation; (10) the La Dentelle Formation is a 15 m-thick quartz-sandstone stratigraphic marker; and (11) the Saint-Chinian and Albigeois formations are 500–1000 m-thick black shales dated to Tremadocian–Floian (Bogdanoff et al., 1984; Guéranjé-Lozes and Guérangé, 1991; Vizcaïno and Álvaro, 2001, 2003); the lower sedimentary pile of the latter includes numerous basaltic flows and sills referred to the Peyrebrune Volcanic Complex.

### 2.2.3. Southern Cévennes

In the Cévennes region, the lower Palaeozoic low-grade sedimentary series are stratigraphically equivalent to those of the Albigeois. They are considered as a single tectonostratigraphic entity, separated by Mesozoic and Cenozoic basins (Ledru et al., 1994), and named the Albigeois-Cévennes Unit. As in the northern Montagne Noire, the Albigeois-Cévennes Unit overthrusts to the south of the southern Cévennes area, equivalent of the Lacaune mountains (Marignac et al., 1980; Guérangé-Lozes, 1987). Various thrust slices have been described involving Cambrian units (Alabouvette, 1988). In the parautochthon, the lower sequence of sandstones and shales is a lateral equivalent of the Marcory Formation (Álvaro et al., 2010). It is overlain by shales and archaeocyatha-bearing limestones, Botoman in age and correlated with the Pardailhan Formation (Debrenne et al., 1976), and then by a thick stack of dolostones equivalent of the Lastours Formation and dated to the Botoman–Toyonian (late early Cambrian). The lower part of this stack contains interbedded acidic to mafic volcanosedimentary deposits and basaltic lava and pyroclastic flows: the Saint-Bresson Volcanic Complex (Verraes, 1979; Alabouvette, 1988).

**Table 5**

Selected chemical analyses of pyroxenes. Microprobe analyses using CAMECA SX 100 at the Camparis Analytical Laboratory of the University of Paris-VI, France.

| Volcanic formation | St-Méen volcanic complex | | | | | | | | St-Méen volcanic complex | | | | | | | | | |
| --- | --- | --- | --- | --- | --- | --- | --- | --- | --- | --- | --- | --- | --- | --- | --- | --- | --- | --- |
| Sample site | St-Méen sill | | | | | | | | Raffanel sill | | | | | | | | | |
| Sample# | Meen | | | | | | | | Raff | | | | | | | | | |
| Rock type | Metadolerite | | | | | | | | Metadolerite | | | | | | | | | |
| Major elements (wt.%) | | | | | | | | | | | | | | | | | | |
| $SiO_2$ | 53.51 | 53.73 | 52.84 | 52.43 | 51.93 | 52.17 | 51.90 | 51.65 | 52.79 | 52.83 | 52.40 | 52.06 | 52.47 | 52.90 | 53.21 | 52.68 | 53.11 | 51.49 |
| $TiO_2$ | 0.54 | 0.57 | 0.78 | 0.81 | 0.50 | 0.53 | 0.87 | 1.03 | 0.72 | 0.79 | 0.60 | 0.59 | 0.44 | 0.20 | 0.21 | 0.31 | 0.05 | 0.21 |
| $Al_2O_3$ | 1.28 | 1.40 | 2.17 | 2.52 | 1.92 | 1.58 | 1.70 | 1.72 | 1.31 | 1.51 | 1.25 | 2.20 | 0.67 | 0.54 | 0.61 | 0.38 | 0.24 | 1.63 |
| $FeO^t$ | 7.68 | 7.84 | 7.34 | 6.92 | 7.88 | 7.74 | 10.66 | 10.91 | 10.66 | 11.02 | 10.31 | 8.39 | 14.28 | 12.15 | 11.93 | 14.33 | 12.52 | 11.03 |
| $Cr_2O_3$ | 0.30 | 0.23 | 0.37 | 0.64 | 0.15 | 0.12 | 0.00 | 0.12 | 0.01 | 0.03 | 0.05 | 0.03 | 0.00 | 0.01 | 0.00 | 0.01 | 0.03 | 0.01 |
| MnO | 0.25 | 0.23 | 0.18 | 0.19 | 0.31 | 0.31 | 0.32 | 0.36 | 0.29 | 0.28 | 0.37 | 0.27 | 0.37 | 0.30 | 0.30 | 0.41 | 0.33 | 0.98 |
| MgO | 17.53 | 17.51 | 16.68 | 16.64 | 15.81 | 15.27 | 15.07 | 14.93 | 16.03 | 15.91 | 15.39 | 15.12 | 13.65 | 13.43 | 13.34 | 13.21 | 12.57 | 11.13 |
| CaO | 18.92 | 18.90 | 19.62 | 20.24 | 19.49 | 20.59 | 18.59 | 18.79 | 18.06 | 17.67 | 18.87 | 20.30 | 17.76 | 19.94 | 20.28 | 18.73 | 21.25 | 22.49 |
| $Na_2O$ | 0.21 | 0.23 | 0.20 | 0.30 | 0.25 | 0.23 | 0.28 | 0.38 | 0.38 | 0.41 | 0.42 | 0.24 | 0.56 | 0.40 | 0.55 | 0.59 | 0.34 | 0.37 |
| $K_2O$ | 0.00 | 0.00 | 0.00 | 0.01 | 0.02 | 0.01 | 0.01 | 0.01 | 0.00 | 0.01 | 0.01 | 0.02 | 0.01 | 0.03 | 0.00 | 0.01 | 0.01 | 0.00 |
| Total | 100.22 | 100.63 | 100.17 | 100.69 | 98.25 | 98.54 | 99.39 | 99.91 | 100.25 | 100.46 | 99.67 | 99.21 | 100.21 | 99.88 | 100.43 | 100.67 | 100.44 | 99.33 |
| | | | | | | | | | | | | | | | | | | |
| Mg% | 49.27 | 49.15 | 47.65 | 47.31 | 45.95 | 44.15 | 43.57 | 42.96 | 45.61 | 45.51 | 44.04 | 43.73 | 39.42 | 38.67 | 38.36 | 37.81 | 35.87 | 32.69 |
| $(Fe^t + Mn)\%$ | 12.51 | 12.71 | 12.05 | 11.34 | 13.35 | 13.06 | 17.81 | 18.19 | 17.48 | 18.15 | 17.16 | 14.06 | 23.73 | 20.10 | 19.72 | 23.67 | 20.56 | 19.82 |
| Ca% | 38.22 | 38.13 | 40.30 | 41.36 | 40.70 | 42.79 | 38.62 | 38.85 | 36.91 | 36.34 | 38.80 | 42.21 | 36.86 | 41.24 | 41.91 | 38.52 | 43.57 | 47.49 |

### 2.2.4. Mouthoumet massif (Corbières)

Finally, the Mouthoumet massif lies south of Montagne Noire and north of the North Pyrenean frontal thrust. It contains four tectonostratigraphic units, from east to west, the Serre de Quintillan, Félines-Palairac and Roc de Nitable thrust slices, and an unnamed parautochthon (Cornet, 1980; Bessière and Schulze, 1984; Bessière and Baudelot, 1988; Bessière et al., 1989; Berger et al., 1997). Mafic and acidic volcanic episodes are widespread in the various stratigraphic units dated from lower Ordovician to Carboniferous.

As in the case of the Pyrénées and Montagne Noire, the middle Ordovician is absent and its gap allows differentiation between a lower Ordovician sedimentary sequence and a para- to unconformable overlying upper Ordovician–Silurian sedimentary package (Álvaro et al., 2016). This package includes black shales that resemble those of the Albigeois and Vendean basins.

The most significant lower Ordovician volcanics consist of (1) a thick flow (ca. 100 m) of porphyritic metarhyolites in the sandstones of the parautochthon and dated to Tremadocian by acritachs (Cocchio, 1982), and (2) flows or sills of metarhyolites overlain by flows of metabasalts in the lower Ordovician shales and sandstones of the lower part of the Serre de Quintillan slice, in its western side and in the Davejean tectonic window. These lower Ordovician volcanics are referred to the Davejean Volcanic Group.

## 3. Magmatic composition of the Cambrian–early Ordovician volcanism

The volcanic products of the above-reported domains dated around the Cambrian and early Ordovician have been sampled for petrographical and geochemical studies. Particular attention was done to the residual magmatic pyroxenes for microprobe analyses. Some accurate chemical analyses from the literature are retained. A significant set of 56 new analyses was performed (GPS coordinates of the analysed samples in Table 3 and chemical analyses in Table 4). Major, trace, and rare earth elements were determined by inductively coupled plasma mass spectrometry (ICP-MS) at ACME-LABS in Canada and at the "Service d'Analyse des Roches et Minéraux du Centre de Recherches en Pétrographie et Géochimie" of Nancy in France. The microprobe mineral analyses were performed at the Camparis Analytical Laboratory of the University of Paris-VI in France. Selected analyses of pyroxenes are available in Table 5.

### 3.1. South Armorican Domain

Magmatic products of interest are located in the following areas from northeast to southwest: (1) Northern Structural Area (Cholet Basin), (2) Central Structural Zone (Montaigu Leptyno-Amphibolite Complex and Chantonnay Basin), (3) Intermediate Structural Zone (Les Essarts Complex and Saint-Martin-des-Noyers Unit), and (4) Western Structural Zone (La Roche-sur-Yon, La Chapelle-Hermier, Saint-Gilles and Bois-de-Céné units).

Only some magmatic units are accurately dated as Cambrian and lower Ordovician. The others are attributed to this time span based on stratigraphic data and structural correlations. For that reason, the magmatic formations are described following the above-reported tectonostratigraphic scheme, and not with chronological order. The accurate or suspected ages are discussed.

### 3.1.1. Cholet Basin

Although the volcano-plutonic rocks of the Cholet Basin are broadly dated as mid Cambrian (Thiéblemont et al., 2001), these volcanics postdate a sedimentary sequence also palaeontologically dated as mid Cambrian (Cavet et al., 1966), so they may be younger.

Major and some trace elements of magmatic interest were presented by Thiéblemont (1988) for 14 metagabbros and metadolerites, 22 metarhyolites and microgranites, and 6 intermediate rocks of the upper magmatic unit. No new analyses were done.

The mafic rocks are metamorphosed in the greenschist and amphibolite facies. Their composition is subalkaline basaltic. Most of these rocks are saturated olivine-basalts ($2.7 < Ol < 16.3$), one being slightly under-saturated ($Ne = 1.86$), and a few others over-saturated tholeiites ($0.1 < Qtz < 4.3$). According to the Mg number, ranging from 70.3 to 45.2, the basaltic rocks are primitive to fairly evolved, fitting with the light rare earth low to moderate values ($8.0$ ppm $< La < 21.8$ ppm). Only La to Tb rare earth elements were analysed except for one sample where Yb was determined. The chondrite normalized La/Tb ratios range from 1.1 to 3.0. Taking into account the profile trends and the Yb analysed sample, the chondrite normalized La/Yb ratios range from 1.4 to 3.7. The complete analysed sample displays a chondrite normalized $(La/Yb)_{NC}$ ratio of 3.0. These values indicate a weak rare earth element fractionation. The lithophile moderate enrichment is illustrated by averaged values of N-MORB-normalized ratio of $(Ta/La)_{NM} = 1.1$, $(Th/La)_{NM} = 2.6$, and $(Rb/La)_{NM} = 8.3$. In spite of the lack of some

| Post-Variscan dyke | | | | | | | | | | Peyrebrune volcanic complex | | | | | | | | | |
|---|---|---|---|---|---|---|---|---|---|---|---|---|---|---|---|---|---|---|---|
| Les Bayles | | | | | | | | | | Peyrebrune flow-sill | | | | | | | | | |
| Bay 1 | | | | | | | | | | Pey 6 | | | | | | | | | |
| Dolerite | | | | | | | | | | Metabasalt | | | | | | | | | |
| 47.83 | 47.13 | 47.45 | 46.62 | 46.64 | 45.82 | 42.36 | 41.59 | 40.09 | 40.17 | 53.02 | 52.48 | 49.63 | 50.74 | 50.33 | 49.95 | 50.26 | 49.16 | 49.05 | 50.67 |
| 2.59 | 2.70 | 2.78 | 3.12 | 3.06 | 3.21 | 4.75 | 4.87 | 5.36 | 5.44 | 0.73 | 0.68 | 1.32 | 1.18 | 1.36 | 1.57 | 1.22 | 1.71 | 2.02 | 1.20 |
| 5.69 | 6.62 | 6.61 | 7.11 | 6.97 | 7.19 | 10.49 | 10.74 | 11.70 | 12.65 | 1.78 | 2.07 | 5.03 | 4.41 | 4.20 | 4.62 | 4.04 | 4.52 | 4.03 | 1.85 |
| 6.21 | 6.53 | 6.69 | 7.21 | 7.36 | 7.65 | 7.24 | 7.78 | 7.83 | 8.50 | 7.34 | 6.60 | 7.46 | 7.37 | 8.23 | 9.27 | 8.66 | 8.93 | 12.96 | 14.74 |
| 0.35 | 0.05 | 0.04 | 0.00 | 0.08 | 0.04 | 0.14 | 0.00 | 0.13 | 0.05 | 0.18 | 0.29 | 0.78 | 0.30 | 0.05 | 0.09 | 0.16 | 0.23 | 0.00 | 0.02 |
| 0.09 | 0.13 | 0.21 | 0.09 | 0.13 | 0.15 | 0.10 | 0.13 | 0.08 | 0.18 | 0.16 | 0.20 | 0.18 | 0.13 | 0.23 | 0.30 | 0.21 | 0.24 | 0.32 | 0.49 |
| 13.78 | 13.34 | 12.92 | 12.53 | 12.49 | 12.46 | 10.71 | 10.70 | 10.45 | 9.78 | 17.15 | 16.62 | 15.45 | 14.84 | 15.09 | 14.99 | 14.83 | 14.80 | 12.40 | 12.21 |
| 23.26 | 23.55 | 23.62 | 23.50 | 23.61 | 23.43 | 23.62 | 23.43 | 23.45 | 23.57 | 20.14 | 21.01 | 19.88 | 20.60 | 20.36 | 19.66 | 20.11 | 20.02 | 19.54 | 18.78 |
| 0.27 | 0.35 | 0.39 | 0.40 | 0.42 | 0.38 | 0.44 | 0.46 | 0.42 | 0.53 | 0.26 | 0.32 | 0.32 | 0.32 | 0.28 | 0.31 | 0.36 | 0.32 | 0.47 | 0.25 |
| 0.00 | 0.00 | 0.03 | 0.01 | 0.03 | 0.00 | 0.03 | 0.02 | 0.02 | 0.02 | 0.01 | 0.00 | 0.00 | 0.00 | 0.00 | 0.00 | 0.00 | 0.00 | 0.01 | 0.00 |
| 100.09 | 100.41 | 100.73 | 100.60 | 100.80 | 100.34 | 99.88 | 99.72 | 99.54 | 100.88 | 100.76 | 100.28 | 100.06 | 99.88 | 100.14 | 100.76 | 99.86 | 99.92 | 100.80 | 100.21 |
| 40.49 | 39.24 | 38.26 | 37.39 | 37.10 | 36.99 | 33.69 | 33.46 | 32.93 | 30.95 | 47.87 | 46.76 | 45.40 | 43.83 | 43.77 | 43.46 | 43.28 | 43.11 | 36.58 | 35.64 |
| 10.40 | 10.99 | 11.46 | 12.21 | 12.49 | 13.00 | 12.94 | 13.87 | 13.97 | 15.42 | 11.74 | 10.74 | 12.61 | 12.43 | 13.78 | 15.57 | 14.53 | 14.98 | 21.98 | 24.95 |
| 49.11 | 49.78 | 50.28 | 50.40 | 50.40 | 50.01 | 53.37 | 52.67 | 53.10 | 53.63 | 40.39 | 42.50 | 42.00 | 43.74 | 42.45 | 40.97 | 42.19 | 41.91 | 41.44 | 39.41 |

key elements (Nb and heavy rare earth elements), the N-MORB-normalized element patterns of the Cholet metabasites are very similar to those of the Montaigu Leptyno-Amphibolite Complex (see the following section) (Fig. 7a). Both magmatic series are characterized by moderate lithophile element enrichment, no enrichment or slight Ta-Nb negative anomalies, and moderate Ti negative anomalies limited to the more evolved rocks. These features are characteristic of continental tholeiites shown by an averaged profile of Holm (1985) in Fig. 7. The continental tholeiite signature is illustrated in the Th-Tb-Ta ternary diagram of Cabanis and Thiéblemont (1988) (Fig. 8a).

The acidic rocks gather microgranular porphyritic, subaphyric and granophyric facies. They are foliated and partly recrystallized in a felsic assemblage of quartz, albite, microcline, muscovite and biotite. All these rocks display similar silica- and alkaline-rich compositions. They are moderately enriched in incompatible elements (La = 31.1 ± 9.2 ppm; Yb = 7.2 ± 2.3 ppm; La/Yb = 4.5 ± 1.2; Th = 13.7 ± 2.9 ppm; Hf = 10.4 ± 4.3 ppm; Ta = 1.3 ± 0.3 ppm). In the Q-Ab-Or diagram (Tuttle and Bowen, 1958 in Thiéblemont, 1988), the rhyolites and micrognanites plot close to the thermal eutectic for $P_{H_2O}$ of 0.5 to 1 kbar. According to the petrographical features, the micropegmatitic texture of microgranites and the perthitic texture of all the alkaline feldspars, and the chemical compositions consistent with anhydrous granitic eutectic, it can be concluded with Thiéblemont (1988) that the rhyolites and micropegmatites are crustal melts derived from low-pressure eutectic liquids. This genetic model is supported by the abundance of rhyolitic and granitic rocks compared with the low volume of mafic rocks that discards a genesis of the acidic magmas from evolving mafic magmas.

The intermediate volcano-plutonic rocks consist of foliated felsic rocks enriched in amphibole and biotite. They display $SiO_2$ values ranging from 54.2 to 66.2 wt.% and MgO from 7.6 to 1.2 wt.%. Similarly, La varies from 12.9 to 26.0 ppm, Rb from 29.2 to 106.0 ppm, Th from 6.7 to 9.9 ppm, Zr from 67 to 193 ppm, and Hf from 1.8 to 5.4 ppm, while Sr decreases from 645 to 92 ppm. Petrographical features suggest that these rocks are mixtures of mafic and acidic rocks, rather more than products of variously evolved magmas (Thiéblemont, 1988). This mixing process is illustrated in the Th-Tb-Ta diagram by the Th enrichment trend from microgabbros to rhyolites (Cabanis and Thiéblemont, 1988) (Fig. 8a). It is noticeable that the rhyolites display the same Th-Tb-Ta ratio than the averaged upper continental crust (UCC; Rudnick and Gao, 2004).

### 3.1.2. Montaigu Leptyno-Amphibolite Complex

The Montaigu Leptyno-Amphibolite Complex (MLAC) comprises a lower thick amphibolite pile and upper alternating amphibolites and leucocrate to mesocrate fine-grained and banded gneisses commonly named "leptynites". A broad Cambro–Ordovician age has been assumed. In the notice of the Montaigu geological map,
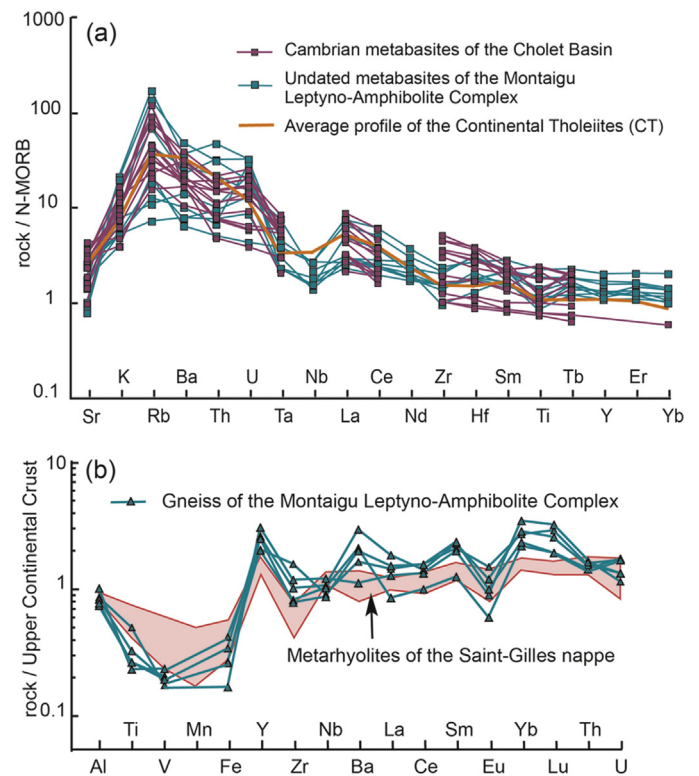


Figure 7. Normalized element diagrams. Analyses from Thiéblemont (1988) and Godard et al. (2010). (a) N-MORB normalized incompatible element diagram of metabasites of the Cholet Basin and the Montaigu Leptyno-Amphibolite Complex. Normalized values after Sun and McDonough (1989). CT, average composition of continental tholeiites after Holm (1985). (b) Upper continental crust normalized element diagram of gneisses of the Montaigu Leptyno-Amphibolite Complex. Comparison with the metarhyolites of the Saint-Gilles nappe (this work). Normalized values after Rudnick and Gao (2004); for abbreviations, see Fig. 5.
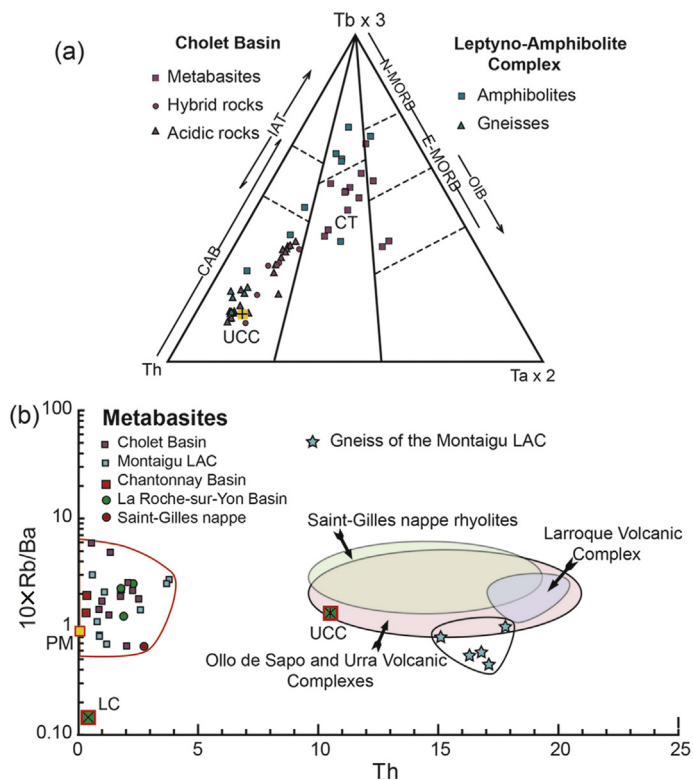
**Figure 8.** (a) Th-Tb-Ta diagram of the Cholet Basin and Montaigu Leptyno-Amphibolite Complex igneous rocks (diagram after Cabanis and Thiéblemont, 1988). Mixing process between continental tholeiitic magma and upper continental crust material. CT, continental tholeiite. UCC, upper continental crust after Rudnick and Gao (2004). (b) Th vs. Rb/Ba diagram of the gneisses from the Montaigu Leptyno-Amphibolite Complex (LAC). UCC, upper continental crust after Rudnick and Gao (2004). LC, lower continental crust after Weaver and Tarney (1984). This diagram discriminates the metabasites and the meta-acidic rocks by the Th enrichment. Compared to the composition of lower Palaeozoic rhyolites of the Variscan realm (Saint-Gilles nappe and Larroque Volcanic Complex of the South Armorican and Occitan domains in this work); compositional area of the Ollo de Sapo and Urra Volcanic formations in the Iberian Domain after Solá et al. (2008) and Díez Montes et al. (2010), the LAC gneisses show a lower Rb/Ba ratio due to low Rb and high Ba.

Godard et al. (2010) analysed 9 amphibolites and 5 gneisses. These data being accurate, no new analyses were done.

The amphibolites are foliated and metamorphosed in the epidote-amphibolite facies. Any residual magmatic textures or minerals are lacking. However, according to their setting in thick elongated massifs, the amphibolites could be former gabbros or basalts. These rocks are subalkaline basaltic in composition. In the normative nomenclature, most of the rocks are over-saturated tholeiites ($1.1 < Qtz < 8.0$) and some others saturated olivine-basalts ($9.6 < Ol < 17.6$). The Mg numbers ranging from 58.9 to 46.2 indicate a fairly evolved mafic magma. The rare earth elements display a weak enrichment with a chondrite normalized $(La/Yb)_{NC}$ ratio of $1.7 \pm 0.7$ for a La value of 5.7 to 18.5 ppm. The N-MORB normalized incompatible element patterns (Fig. 7a) show a lithophile element enrichment, except Sr and K, with $(Th/La)_{NM} = 4.6 \pm 2.5$, $(Rb/La)_{NM} = 11.8 \pm 10.3$, and $(Ba/La)_{NM} = 4.9 \pm 2.4$. However, Ta is not enriched, $(Ta/La)_{NM} = 1.1 \pm 0.6$ and Nb is relatively depleted, $(Nb/La)_{NM} = 0.6 \pm 0.2$. In addition, a moderate negative anomaly concerns the titanium ($Ti/Ti^* = 0.7 \pm 0.1$). These geochemical features (lithophile element enrichment, lack of Ta enrichment, and moderate Nb and Ti negative anomalies) are common in continental tholeiites (Holm, 1985). Orogenic calc-alkaline magmas have a similar lithophile enrichment, but with less Rb-enrichment, more important Ta-Nb negative anomalies

(andesites) or less rare earth element abundances (arc tholeiites) (Holm, 1985). In the Th-Tb-Ta diagram (Fig. 8a) amphibolites display a Th enrichment suggesting mixing with gneisses.

The gneisses have silica- and alkaline-rich compositions. They are ferroan, calc-alkalic and peraluminous in the classification of Frost et al. (2001). They are moderately enriched in incompatible elements, fractionated in light rare earth elements in showing a negative anomaly of Eu, and undepleted in the heavy rare earth elements (La = $43.2 \pm 11.3$ ppm; Yb = $5.3 \pm 1.0$ ppm; Th = $16.6 \pm 1.0$ ppm; Nb = $12.2 \pm 1.6$ ppm; La/Yb = $8.2 \pm 2.2$; Eu/Eu* = 0.3–0.4). Compared to the average composition of the upper continental crust (Rudnick and Gao, 2004), the gneisses display depletions in Ti, V, Fe, and Eu that may be explained by magmatic fractionation of oxides and plagioclase (Fig. 7b). Profiles are plotted with those of the neighbouring South Armorican rhyolites, e.g. the Saint-Gilles nappe. In the Th-Tb-Ta diagram (Fig. 8a), the gneisses are close to the acidic magmatic rocks of the Cholet Basin. But, compared to the composition of lower Palaeozoic rhyolites of the Variscan realm [Saint-Gilles nappe and Larroque Volcanic Formation of the South Armorican and Occitan domains in this work, and Ollo de Sapo and Urra volcanic formations in the Iberian Domain (Solá et al., 2008; Díez Montes et al., 2010)], the gneisses of the MLAC show a lower Rb/Ba ratio due to low Rb and high Ba (Fig. 8b), and high Yb and Y contents. Taking into account the very high silica content and the ferroan, calc-alkalic and peraluminous features, the gneisses look like former silty clay or volcano-sedimentary sediments instead of acidic lava.

### 3.1.3. Chantonnay Basin

A suspected synsedimentary magmatic activity is recorded in the lower Cambrian formations. It consists of scarce sills of metabasites and volcanosedimentary beds including mafic and acidic debris (Wyns et al., 1988; Bouton and Branger, 2007). No analytical data are available, not even from volcanic products of the neighbouring similar formations of the Haut-Bocage Basin (Wyns et al., 1988).

More significant volcanic activity is widespread in the Furongian formations with numerous sills and flow-sills of metabasites. Most of these sills are metre-sized in thickness, but there are some decametre-sized laccoliths (Fig. 3). Thick sills of rhyolites are set in the upper part of the formation. They are related to the overlying Tremadocian flows of the La Châtaigneraie Volcanic Formation (Table 2). Chemical analyses of major elements and a few minor elements are available from Thiéblemont (1988), namely eight metabasites and one rhyolite. Boyer (1974) analysed twelve rhyolites for the major elements. New and complete analyses were done for two samples of the Antigny mafic laccolith in the upper sequence of the Bourgneuf Formation (Ant, Fig. 3; samples Ant 1-3, Tables 3 and 4).

The metabasites are foliated and metamorphosed in the greenschist facies. Relics of doleritic texture are discernible in the centre of the thicker sills, with intersertal ordering of pseudomorphosed plagioclase and actinolite and with residual magmatic clinopyroxene in the core of phenoblastic amphibole. Chemical compositions of the new analyses are subalkaline to fairly alkaline. In the normative nomenclature, they range from tholeiites ($0.1 < Qtz < 3.5$) to olivine-basalts ($5.0 < Ol < 15.4$), one being slightly under-saturated (Ne = 1.1). According to the Mg number ranging from 67.2 to 49.9, the basaltic rocks are primitive to fairly evolved, in good agreement with the light rare earth low to moderate contents ($3.2 < La < 11.9$). Only La, Eu and Tb rare earth elements were analysed in the eight data from the literature. All the rare earth and incompatible trace elements are provided in the new analyses. The chondrite normalized La/Tb ratios range from 1.1 to 2.4 for the whole samples. The more complete analysed samples display a chondrite normalized La/Yb ratio of 1.1–1.7. Taking into account the profile trends for the Yb estimated values and the Yb analysed

values, the chondrite normalized La/Yb ratios range from 1.1 to 1.7 for the whole samples. These ratios indicate a lack of rare earth element fractionation. The lithophile moderate enrichment is expressed with averaged values of N-MORB-normalized ratio, $(Th/La)_{NM} = 2.9$, $(Rb/La)_{NM} = 27.1$, and $(Ba/La)_{NMB} = 13.3$. Ta and Nb display a moderate negative anomaly, $(Ta/La)_{NM} = 0.8$ and $(Nb/La)_{NM} = 0.7$. The N-MORB-normalized element patterns of the Chantonnay metabasites are similar to those of the amphibolites in the Montaigu Leptyno-Amphibolite Complex (Fig. 9a). Again, the geochemical fingerprints agree with a continental tholeiitic magma.

The rhyolites of the La Châtaigneraie Volcanic Formation show a felsitic groundmass including 15% to 30% of quartz and microcline phenocrysts. The magmatic texture is devitrified and fine-grained porphyritic or eutaxitic corresponding to thick lava flows and to ignimbritic flows. The metamorphism led to recrystallization of the groundmass in sodo-potassic feldspar, quartz and sericite. Close to St-Pierre-du-Chemin (Fig. 3), a rhyolitic body is elongated in a shear zone, severely mylonitized and finely recrystallized in quartz, sericite, chloritoid and pyrophyllite. The rock termed "pierre des plochères" has been worked in quarries for using in lime kiln because of its refractory property. We determined this rock as a "blaviérite" in the sense of Munier-Chalmas (1881-82).

Chemical composition is silica- and alkaline-rich with potassium overtopping sodium, though alkali contents may have been reduced by secondary leaching. $SiO_2$ ranges from 71 to 77 wt.%. $Na_2O$ averages 3 wt.% and $K_2O$ is 6 wt.%. Analyses of the "pierre des plochères" show a complete leaching of alkalies and secondary silica or alumina enrichments (Poncet and Bouton, 2010: Table 2). In the single analysis made for trace elements, lithophile elements are fairly enriched: Rb = 144 ppm, La = 44 ppm, Th = 13.7 ppm with values in the range of those of the Choletais rhyolites and gneisses of the Montaigu Leptyno-Amphibolite Complex.

### 3.1.4. Les Essarts Complex

The Les Essarts Complex is notorious for the abundance of eclogitic and peridotitic lenses enclosed in orthogneisses and paragneisses as a tectonic mélange. The Tremadocian orthogneiss (483 ± 4 Ma; Lahondère et al., 2009) is contemporaneous with the orthogneisses of Montaigu and Mervent, and with the rhyolites of the Chantonnay Basin and of the Saint-Gilles nappe.

The eclogites have been analysed for major elements and some minor elements by Montigny and Allègre (1974), Godard (1981, 1988), and Bernard-Griffiths and Cornichet (1985). Most of the eclogites show a tholeiitic composition with a light rare earth depletion in the chondrite-normalized diagram ($(La/Yb)_{NC} = 0.6-0.3$) indicating a depleted source and N-MORB signature. Some eclogites are enriched in Mg, Cr and Ni, but depleted in the whole rare earth elements with a Eu positive anomaly featuring a feldspar-olivine-pyroxene cumulative process. Some other eclogites are enriched in the light rare earth elements suggesting a different and enriched source ($(La/Yb)_{NC} = 4.5$).

For comparison, both types of eclogites are present in the Champtoceaux Complex with a flat chondrite normalized pattern ($(La/Yb)_{NC} = 1.4$; Bernard-Griffiths and Cornichet, 1985), or a fractionated pattern ($(La/Yb)_{NC} = 9.1$; Paquette et al., 1985). The eclogites of Limousin show a fractionated pattern ($(La/Yb)_{NC} = 4.1-4.7$; Bernard-Griffiths and Jahn, 1981).

### 3.1.5. Saint-Martin-des-Noyers Unit

Amphibolites and gneisses of the Saint-Martin-des-Noyers Unit have been analysed by Thiéblemont et al. (1987b) and Thiéblemont (1988) for major elements and some trace elements. We add two complete analyses of amphibolites (Smn 1 and 2, Fig. 3, Tables 3 and 4). The analyses are set in amphibolites, amphibole-bearing gneisses, and felsic gneisses.
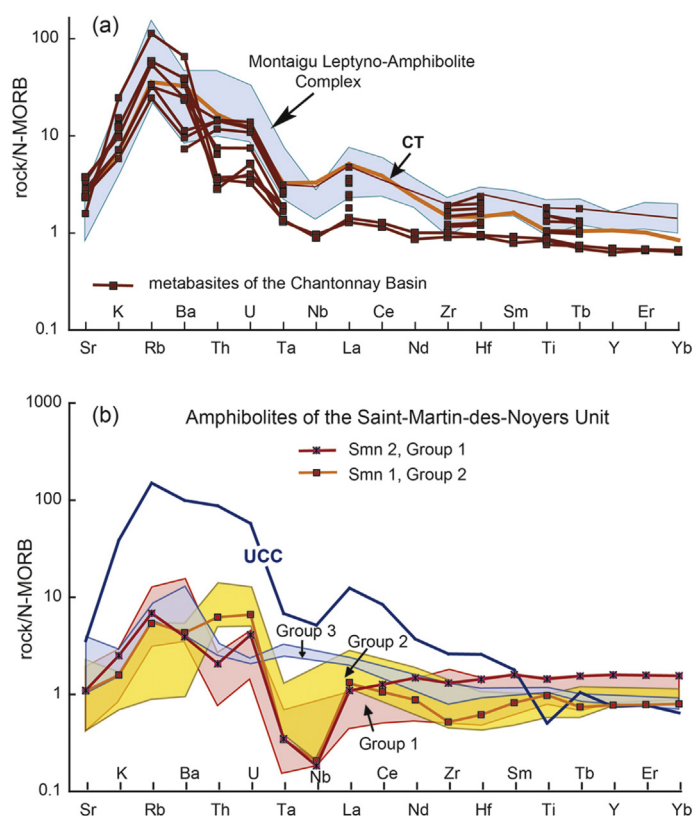


**Figure 9.** (a) N-MORB normalized incompatible element diagram of Furongian metabasites from the Chantonnay Basin. Normalized values after Sun and McDonough (1989). Partial analyses of Thiéblemont (1988) and complete analyses of this work (Ant 1 and 3). CT, average composition of continental tholeiites after Holm (1985). Comparison with the amphibolites of the Montaigu Leptyno-Amphibolite Complex (LAC, analyses of Godard et al., 2010) displays close similarities except a higher enrichment of Th and U in the LAC. (b) N-MORB normalized incompatible element diagram of metabasites of Saint-Martin-des-Noyers Unit. Magmatic groups of Thiéblemont et al. (1987b); Group 1, amphibolites of Pont-Charron (south of Chantonnay); Group 2, amphibolites of Petit-Lay (south-west of Chantonnay); Group 3, metadolerites of the Pont-Charron interbedded intrusion. New analyses have been done in the Pont-Charron site: Smn 2 belonging to Group 1, and to south-west Chantonnay: Smn 1 belonging to Group 2 and indicating that this site includes amphibolites of both groups 1 and 2. The Group 1 rocks are pure basaltic lavas depleted in the light rare earth elements and moderately enriched in the lithophile elements. The Group 2 rocks are basaltic lavas contaminated or mixed with sialic crustal material as shown by the UCC profile. The Group 3 metadolerites have different profiles with REE fractionation and the lack of Ta and Nb negative anomalies.

The amphibolites are either massive or banded with a granonematoblastic texture of hornblende, plagioclase, epidote, magnetite and garnet. Only few amphibolites display remains of doleritic texture of former magmatic plagioclase and clinopyroxene transformed to amphibole. All these mafic rocks can be termed metabasites having a chemical composition of subalkaline to fairly alkaline olivine basalts. The Mg number ranging from 64.7 to 38.9 shows that the rocks are primitive to evolved. The amphibole-bearing gneisses are intermediate in composition and may be considered as either evolved lavas or mixed volcanosediments. The gneisses are silicic and may have derived from sediments or acidic volcano-sediments.

Rare earth elements and some key incompatible elements (Rb, Sr, Zr, Ba, Hf, Ta, Th and U) were analysed in the data from the literature. Complete analytical data are given in the new analyses. Based on the trace element covariation diagrams, the metabasites are distributed into three groups as shown in the Hf vs. Ta diagram (Fig. 10a). The incompatible element patterns are illustrated in the N-MORB normalized diagram (Fig. 9b). Group 1 is depleted in the

light rare earth elements and Ta, and enriched in Rb and Ba. This group is located southwest and south of Chantonnay and includes the new analysed sample Smn2. Group 2 is very fairly enriched in light rare earth elements. The Ta depletion is moderate, but Th and U are greatly enriched. This group gathers the banded amphibolites located to the west of Chantonnay and includes the new sample Smn1. Group 3 is significantly enriched in light rare earth elements, Ta, Ba and Rb. It is limited to the doleritic metabasite forming a thick interbedded body in the amphibolites of SW-Chantonnay, and is interpreted as a lately intruded sill.

The magmatic chemical features are interpreted in the Ta/Tb vs. Th/Tb diagram (Fig. 10b). Group 1 takes place in the mantle array close to the depleted MORB mantle and derived from a depleted source. However, the lithophile enrichment suggests either a former and limited enrichment of this source, or a crustal contamination of the magma. This second explanation is retained for the Group 2 magma because of the high Th values placing the lavas in a trend from Group 1 composition to the upper continental crust composition (UCC). Mixing of the depleted magma with crustal material would explain the overall element enrichment from Group 1 to Group 2 rocks as shown by the UCC profile drawn in Fig. 9b. The simplest explanation would be that the banded amphibolites were formerly a volcanosedimentary material. Group 3 is enriched in all the elements and derived from a slightly enriched source very different to the depleted source of Group 1. Owing to the suspected intrusive setting of the doleritic meta-basites, Group 3 lavas are related to a second and distinct magmatic activity that resembles the continental tholeiite activity commonly present in the neighbouring lithostructural units. Concurrently, the Group 1 depleted source may be close to the depleted source of the eclogites though this latter source is only known by the rare earth element analyses in the eclogites.

The trace element contents and ratios of the felsic gneisses do not fit well with composition of acidic magmatic rocks. These gneisses are more probably of sedimentary origin and derived from clayey sandstones and shales with variable contribution of mafic volcano-clastic material as shown by the Ta/Tb vs. Th/Tb diagram (Fig. 10b).

### 3.1.6. La Roche-sur-Yon Unit

The volcanic products of the La Roche-sur-Yon Unit are limited to the Les Sables-d'Olonne Formation in the lower sequence of the basin dated to Tremadocian (Fig. 4, Table 2). They consist of meta-basalts and metarhyolites interbedded in shales and averaging some ten metres in thickness and some hundred metres in width, except a few km-sized rhyolitic massifs.

The metabasalts are moderately foliated and recrystallized in the greenschist facies. Relics of intersertal and intergranular doleritic textures are preserved with laths of plagioclase and sub-idiomorphic pyroxene transformed to amphibole. We selected samples in a 20 m-thick and 150 m-wide sill close to Talmont-Saint-Hilaire and far from the Variscan granite intrusives (TSH, Fig. 4; analyses Tsh 1, 2 and 3, Tables 3 and 4).

The metarhyolitic large bodies appear under two facies, either as porphyritic facies rich in phenocrysts of alkaline feldspars and quartz or as finely bedded aphyric facies, related to lava flows and to pyroclastic flows from an aerial or a shallow-water volcanic activity. The metamorphic effect led to crystallization of muscovite and quartz and to abundant silica impregnation. Due to the latter effect, no analysis was attempted.

The chemical composition of the metabasalt is subalkaline tholeiitic (Qtz = 3). The Mg number averaging 40.5 complies with an evolved magma. The rare earth elements are moderately fractionated (La = 16.7 ppm; $(La/Yb)_{NC}$ = 3.2) and the lithophile elements slightly enriched as shown by the averaged values of N-MORB-normalized ratio, $(Th/La)_{NM}$ = 2.5 and $(Rb/La)_{NM}$ = 2.1
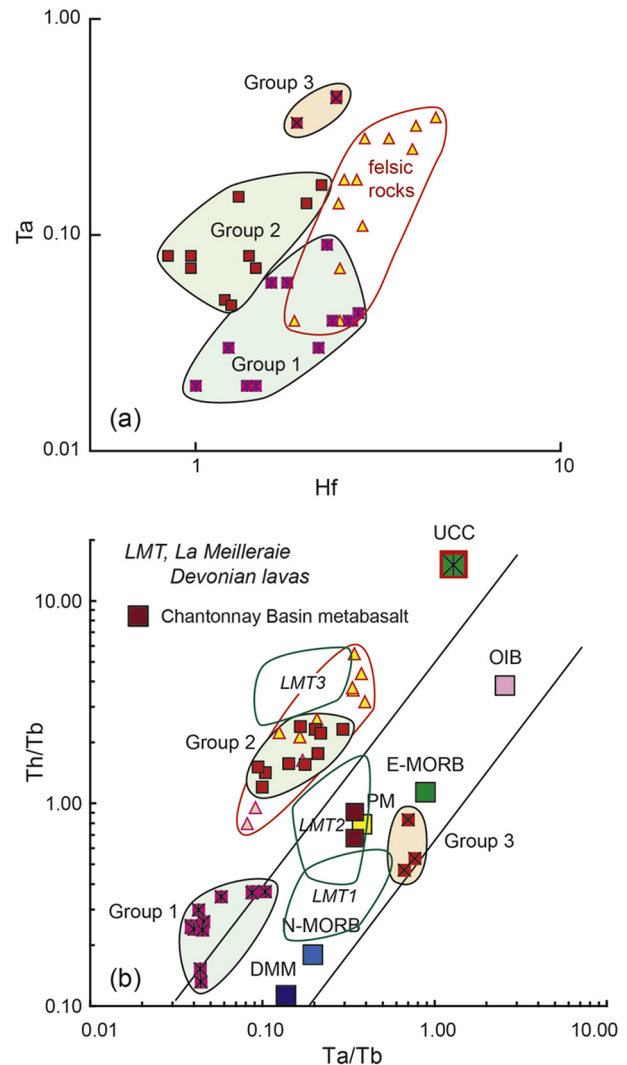


**Figure 10.** (a) Hf vs. Ta diagram for the Saint-Martin-des-Noyers amphibolitic groups. Note depletion of Group 1 and enrichment of Group 3. (b) Ta/Tb vs. Th/Tb diagram for the Saint-Martin-des-Noyers amphibolitic groups compared to the Devonian La Meilleraie metatholeiites of the Chantonnay Basin. DMM, depleted MORB mantle after Workman and Hart (2005). N-MORB, PM (primitive mantle), E-MORB and OIB (oceanic island basalt) after Sun and McDonough (1989). UCC after Rudnick and Gao (2004). Group 1 originated from a depleted source and Group 3 from an undepleted source. Group 2 was probably contaminated by crust material. LMT1, 2 and 3 areas: La Meilleraie Devonian basalts after analyses of Thiéblemont (1988), see text in Section 4.1.

(Fig. 11). Ta and Nb display an insignificant weak negative anomaly, $(Ta/La)_{NM}$ = 0.9 and $(Nb/La)_{NM}$ = 0.9. The normalized profiles are close to the averaged continental tholeiitic pattern (CT), and more precisely to the initial rift tholeiite pattern (IRT), as illustrated by the Ti-Nb-Th diagram of Holm (1985) (Fig. 12a). The IRT composition is explained by a mixed source from lithospheric and asthenospheric mantles. This mixing process implied upwelling of hot asthenospheric material that induced lithosphere thinning and mantle melting, in the case of intracontinental rift initiation. Unless the asthenospheric contribution, the magmatic composition of the metabasalt resembles that of the mafic rocks of the regional tectonostratigraphic units: the Chantonay and Cholet Basin meta-basites, and the MLAC amphibolites (Fig. 12b).

In the Ta/Yb vs. Th/Yb diagram (Fig. 13a), the metatholeiite plots in the mantle array between E-MORB and OIB and are clearly related to an enriched source. The La/Yb and Sm/Yb values and the lack of heavy rare earth element depletion comply with a mantle

source of spinel lherzolite. Batch melting calculations using rare earth elements give a partial melting degree averaging $15 \pm 5\%$. It is concluded that the metatholeiite of the La Roche-sur-Yon Basin resulted from partial melting of a continental lithosphere that was probably thinned owing to the high degree of melting and the contribution of the asthenospheric component.

### 3.1.7. La Chapelle-Hermier, Saint-Gilles-sur-Vie, and Mareuil-sur-Lay units

The La Chapelle-Hermier Unit slices, the lower part of the Saint-Gilles nappe (La Sauzaie Volcanic Formation), and the Mareuil nappe consist of rhyolitic lavas sharing similar petrographical features and ages. Dated and analysed by Béchennec et al. (2008, 2010) and Ballèvre et al. (2012), they consist of subvolcanic plugs and of subaerial lava and pyroclastic flows of porphyritic and aphyric rhyodacites and rhyolites. From the published data, we retained a set of fourteen analyses of major and trace elements. The data being accurate, no new analyses were done. $SiO_2$ ranges from 67.1 to 77.6 wt.%, $Na_2O$ from 0.3 to 3.3 wt.% and $K_2O$ from 4.6 to 9.8 wt.%. The lowest alkali contents can be due to secondary leaching. In spite of this effect, rhyolites are alkali-calcic in the nomenclature of Frost et al. (2001). The $Al_2O_3/(CaO + Na_2O + K_2O)$ mole ratio is peraluminous (1.1–2.0). The rare earth elements are moderately abundant (22 ppm < La < 39 ppm) and fractionated (chondrite normalized ratio: $5.5 < (La/Yb)_{NC} < 15.4$), with increasing values from dacites to rhyolites. The $Eu/Eu^*$ negative anomaly varies from 0.6 to 0.2, from rhyodacites to rhyolites. Trace element compositions are close to that of the upper continental crust (UCC) (Rudnick and Gao, 2004), except depletion of Ti, Fe and Mn explained by oxide and Ti-bearing phase fractionation. Negative anomalies of Zr and Eu suggest zircon and feldspar fractionations (Fig. 14a). The result of these fractionations is illustrated in the Zr/Hf vs. Nb/Ta diagram according to experimental studies of Linnen and Keppler (2002) concerning the zircon fractionation in peraluminous melts and the data of Pfänder et al. (2007) (Fig. 13b).

Acidic, peraluminous and potassium-rich characters together with the rare earth and trace element patterns are typical of S-type peraluminous granites. These rhyolitic rocks possibly derived from melting of crustal material according to experimental studies Patiño-Duce and Johnson, 1991; Patiño-Duce and Beard, 1995). A peraluminous and potassic shale or metamorphic equivalent is the best candidate. The crustal origin for the rhyolites is also supported by the abundance of inherited zircons dated around 600 Ma and between 1.8 and 2.6 Ga (Béchennec et al., 2008, 2010).

The metabasites capping the rhyolites of the second volcanic sequence are recrystallized in a planar fabric of fine granular
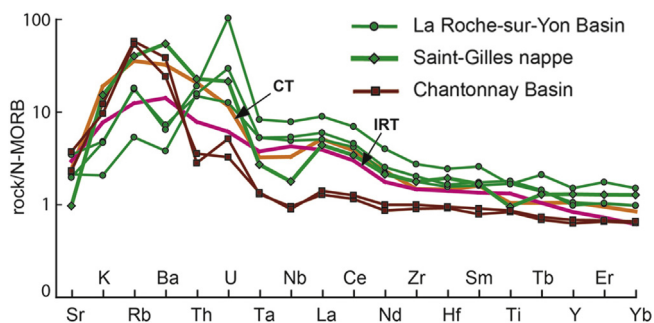


**Figure 11.** N-MORB normalized incompatible element diagram of Tremadocian metabasites of the La Roche-sur-Yon Basin (Tsh) and Saint-Gilles nappe (Lfr). The La Roche-sur-Yon metatholeiites have features of initial rift tholeiites (IRT) whilst the Saint-Gilles mafic lava is close to continental tholeiites (CT). Metabasites of the Chantonnay Basin (Ant 1 and 3) are plotted for comparison as they show typical CT profiles. IRT and CT after Holm (1985) and Pouclet et al. (1995).
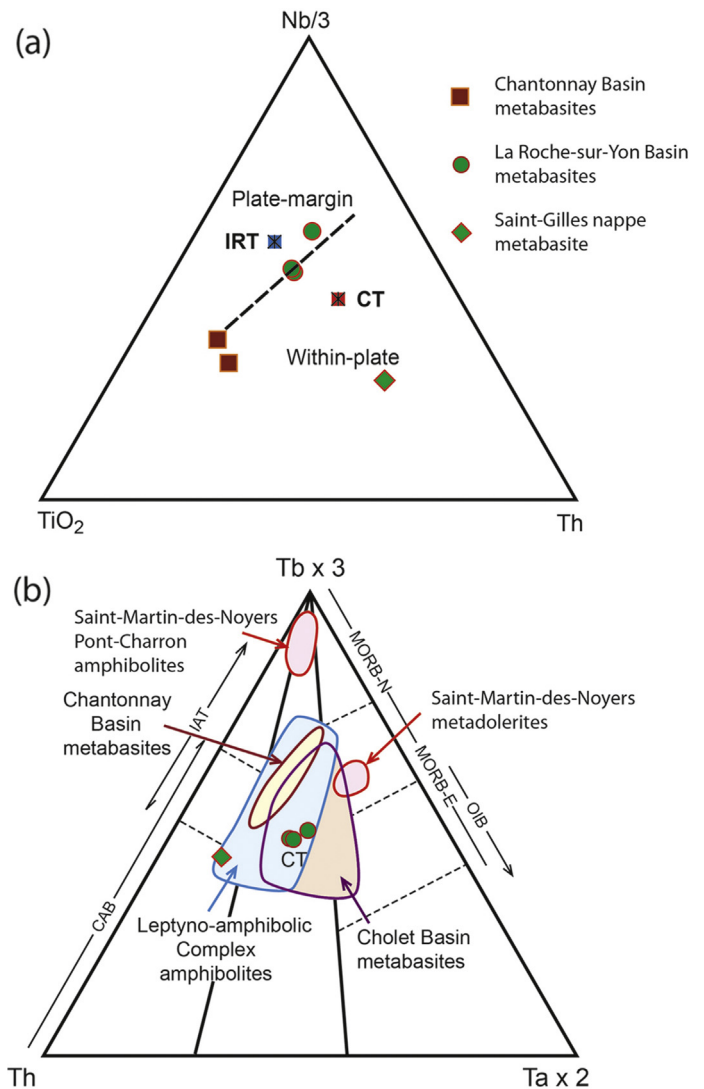




**Figure 12.** (a) Ti-Nb-Th diagram of Holm (1985) for distinguishing tholeiites from plate-margin (La Roche-sur-Yon metatholeiites) and within-plate (Saint-Gilles metabasite). (b) Th-Tb-Ta diagram of the La Roche-sur-Yon and Saint-Gilles metabasites compared to those of the neighbouring South Armorican units. Most of the mafic rocks plot in the continental tholeiite compositional area except the Pont-Charron amphibolites that are close to the N-MORB composition.

actinolite, epidote, chlorite, albite and quartz, as a consequence of thrust shearing. One sample of the Le Fenouiller volcanic Member has been analysed (Lf, Fig. 2). The composition is subalkaline ($SiO_2$ = 55.6 wt.%; $TiO_2$ = 1.2 wt.%; MgO = 5.5 wt.%; $Na_2O$ = 5.0 wt.%; $K_2O$ = 1.1 wt.%) though albitization is suspected. In the normative nomenclature, the lava is a tholeiite (Qtz = 2). The Mg number of 54.6 corresponds to a slightly evolved magma. The rare earth element contents are low and very moderately fractionated (La = 11.1 ppm; $(La/Yb)_{NC}$ = 1.9) with slight Eu negative anomaly ($Eu/Eu^*$ = 0.6). The N-MORB normalized diagram shows a clear enrichment of the lithophile elements: $(Th/La)_{NMB}$ = 5.2, $(Rb/La)_{NMB}$ = 9.2 and $(Ba/La)_{NMB}$ = 12.4 (Fig. 11). Ti, Ta and Nb display moderate negative anomalies: $Ti/Ti^*$ = 0.6, $(Ta/La)_{NMB}$ = 0.6 and $(Nb/La)_{NMB}$ = 0.4. The normalized profile mimics that of the averaged continental tholeiite (CT). Taking into account a weak Th-enrichment possibly due to crustal contamination, the Saint-Gilles nappe metabasalt is close to the mafic rocks of the regional tectonostratigraphic units: Chantonay and Cholet Basin metabasites, and MLAC amphibolites (Figs. 12b and 13a).
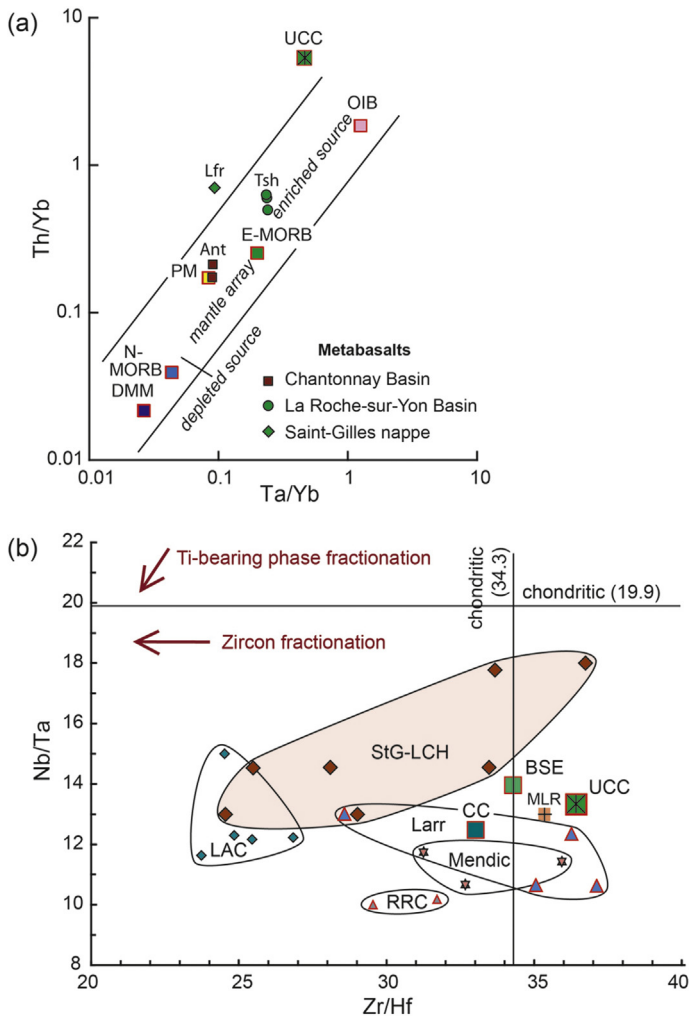
**Figure 13.** (a) Ta/Yb vs. Th/Yb diagram of the Tremadocian La Roche-sur-Yon and Saint-Gilles metabasites showing a magmatic origin from an enriched mantle source. Comparison with the Chantonnay Basin. (b) Zr/Hf vs. Nb/Ta diagram for the Saint-Gilles, Mareuil-sur-Lay and La Chapelle-Hermier Tremadocian metarhyolites. Fractionation of both Ti-bearing phase and zircon is suspected in a peraluminous melt. Comparison with meta-acidic rocks of the Montaigu Leptyno-Amphibolite Complex (LAC), Rivernous Complex (RRC), Larroque Unit (Larr), Mendic pluton, and Montjoi-Quintillan (MLR) dominated by zircon fractionation. BSE, bulk silicate earth and CC, continental crust as in Pfänder et al. (2007).



**Figure 14.** Upper continental crust (UCC) normalized element diagrams of the meta-acidic rocks of the La Chapelle-Hermier slices, Saint-Gilles and Mareuil nappes (analyses from Béchennec et al., 2008, 2010) (a), and of the Occitan Domain (b and c). Normalized values after Rudnick and Gao (2004). Ti, Cr, Mn, and Fe depletions mainly resulted from oxide fractionations. The incompatible element profiles are close to UCC taking into account Zr-Hf and Eu negative anomalies due to zircon and feldspar fractionations, respectively. Light rare earth element depletions in the Rivernous metarhyolites and particularly the Murat-sur-Vèbre one and in the Mendic metamicrogranite are explained by apatite and/or allanite fractionation.

### 3.1.8. Bois-de-Céné klippe

Interbedded metabasites of the Bois-de-Céné klippe are highly altered and impregnated with calcite. No analysis can be done. It is impossible to decipher the initial petrographical composition.

### 3.2. Limousin and Occitan Domain

In the Limousin and Occitan Domain of the Massif Central, the magmatic products consist of abundant volcanic rocks distributed in lower Palaeozoic sedimentary basins. The synsedimentary volcanic activities are only dated by their chronostratigraphic position. We can then describe the volcanics following a chronological succession and organizing them in volcanic complexes.

Many petrographical and geochemical studies have been done for these rocks (e.g. Durand and Gagny, 1966; Boyer, 1974; Prian, 1980; Gachet, 1983; Alsac et al., 1987; Guérangé-Lozes, 1987; Béziat et al., 1992; Pin and Marini, 1993). As a general rule, the chemical data were limited to major elements and a short selection of trace elements and many samples are not carefully localized.

Consequently, no accurate data have been retained from the literature. For that reason, an important set of new and complete analyses has been obtained from a thorough sampling (Fig. 5; Tables 3 and 4).

### 3.2.1. Rivernous Rhyolitic Complex

The Rivernous Rhyolitic Complex was emplaced in the Ediacaran–Cambrian boundary interval between the Grandmont and Layrac formations (Fig. 6). The rhyolites are historically known as "blaviérites" (Bergeron, 1888). This term, coined by Munier-Chalmas (1881-82), is applied to slaty silicic and sericite-rich rocks that are refractory, easy to carve in brick-shape and traditionally used for lime or brick kiln. Bergeron (1888) correctly used the term "blaviérite" for very fine-grained micaceous talcschists located in fault zones close to rhyolitic bodies that he named "porphyroïdes". Unfortunately, the following authors wrongly used the term "blaviérite" for the whole rhyolite formations by neglecting or ignoring the right determination. Earliest petrographical examination proved that blaviérites are metarhyolites (de Lapparent, 1909) severely mylonitized and totally recrystallized in quartz, sericite, paragonite

and pyrophyllite (explaining the refractory property) in a planar fabric. The ultramylonitic features defining the blaviérites were highlighted in the Tremadocian and Tournaisian blaviérites of the Armorican Massif by Klein and Trichet (1968). These rocks occur in shear zone corridors across or along rhyolitic bodies. Ordinary Rivernous rhyolites are moderately deformed with a fracture cleavage and do not comply with the original blaviérite mineralogical and tectonic definition, except in limited fault zones.

Three rhyolites have been analysed from (1) the Layrac summit, (2) the stratotype (LOD) at the Rivernous rivulet, both in the Avène-Mendic Unit, and (3) the Murat-sur-Vèbre area (Bl, Ld, Mu, Fig. 5). The composition is silica-rich (68.7 wt.% < $SiO_2$ < 77.0 wt.%) and alkali-potassic (0.6 wt.% < $Na_2O$ < 2.8 wt.%; 4.1 wt.% < $K_2O$ < 6.0 wt.%). The $Al_2O_3$/(CaO + $Na_2O$ + $K_2O$) mole ratio (A/CNK) is peraluminous (1.3–2.6). Acidic, peraluminous and potassium-rich characters may be related to S-type peraluminous granitic melt.

In the Layrac and Rivernous stratotype rhyolites, the rare earth elements are moderately abundant (14.5 ppm < La < 18.9 ppm) and fractionated (chondrite normalized ratio: 4.2 < $(La/Yb)_{NC}$ < 5.8) with Eu negative anomalies (0.24 < $Eu/Eu^*$ < 0.40). Compared with the upper continental crust (UCC), the light rare earth elements (LREE) are depleted (0.38 < $(La/Ta)_{UCC}$ < 0.40) (Fig. 14b). As commonly recorded in rhyolites, depletion of Ti, V, Fe and Mn are due to oxide fractionation. Negative anomalies of Zr and Eu suggest zircon and feldspar fractionations, respectively. Depletion of the light rare earth elements (LREE) can be due to apatite and/or allanite fractionation according to their mineral/melt distribution coefficients in acidic rocks (Henderson, 1984). Fractionation is particularly important in the Murat-sur-Vèbre rhyolite with high LREE depletion (La = 4.7 ppm; $(La/Yb)_{NC}$ = 3.2).

Compared with the Ordovician rhyolites, the Rivernous Complex rhyolites are discriminated by higher Rb/Ba ratios.

### 3.2.2. Ensèges and Moulergues Volcanic Complexes

The Ensèges and Moulergues Volcanic Complexes comprise the lower Ensèges mafic lava pile and the upper Moulergues mafic to acidic lava and volcaniclastic counterpart.

*The Ensèges lava pile* conformably underlies the Atdabanian–Botoman Pardailhan Formation in the northern part of the Brusque slice (En, Fig. 5). It consists of a ca. 300 m thick basaltic under-water pyroclastic flow pile exposed along a 10 km-long outcrop (Gachet, 1983). Lava outpouring occurred on a steep slope that explains the fragmentation of the quenched lava. Gravity driven aggregation of plastic debris produced decimetre-sized subrounded loaves. The highly brecciated rock is a mixture of angular fragments of vitreous to microlitic lava with plagioclase phenocrysts (An 74-80), partly transformed to albite and pyroxene transformed to actinolite. The lava was palagonitized and locally spilitized with recrystallization of epidote, actinolite, albite and calcite. Quartz and feldspar xenoliths are abundant.

Two samples were selected for analyses from the middle part of the flow pile (Ens 1 and 2, Table 4). The chemical composition is subalkaline (44.3 wt.% < $SiO_2$ < 44.6 wt.%; 0.8 wt.% < $TiO_2$ < 0.9 wt.%; 12.9 wt.% < MgO < 14.6 wt.%; 1.9 wt.% < $Na_2O$ < 3.5 wt.%; 0.3 wt.% < $K_2O$ < 0.8 wt.%). The high Mg number averaging 75 and the high MgO, Cr and Ni contents (Cr = 240 ppm; Ni = 140 ppm) are features of an olivine-pyroxene cumulate lava. But the rock is greatly altered (LOI = 6), and no residual olivine can be discerned. In the normative nomenclature, the lava is saturated (Qtz = 0), rich in olivine and hypersthene (Ol = 16–26; Hy = 12–30), and thus determined as an olivine-tholeiite. The rare earth elements (REE) are poor (La = 1.5 ppm) and depleted in the LREE (La/Yb = 0.69; $(La/Yb)_{NC}$ = 0.47). However, the lithophile elements are enriched as shown by the averaged values of N-MORB-normalized ratio ($(Th/La)_{NM}$ = 2.1; $(Rb/La)_{NM}$ = 31–71; $(Ba/La)_{NM}$ = 12.7)

(Fig. 15a). There are no significant Nb and Ta anomalies compared to N-MORB.

The REE pattern is that of the N-MORB and implies a depleted mantle source, as it is also documented in the Ta/Yb vs. Th/Yb diagram (Fig. 16a). The lithophile element enrichment suggests a magmatic calc-alkaline affinity. But, compared with the average pattern of the island arc tholeiites, the N-MORB normalized profiles of the Ensèges tholeiite show a lack of Nb-Ta anomalies and a distinct enrichment of Rb. This latter feature can be properly explained by a crustal contribution as shown by the upper crust continental average composition (Rudnick and Gao, 2004) (UCC, Fig. 15b). Although the lava includes quartz and feldspar xenolithic fragments that are not easy to eliminate in the sample preparation, the major element composition is not really modified by mechanical contamination of felsic material. The crustal contamination only concerns the mobile lithophile elements that are commonly transported by volatile phases. It is thus inferred that the tholeiitic magma was contaminated by volatile transfer during the crustal passage.

*The Moulergues Complex* overlies the Ensèges flows in two neighbouring areas of the Brusque slice: the Moulergues-Lacan subcomplex to the southwest and the Rocozels-Soubras subcomplex to the northeast (Lc, Bg, Kb, Fig. 5) (Guérangé-Lozes and Guérangé, 1990; Álvaro et al., 2014a). Both subcomplexes are encased in the lower part of the Pardailhan Formation dated to the Atdabanian–Botoman transition (Álvaro et al., 1998).

The basal part is made of volcaniclastic deposits of basaltic and rhyolitic composition (20–40 m) followed by an alternation of basaltic lava and pyroclastic flows, basaltic and rhyolitic breccias, detrital volcanosedimentary layers, and dolostone/shale interbeds (100–200 m thick). The upper part is a thick outpouring of quartz- and albite-rich rhyolitic breccias overlain by a felsic tephra layer (ca. 100 m). The mafic component is common in the Moulergues-Lacan sector, but rare in the Rocozels-Soubras sector.

The mafic lava flows are hyalo-microlitic with more or less abundant feldspar phenocrysts. Most of the flows are auto-brecciated and invaded by quartz and sodic feldspar angular fragments of various sizes. The acidic lavas are rich in quartz and albite phenocrysts. All the lavas are highly spilitized and display albito-phyre or keratophyre facies.

Two basaltic rocks were analysed in lava flows of the Lacan area (Lacan 1 and 3, Table 4). The chemical composition is subalkaline (43.5 wt.% < $SiO_2$ < 44.6 wt.%; 0.8 wt.% < $TiO_2$ < 0.9 wt.%; 11.6 wt.% < MgO < 12.9 wt.%; 2.7 wt.% < $Na_2O$ < 3.8 wt.%; 0.6 wt.% < $K_2O$ < 2.6 wt.%). The high Mg number averaging 73 and the high MgO, Cr and Ni contents (Cr = 277 ppm; Ni = 175 ppm) indicate a cumulate facies. The rock is highly altered (LOI = 6.5), and no residual olivine was observed. In the normative nomenclature, the lava is saturated (Qtz = 0), rich in olivine and hypersthene (Ol = 24%; Hy = 13%), and thus determined as an olivine-basalt close to an olivine-tholeiite. The rare earth elements (REE) are poor (La = 1.2–1.9 ppm) and depleted in the LREE (La/Yb = 0.6–1; $(La/Yb)_{NC}$ = 0.4–0.7). However, the lithophile elements are enriched as shown by the averaged values of N-MORB-normalized ratio ($(Th/La)_{NM}$ = 2.6–3.3; $(Rb/La)_{NM}$ = 64–101; $(Ba/La)_{NM}$ = 105–120) (Fig. 15a). There are no significant Nb and Ta anomalies compared to N-MORB. The whole chemical features are strictly similar to those of the Ensèges lavas assuming the same scenario, that of magma tapping a depleted mantle source (Fig. 16a), enriched in mobile lithophile elements from the crust.

Associated pyroclastic and volcanosedimentary brecciated rocks have been analysed in three samples. Due to the felsic component, silica and alumina are moderately enriched, and magnesia depleted ($SiO_2$ = 54–62 wt.%; $Al_2O_3$ = 16–20 wt.%; MgO = 1.1–3.3 wt.%). The spilitization effect caused anomalous enrichment in $Na_2O$ (7–8 wt.%) and leaching of CaO and $K_2O$. The minor element
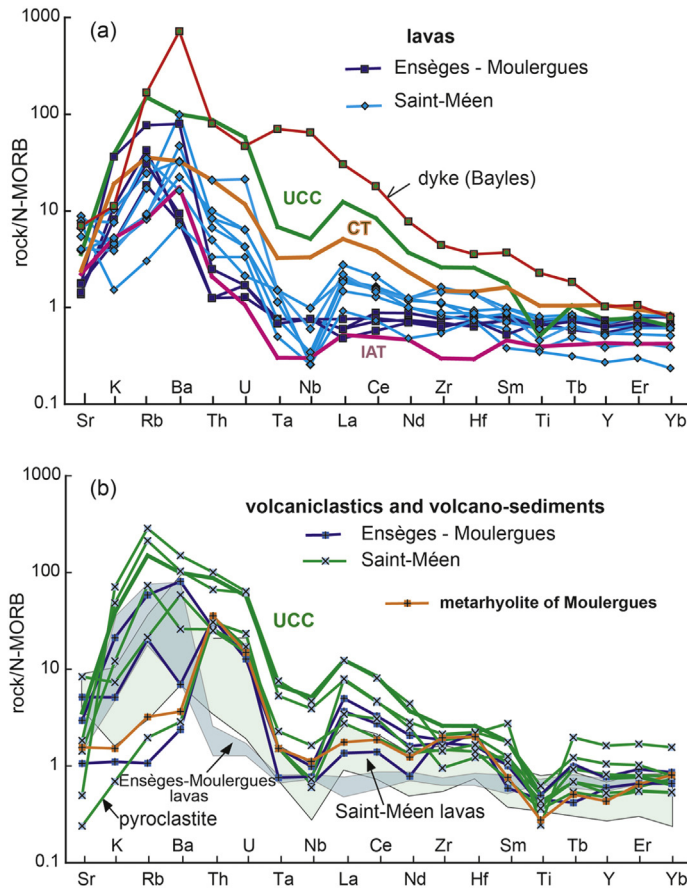
**Figure 15.** N-MORB normalized incompatible element diagrams of the metabasaltic and metadoleritic lavas (a) and of the metavolcaniclastics and volcanosediments (epiclastites) (b) of the Ensèges-Moulergues and Saint-Méen Volcanic Complexes. Island arc tholeiites (IAT) and continental tholeiites (CT) average profiles after Holm (1985). Upper continental crust (UCC) after Rudnick and Gao (2004). Note the different and OIB-like profile of the dolerite of the Bayles dyke originated to a post-Variscan continental fracturing event.

contents recorded the felsic contribution with enrichment in LILE and lithophile elements, but not in Nb and Ti (Fig. 15b). The mafic lavas, volcanosediments and rhyolites are discriminated in the Th vs. Rb/Ba diagram (Fig. 17) due to the positive correlation between Th and Rb enrichments. The volcanosediments properly plot between the mafic lavas and the felsic rocks.

The rhyolite of a brecciated dyke displays a keratophyric facies rich in quartz and albite ($SiO_2$ = 74.5 wt.%; $Na_2O$ = 6.7 wt.%). The A/CNK mole ratio is peraluminous (1.1). The trace elements are moderately enriched except Th and U indicating crustal contribution (Fig. 16a, b). The Ti negative anomaly can be explained by oxide fractionation. Owing to the spilitization effect, with leaching of the mobile elements, it is not possible to decipher about the acidic magma source.

### 3.2.3. Saint-Méen Volcanic Complex

Abundant volcanic products are interbedded in the Série Noire Formation from the central part to the southwesternmost Merdelou slice and in the northeastern corner of the Barre-Peux slice (Cd, Cf, Dg, La, LB, Lb, Mm, Mon, Po, Rf, Sm, Fig. 5) (Gachet, 1983; Guérangé-Lozes and Guérangé, 1990; Alsac, 1991; Béziat et al., 1992; Demange et al., 1995; Guérangé-Lozes and Alabouvette, 1999; Álvaro et al., 2014a). Consequently, renewal of the volcanic activity took place in the latest early Cambrian (Botoman–Toyonian).

The volcanic succession is composed of a basal thick deposit of volcanic and sedimentary breccia mingling mafic and felsic
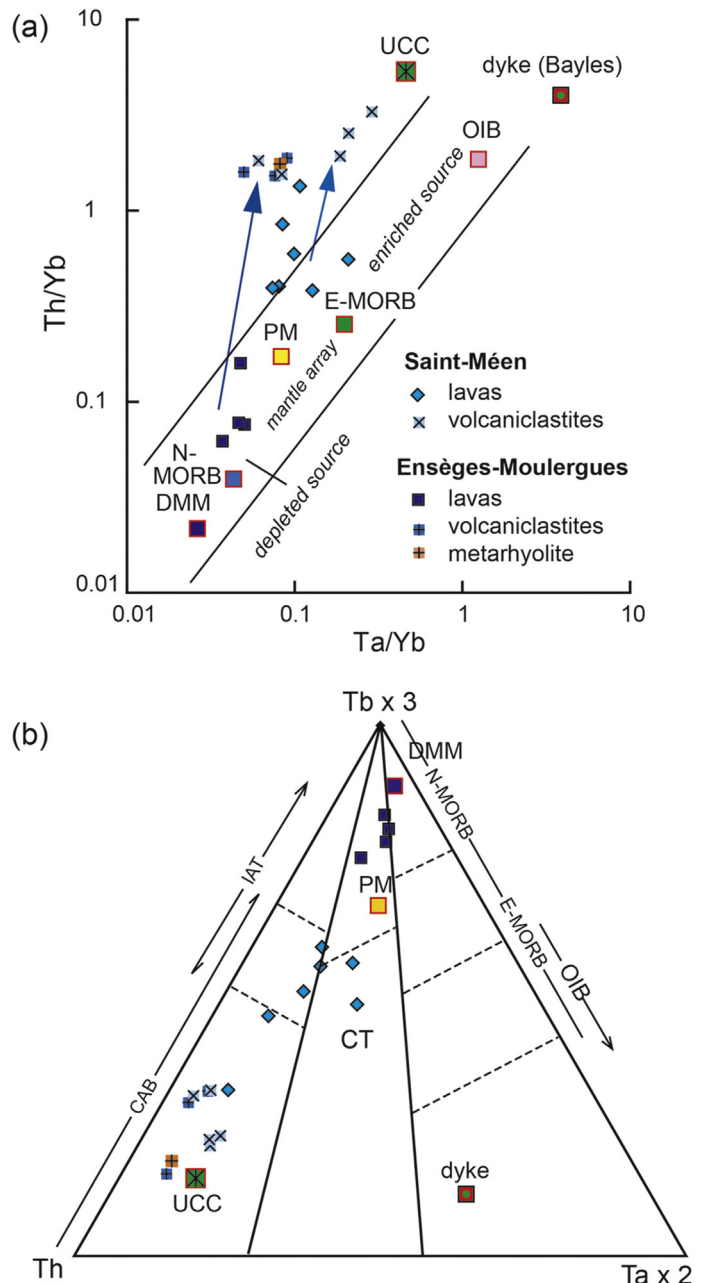


**Figure 16.** (a) Ta/Yb vs. Th/Yb and (b)Th-Tb-Ta diagrams of the Ensèges-Moulergues and Saint-Méen Volcanic Complexes. PM, primitive mantle after Sun and McDonough (1989). DMM, depleted MORB mantle after Workman and Hart (2005). The Ensèges and Moulergues magmas derived from a source intermediate between the depleted N-MORB source and the primitive mantle undepleted source. The Saint-Méen magma derived from an undepleted or weakly enriched source. The volcaniclastic and volcanosedimentary rocks were more or less contaminated by crustal components. The dolerite of the Bayles dyke derived from a very different and enriched source.

pyroclastites, commonly transformed to albitophyres and keratophyres (ca. 100 m). The following is an alternation of dolostone layers and volcanic material consisting of lava and pyroclastic flows and brecciated tephra deposits of mafic and felsic compositions (200–300 m). In the middle to upper parts of the sequence, numerous mafic sills are conformably interbedded, notwithstanding local tectonic disconformities. They recorded the same deformation and metamorphism than the encasing sediments. Their thickness ranges from 10 to ca. 100 m, and their length from 50 m to 4 km. The rock is massive and doleritic in texture. Some sills

are clearly associated with overlying lava flows. It can be inferred that the setting of these sills was subcontemporaneous with the sedimentation. The Saint-Méen sill is one of the largest subvolcanic bodies and gives the name to the complex.

Few mafic dykes have been encountered, particularly in the Lacaune area. Most of them are not deformed and metamorphosed, so they are related to post-Variscan tectonomagmatic events and not to the synsedimentary volcanism. The question of the feeding dykes of the interbedded sills is discussed in the following section.

Samples have been obtained from four lava flows, three sills, and five pyroclastic and volcanosedimentary deposits.

*3.2.3.1. Composition of flows and sills.* The lavas are autoclastic and pyroclastic flows including fragments of hyalo-microlitic and porphytitic lavas and quartz-feldspar xenoliths. The sills are subophitic dolerites with phenocrysts of clinopyroxene, aggregated plagioclase and clinopyroxene, and local poecilitic clinopyroxene. Flows are more or less severely spilitized with high albite content. The low grade metamorphic effect developed a fracture cleavage and recrystallization of the groundmass and phenocryst margins in the greenschist facies with actinolite to Mg-hornblende ($Mg/(Mg + Fe) = 0.67-0.81$), albite, chlorite, clinozoisite (Cz 65–89), pumpellyite, calcite, muscovite and quartz. Chlorite is pycnochlorite and crystallized at $252 \pm 21\ °C$ according to the Zang and Fyfe's (1995) thermometer (36 measurements).

Magmatic plagioclases have the composition of calcic labradorite (An 61–74) only preserved in the core of phenocrysts of lava flows and sills. Best preserved pyroxenes have been analysed in the sills of Saint-Méen and Raffanel. In the Mg-Ca-Fe$^t$ + Mn diagram, they show a calcic augite composition ($32\ wt.\% < MgO < 45\ wt.\%$; $14\ wt.\% < FeO^t + MnO < 24\ wt.\%$; $38\ wt.\% < CaO < 45\ wt.\%$) (Fig. 18). Covariation diagrams attest for low contents of Tschermak moles (Fig. 19). The averaged mole composition is made of diopside (55%), hedenbergite (20%), enstatite (15%), ferrosilite (5%), and acmite + jadeite + Tschermak moles (5%). These features are consistent with pyroxenes of tholeiitic magmas. The composition of the parental magma is estimated by assuming that pyroxenes were in equilibrium in the magma chamber using tests based on Putirka (1999) models. It can be achieved with the composition of the sills if the lava was moderately cumulative in Fe-Mg phases, as supported by Cr, Ni and Co contents. Then, the pyroxene thermobarometer of

Putirka et al. (2003) fully available in Putirka (2008) is applied and gives a crystallizing pressure between 5 and 6 kbar.

The composition of flows and sills is subalkaline ($49.3\ wt.\% < SiO_2 < 50.0\ wt.\%$; $0.44\ wt.\% < TiO_2 < 1.02\ wt.\%$; $4.5\ wt.\% < MgO < 8.8\ wt.\%$; $2.5\ wt.\% < Na_2O < 5.5\ wt.\%$; $0.59\ wt.\% < K_2O < 2.62\ wt.\%$). Spilitized lavas are commonly enriched in $Na_2O$. The high Mg number between 63.8 and 73.1 indicates a partly cumulate facies. However, rocks are altered ($LOI = 3.2-7.1$) and no residual olivine has been observed. In the normative nomenclature, discarding the contaminated samples, lavas are saturated ($Qtz = 0$), moderately rich in olivine ($Ol = 3.5-6.9\%$), and defined as olivine-basalts. The rare earth element content (REE) is low ($La = 1.9-2.3\ ppm$) and very weakly fractionated in LREE ($La/Yb = 1.9-4.2$; $(La/Yb)_{NC} = 1.3-2.9$). However, the lithophile elements are enriched as shown by the N-MORB-normalized ratios ($(Th/La)_{NM} = 3.4-9.5$; $(Rb/La)_{NM} = 3.0-23.5$; $(Ba/La)_{NM} = 7.8-51.6$) (Fig. 15a). There is a significant negative anomaly for Nb, and moderate for Ta compared to N-MORB ($(Nb/La)_{NM} = 0.2-0.5$; $(Ta/La)_{NM} = 0.4-1.0$). The magmatic source may be undepleted or less depleted than that of the Ensèges-Moulergues lavas (Fig. 16a). Magmas of the Ensèges-Moulergues and Saint-Méen complexes are quite different (Fig. 16b) though a similar scenario may be pertained for the magma genesis with mobile lithophile element enrichment from the crust.

*3.2.3.2. Compositions of tephra and volcanosediments.* Tephra deposits are pyroclastic layers rich in felsic clasts and impregnated with calcite. The quartz-feldspar xenocrysts are mantled with clinopyroxene in a reaction rim indicating their origin from the magma chamber or dyke walls. The volcanosediments are volcaniclastic mixtures of angular fragments of lava and silico-aluminous sediments. Lava fragments are either spilitized or fresh.

Due to the felsic component, silica and alumina are enriched ($SiO_2 = 59-69\ wt.\%$; $Al_2O_3 = 19\ wt.\%$). The minor element contents recorded the felsic contribution with enrichment in LILE and lithophile elements in the N-MORB normalized diagram (Fig. 15b). Taking into account this enrichment, the patterns mimic those of the lavas with LILE fractionation and Nb and Ta anomalies. The conspicuous feature is the heavy depletion of Ti, the single element that is not enriched. The crustal contribution is illustrated in Figs. 16 and 17.
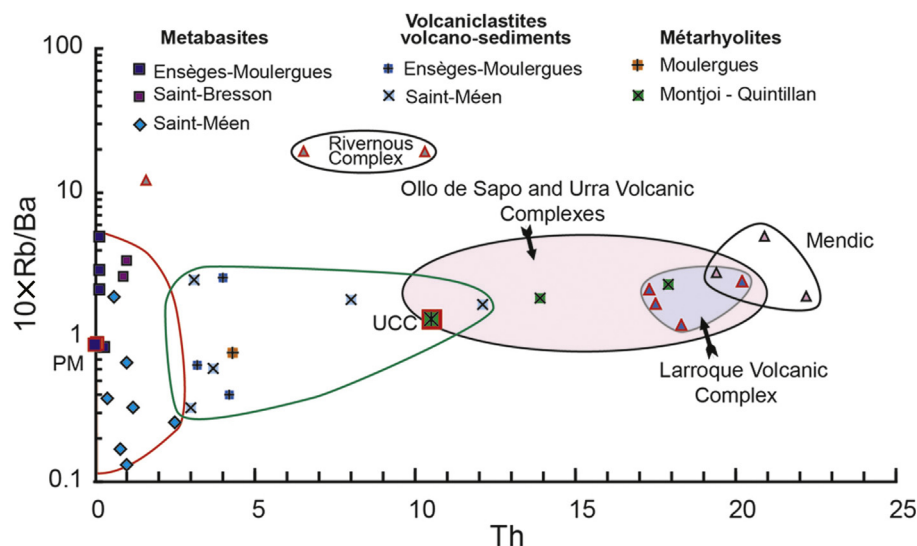
**Figure 17.** Th vs. Rb/Ba diagram for the Ensèges-Moulergues, Saint-Méen and Saint-Bresson metabasites, volcaniclastics and volcanosediments, and for the Rivernous, Moulergues, Larroque and Mendic felsic rocks. Compositional area of the Ollo de Sapo and Urra metarhyolites using data from Solá et al. (2008) and Díez Montes et al. (2010).
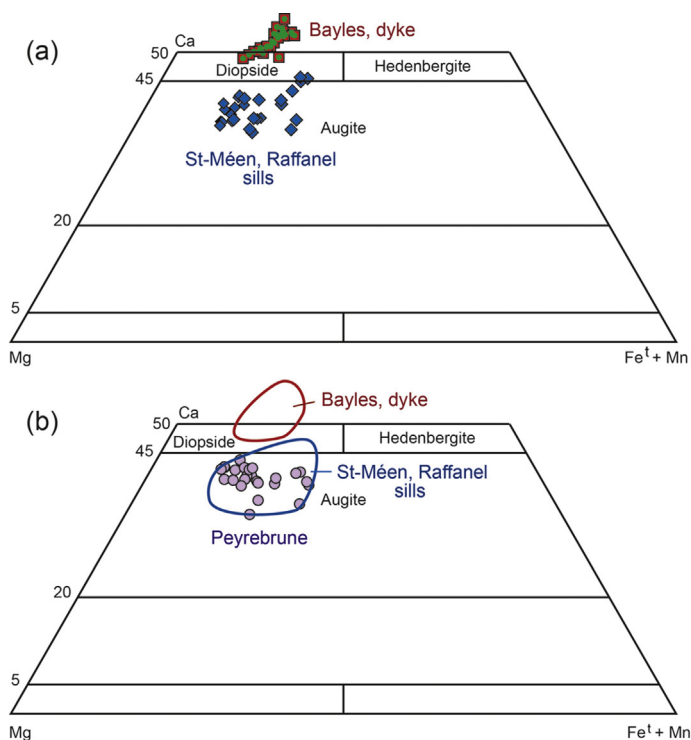
**Figure 18.** Mg-Ca-Fe$^t$+Mn diagram of pyroxenes of Saint-Méen − Raffanel sills and Bayles dyke (a), and of Peyrebrune flow-sills (b). Saint-Méen, Raffanel and Peyrebrune are similar with average composition of calcic augite indicative of a sub-alkaline magma. Bayles is different with a fassaitic diopside composition characteristic of an alkaline magma.

*3.2.3.3. The question of the feeding dykes.* A number of doleritic dykes can be encountered when sampling the Merdelou-Lacaune volcanic formations. Many of them are post-tectonic and devoid of schistosity and metamorphism. They commonly display an alkaline signature: ophitic texture with olivine phenocrysts. It has been suggested that these dykes fed the sills of the Saint-Méen Volcanic Complex, and then, these sills did not belong to the Saint-Méen Complex but to a late- or post-Variscan magmatic event, contradicting the interpretation given in this study. In return, there are a few planar intrusions of lamprophyres (spessartites *sensu* Béziat et al., 1992, 1993) in the Lacaune area, having an ultramafic calc-alkaline to alkaline composition drastically different to that of the metabasite sills. These intrusions are fractured and sheared but not metamorphosed.

To test the feeding dyke hypothesis, a doleritic dyke has been sampled for microprobe and geochemical analyses in the Bayles area, northeastern part of the Merdelou slice. The dyke (Bayles-1) is 1 to 2 m wide, displays a prismatic jointing and crosscuts subvertically the Série Noire and the lower part of the overlying Coulouma Formation, whose lithostratigraphic contact is marked by an interbedded volcanosedimentary level (Bayles-2). The rock is unfolded and devoid of metamorphism unless a late hydrothermal alteration.

The rock is an ophitic olivine-rich dolerite dominated by phenocrysts of olivine and clinopyroxene in an aggregated clinopyroxene-plagioclase groundmass with Ti-magnetite (TiO$_2$ = 19−20 wt.%), apatite and secondary actinolite, pumpellyite, sodic feldspar and clinozoisite. The olivine composition is forsterite-rich (Fo 86−88). The olivine-liquid equilibrium temperature is calculated at 1260 °C (Putirka et al., 2007). The pyroxene is a fassaitic diopside overlapping the 50 Ca limit of the Mg-Ca-Fe ternary diagram (29.4 wt.% < MgO < 39.2 wt.%; 10.4 wt.% < FeO$^t$ + MnO < 19.7 wt.%; 49.1 wt.% < CaO < 56.0 wt.%) (Fig. 18). This is due to high Tschermak mole substitutions
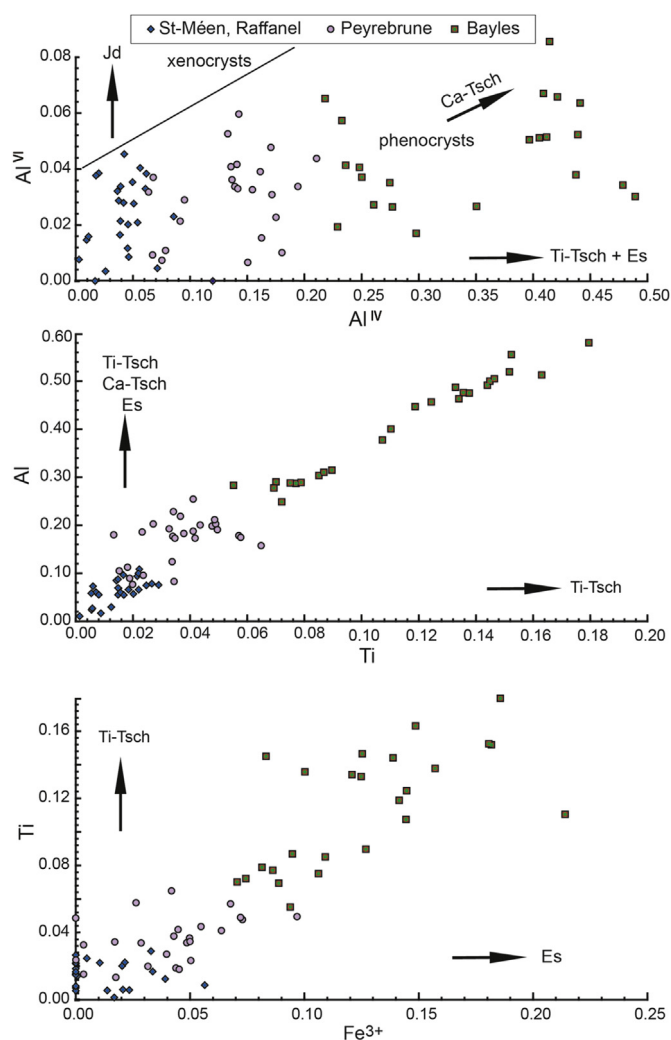


**Figure 19.** Al$^{IV}$-Al$^{VI}$, Ti-Al, and Fe$^{3+}$-Ti covariation diagrams of per formula unit values of pyroxenes to distinguish the Saint-Méen − Raffanel, Peyrebrune and Bayles chemical compositions. All the pyroxenes are in the phenocrystic area. Compared to Saint-Méen − Raffanel, Peyrebrune pyroxenes are slightly enriched in Ca-Tschermakite, Ti-Tschermakite and Esseneite moles. In contrast, Bayles pyroxenes are highly enriched in the Tschermak moles, explaining the fassaitic feature related to alkaline magma composition.

averaging 25% as shown by the covariations diagrams (Fig. 19). The averaged mole composition is made of diopside (57%), hedenbergite (11%), enstatite (2%), ferrosilite (1%), jadeite + acmite (4%), esseneite (12%), Ti-tschermakite (11%) and Ca-tschermakite (2%). Such a composition is symptomatic of an alkaline magma. Using the pyroxene thermobarometer of Putirka et al. (2003), the crystallizing pressure averages 10 kbar.

The chemical composition is titanian- and magnesian-rich (TiO$_2$ = 2.9 wt.%; MgO = 7.8 wt.%; Mg$^\#$ = 60). The rock has experienced a weak hydrothermal alteration and shows high loss on ignition (8.1 wt.%). Leaching of alkalis probably occurred and the norm calculation has no sense. Owing to the olivine and fassaitic diopside mineral composition, the rock is representative of an undersaturated olivine-basalt magma. Except the most mobile elements (Ba, Rb, K, Sr), the incompatible elements are not too severely modified and their ratios are preserved. The rare earth elements are enriched and highly fractionated (La = 76 ppm; La/Yb = 32; (La/Yb)$_{NC}$ = 21.5). Enrichments in Ta, Nb and Th can be considered. The N-MORB normalized profile is characteristic of an alkaline basalt (Fig. 15a) and

drastically different to the lavas of the Saint-Méen Volcanic Complex and all the regional Cambrian volcanic complexes.

The mineral composition and the salient chemical features of the dyke clearly advocate for a magmatic alkaline signature and an enriched mantle source (Fig. 16). It is concluded that the dyke as well, as all the similar alkaline dykes, are not related to the Cambrian−lower Ordovician sills showing very different composition, but belong to a drastically distinct magmatic phase. Structural features indicate that these dykes were linked to a post-Variscan intracontinental fracturing.

### 3.2.4. Larroque Volcanic Formation

The most noteworthy facies of the Larroque volcanic rocks is represented by the sheared porphyroclastic rhyolites or microgranites rich in lacunous quartz (rhyolitic quartz) and alkali feldspar largely fragmented phenocrysts giving the name of "porphyroid" commonly used in the whole Variscan realm for these widespread Ordovician metarhyolites. These rocks are also named "augen gneiss" though they do not show a high-grade gneiss paragenesis but, in most cases, a lower grade metamorphic mineralogy. Because of the large bluish quartz phenocrysts, similar rocks are nicknamed "Ollo de sapo" in Portugal and Spain. These porphyritic lavas belong to thick rhyolitic flows and to sills. Meanwhile, many other facies are associated such as aphyric lava flows, aphyric and porphyritic pyroclastic flows of welded or unwelded ignimbritic types, fine to coarse tephra deposits, and volcaniclastic or epiclastic deposits with variable sedimentary contribution.

We analysed four porphyroclastic rocks from the Larroque and Saint-Géraud areas in the Saint-Sernin-sur-Rance nappe and the Saint-André klippe above the Saint-Salvi-de-Carcavès nappe, respectively (Am, Sa, Sg, Fig. 5). Composition ranges from potassic-rich dacite to rhyolite (66.7 wt.% < $SiO_2$ < 75.0 wt.%; 0.8 wt.% < $Na_2O$ < 1.6 wt.%; 4.0 wt.% < $K_2O$ < 9.3 wt.%), and belongs to the alkalic group in the nomenclature of Frost et al. (2001). The A/CNK ratio is peraluminous (A/CNK = 1.3−2.4). The rare earth elements are enriched and fractionated (33.2 ppm < La < 45.6 ppm; 11.2 < La/Yb < 14.5). The upper continental crust normalized diagram (Fig. 14b) shows negative anomalies of Ti, V, Cr, Mn and Fe linked to oxide fractionation, of Zr and Hf linked to zircon fractionation, and of Eu linked to plagioclase fractionation. Profiles are similar to those of the Vendean Saint-Gilles rhyolites. Fractionation of zircon in peraluminous melt is illustrated in Fig. 13b. The Th vs. Rb/Ba features are also similar to those of the Saint-Gilles rhyolites, as well as those of the Iberian Ollo de Sapo and Urra rhyolites (Solá et al., 2008; Díez Montes et al., 2010) (Fig. 17).

### 3.2.5. Mendic Pluton

Though it is not a volcanic formation, the Mendic Pluton is concerned by this study because it may be related to the same magmatic activity than the Larroque Volcanic Formation. The Mendic metagranite is a biotite-muscovite porphyritic granite showing subhedral potassic feldspar in granular aggregates of micas, sodic plagioclase (An 10−30), alkaline feldspar, quartz and accessory magnetite, apatite and zircon. The initial granular texture is heavily constrained by a protomylonitic planar deformation. Dykes are dominated by microgranites recording the same deformation than the intruded metasediments.

We analysed two granites and one microgranite (Md, Fig. 5; Men 1-2 and Gra2, Tables 3 and 4). The granite is silica rich and sodo-potassic ($SiO_2$ = 75 wt.%; $Na_2O$ = 5.0−5.8 wt.%; $K_2O$ = 1.4−5.0 wt.%). The microgranite is more potassic ($K_2O$ = 7.0 wt.%). The A/CNK ratio is peraluminous (1.2). The rare earth elements are enriched and fractionated (La = 35.5−36.9 ppm, La/Yb = 9.5−11.0). The lithophile elements are enriched (Rb = 57−143 ppm; Ba = 113−511 ppm; Th = 19−21 ppm). The microgranite is

characterized by depletion of light rare earth elements (LREE) but not of lithophile elements. An apatite fractionation may be assumed for the REE loss. The upper continental crust normalized patterns are similar to those of the Larroque metarhyolites (Fig. 14c). The noteworthy LREE depleted trend of the microgranite is evidence of apatite and/or allanite fractionation based on their mineral/melt distribution coefficients in acidic rocks (Henderson, 1984). The negative Eu anomaly is symptomatic of plagioclase fractionation. The Th vs. Rb/Ba diagram supports a geochemical similarity of the Mendic metagranite with the Larroque metarhyolites (Fig. 17).

### 3.2.6. Peyrebrune Volcanic Complex

The Peyrebrune Volcanic Complex includes several decametre-thick metadoleritic sills and metre-thick metabasaltic flows and pyroclastites encased in the black shales of the lower Ordovician Albigeois Formation of the Saint-Salvi-de-Carcavès and Saint-Sernin-sur-Rance nappes (Guérangé-Lozes, 1987; Guérangé-Lozes et al., 1996; Guérangé-Lozes and Mouline, 1998; Guérangé-Lozes and Alabouvette, 1999). The complex is named after the notorious mining area of Peyrebrune, western side of the Saint-Salvi-de-Carcavès nappe, where well preserved pillowed lava flows were described by Durand and Gagny (1966), Alsac et al. (1987), and Marini (1987).

Metabasites have been sampled in the Peyrebrune-Teillet area and in the Bonneval-La Roque-Trebas-Mercadial area, located in the western and northern parts of the Saint-Salvi-de-Carcavès nappe, respectively (Py, Te, Bo, Lq, Tr, Fig. 5). The rocks recorded a moderate brittle deformation and recrystallized in the greenschist facies. The metamorphic chlorites are Fe-ripidolite to pycnochlorite and crystallized at 254 ± 18 °C according to the Zang and Fyfe's (1995) thermometer (17 measurements). Spilitization process has occurred with phenoblastic albite enrichment at the base and top of the flows. Magmatic textures are always visible and residual magmatic clinopyroxene has been analysed. The lavas are microlitic porphyritic with phenocrysts of plagioclase ($An_{61-68}$) partly changed to albite and clinopyroxene partly replaced by secondary actinolite. The inner part of the thickest lava flows (more than 4 m) and the sills are doleritic intergranular and locally porphyritic.

Several pyroxenes have been analysed in flow-sills of Peyrebrune. In the Mg-Ca-$Fe^t$ + Mn diagram, they display a calcic augite composition (36 wt.% < MgO < 48 wt.%; 11 wt.% < $FeO^t$ + MnO < 25 wt.%; 34 wt.% < CaO < 44 wt.%) (Fig. 18). These data comfort previous analyses performed by Marini (1987). The Peyrebrune pyroxenes seem to resemble those of the Saint-Méen Volcanic Complex but include higher contents of Tschermak moles (Fig. 19). The averaged mole composition is made of diopside (51%), hedenbergite (17%), enstatite (15%), ferrosilite (5%), acmite + jadeite (3%), Ti-Tsch (4%), esseneite (4%) and Ca-Tsch (1%), for a total of 9% of Tschermak moles. The pyroxene composition is consistent with enriched tholeiitic or transitional magmas. The composition of the parental magma is estimated by assuming that pyroxene was in equilibrium in the magma chamber (Putirka, 1999). The pyroxene thermobarometer of Putirka et al. (2003) gives a crystallizing pressure between 6 and 7 kbar.

The chemical composition of the flows and sills is subalkaline (48 wt.% < $SiO_2$ < 52 wt.%; 2 wt.% < $TiO_2$ < 4 wt.%; 4.3 wt.% < MgO < 7.4 wt.%; 2.6 wt.% < $Na_2O$ < 3.9 wt.%; 0.3 wt.% < $K_2O$ < 0.6 wt.%), discarding spilitized and sialic contaminated lavas. The Mg number between 40 and 57 corresponds to mafic to slightly evolved magmas. In the normative nomenclature, the lavas are oversaturated to saturated with Qtz or Ol and Hy (0 < Qtz = 8; 0 < Ol < 10; 14 < Hy < 23), and then defined as tholeiites and olivine-tholeiites. The rare earth element content (REE) is moderate to high (La = 7.9−50.0 ppm) and fractionated in LREE (La/Yb = 2.3−5.8; (La/Yb)$_{NC}$ = 2.2−5.5). The lithophile elements are enriched as shown by the N-MORB-normalized

ratios (($Th/La)_{NM} = 1.6$–$6.9$; $(Rb/La)_{NM} = 1.0$–$5.3$; $(Ba/La)_{NM} = 1.9$ –$6.9$) (Fig. 20a). There are no anomalies for Nb, and Ta compared to N-MORB. The normalized spectra are parallel, indicating that all the lavas were evolved from the same magmatic batch. The more evolved lava shows a Ti negative anomaly. The profiles are compared with the averaged compositions of initial rift tholeiite (IRT) that fits very well with the profiles of mafic terms (neglecting secondary loss of K). The IRT signature is illustrated in the Ti-Nb-Th diagram (Fig. 21a). This conclusion is in good agreement with the previous data of Marini (1988) and Pin and Marini (1993) concerning some lavas of Peyrebrune. The IRT composition is explained by mixing of lithospheric and asthenospheric materials, which occurred during lithosphere thinning and intracontinental rift initiation. In the Ta/Yb vs. Th/Yb diagram (Fig. 21b), the tholeiites plot in the mantle array and may be related to a moderately enriched source. The La/Yb and Sm/Yb values and the lack of heavy rare earth element depletion comply with a mantle source of spinel lherzolite. Batch melting calculations using rare earth elements give a partial melting degree greater than 10%.

### 3.2.7. Southern Cévennes, the Saint-Bresson Volcanic Complex

The Saint-Bresson Volcanic Complex gathers mafic lavas, pyroclastites and volcanosediments of mixed acidic and mafic components (Vg, Fig. 5). Two basaltic flows were analysed. The rock is a crystal-rich pyroclastite with phenocrysts of pyroxene replaced by actinolite. Lava fragments are microlitic porphyritic and severely altered in secondary actinolite, albite, epidote and chlorite. Rounded xenoliths of quartz and feldspar are locally abundant. The matrix is enriched in sericite and calcite. The chemical composition is subalkaline (44 wt.% < $SiO_2$ < 48 wt.%; 0.8 wt.% < $TiO_2$ < 0.9 wt.%; 12.3 wt.% < MgO < 12.6 wt.%). The high Mg number averaging 74 and the high MgO, Cr and Ni contents (Cr = 255 ppm; Ni = 70 ppm) are features of an olivine-pyroxene cumulate lava, but due to alteration, no residual olivine can be discerned. The rock alteration (LOI > 8) implies losses of lime and alkalis, so, the norm calculation has no sense. The rare earth elements (REE) are low (La = 5–5.5 ppm) and very slightly fractionated in the LREE (La/ Yb = 2.6; $(La/Yb)_{NC} = 1.8$). The lithophile elements are enriched as shown by the averaged values of N-MORB-normalized ratio ($Th/La_{NM} = 4.2$; $(Rb/La)_{NM} = 14$–$112$; $(Ba/La)_{NM} = 3.7$–$8.7$) (Fig. 20b). The highest contents of Rb (and K) are explained by the sericite secondary invasion. There are negative Nb and Ta anomalies (($Nb/La)_{NM} = 0.4$–$0.5$; $(Ta/La)_{NM} = 0.4$–$0.8$).

The REE pattern is close to that of the E-MORB and CT. The Nb-Ta negative anomalies and the LILE enrichment are more consistent with the CT pattern, allowing that the lower contents of REE are explained by cumulation process. In the Ta/Yb vs. Th/Yb diagram, the mantle source was probably slightly depleted, considering that the moderate Th enrichment resulted from crustal assimilation as suggested by the submelted felsic xenoliths (Fig. 21b).

### 3.2.8. Mouthoumet Massif, the Davejean Volcanic Complex

A Tremadocian metarhyodacite flow of the parauthochton has been sampled in the Lairière volcanic dome, close to Montjoi village, at the northeastern corner of the Quillan geological map (northwest of Mouthoumet) (Mj, Fig. 5). A metarhyolite flow interbedded between shales and sandstones of the lower Ordovician sequence of the Serre de Quintillan slice has been sampled in the Quintillan-Forest area. Metabasaltic flows were investigated in the Davejean window and in the Maisons village, west of the Serre de Quintillan slice (Dj, Ms, Qu, Fig. 5).

The rhyolites are suspected to belong to the oldest volcanic event. Composition ranges from sodo-potassic dacite to rhyolite (69 wt.% < $SiO_2$ < 76 wt.%; 2.1 wt.% < $Na_2O$ < 3.7 wt.%; 2.4 wt.% < $K_2O$ < 3.8 wt.%) and is alkali-calcic (Frost et al., 2001).
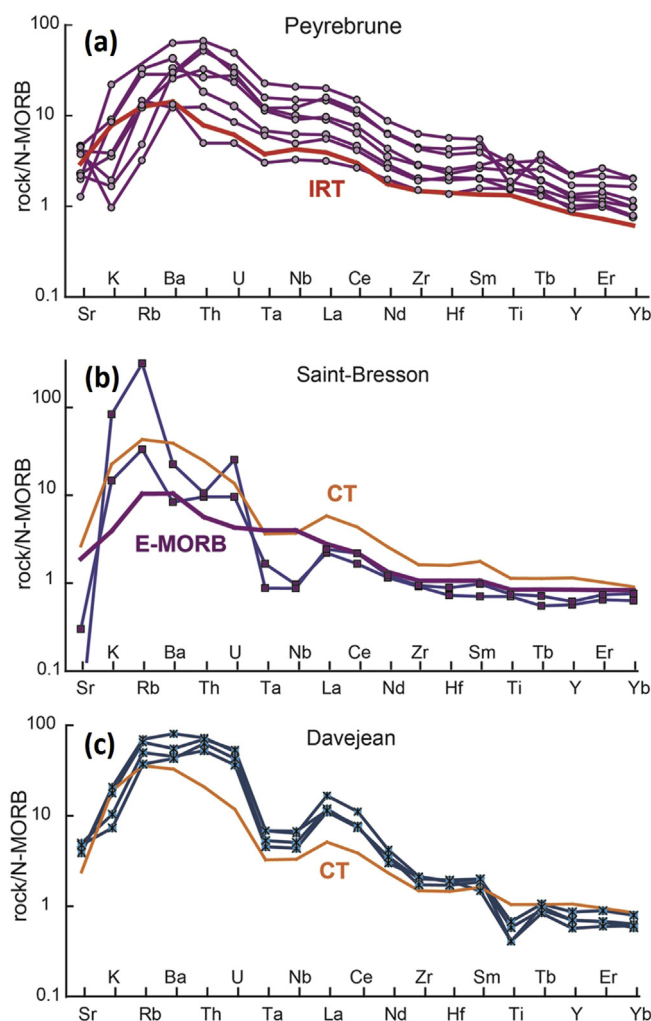


**Figure 20.** N-MORB normalized incompatible element diagrams of the metabasaltic lavas of the Peyrebrune (a), Saint-Bresson (b), and Davejean (c) volcanic complexes. IRT and CT average profiles after Holm (1985) and Pouclet et al. (1995). E-MORB composition after Sun and McDonough (1989). Note the IRT fingerprint of Peyrebrune.

The A/CNK ratio is peraluminous (1.7–2.0). The rare earth elements are enriched and fractionated (59 ppm < La < 63 ppm; 28 < La/ Yb < 38). The lithophile elements are enriched (75 ppm < Rb < 75 ppm; 400 ppm < Ba < 657 ppm; 14 < Th < 18). The upper continental crust normalized patterns are similar to those of the Larroque metarhyolites (Fig. 14c), taking into account a more important fractionation of zircon in the more evolved rhyolite. The Th vs. Rb/Ba diagram supports the similarity with the Larroque metarhyolites (Fig. 17).

The basaltic lava flows are microlitic porphyritic and range from mafic composition with abundant phenocrysts of pyroxene and plagioclase to intermediate composition enriched in plagioclase and alkaline feldspar. They were metamorphosed with complete recrystallization of magmatic minerals and matrix in the greenschist facies paragenesis. In addition, many flows were spilitized and enriched in sodium (albite). Weathering alteration is widespread. Consequently, the sampling is hazardous and many analytical results have been discarded.

Based on few available analyses, the chemical composition is basaltic to moderately evolved (57 wt.% < $SiO_2$ < 64 wt.%; 0.5 wt.% < $TiO_2$ < 0.9 wt.%; 2.3 wt.% < MgO < 4.6 wt.%; 5.4 wt.% < $Na_2O$ < 6.5 wt.%; 0.5 wt.% < $K_2O$ < 1.5 wt.%), as shown by the $Mg^{\#}$ (54–62). The norm calculation, though poorly constrained
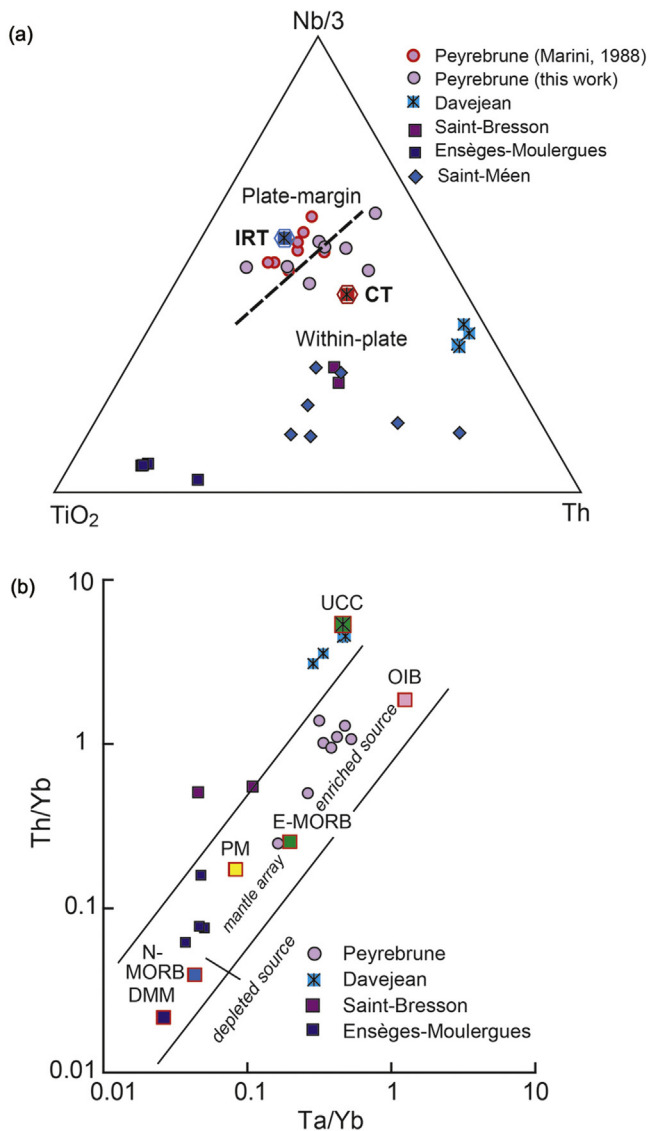
**Figure 21.** Ti-Nb-Th (a) and Ta/Yb vs. Th/Yb (b) diagrams of the Peyrebrune, Saint-Bresson and Davejean volcanic complexes. Comparison with Ensèges-Moulergues and Saint-Méen volcanic complexes. The IRT-like magma of Peyrebrune derived from a slightly enriched mantle source. Saint-Bresson lavas are contaminated and could provide from a depleted source. Davejean lavas display a severe crustal contamination and cannot be defined.

due to post-magmatic processes, favours an oversaturated tholeiitic magmatic composition ($7 < Qtz < 15$; $11 < Hy < 20$). In return, the incompatible trace element abundances are relatively well preserved. The rare earth elements are enriched and fractionated ($28$ ppm $<$ La $< 42$ ppm; $12 <$ La/Yb $< 21$; $8.8 <$ (La/Yb)$_{NC} < 15.3$). The N-MORB normalized diagram shows parallel profiles of the mafic and evolved lavas belonging to the same magmatic batch (Fig. 20c). The lithophile elements are enriched ((Th/La)$_{NM}$ = 4.4–6.1; (Rb/La)$_{NM}$ = 3.1–5.7; (Ba/La)$_{NM}$ = 3.6–4.9). Nb and Ta negative anomalies are important ((Nb/La)$_{NM}$ = 0.4–0.6; (Ta/La)$_{NM}$ = 0.4–0.6). The Ti negative anomaly (Ti/Ti* = 0.3–0.4) may be partly a magmatic feature and the result of oxide fractionation in the differentiated facies. Compared to the CT average composition, the lavas can be defined as continental tholeiites, also shown by the Ti-Nb-Th ratios (Fig. 21a). In the Ta/Yb vs. Th/Yb diagram, the mantle source cannot be defined because of the Th enrichment resulting from crustal contamination as suggested by the abundant felsic xenoliths (Fig. 21b).

## 4. Timing of the magmatic activities and geodynamic significance

### 4.1. South Armorican magmatic activities

In the South Armorican Domain, magmatic activities lasted from mid Cambrian to mid Devonian times according to their dated host sedimentary basin formations. The Cambrian to lower Ordovician volcanic rocks comprise middle Cambrian–Furongian olivine-basalts and tholeiites and Tremadocian rhyolites with a few overlying tholeiites. These mafic rocks share a common signature of continental tholeiites (CT) generated by melting of an enriched source of the continental lithosphere (Fig. 13a). Nevertheless, some Tremadocian tholeiites display an initial rift tholeiite signature (IRT) implying the contribution of a depleted source, and are indicative of an incipient rifting process. The acidic rocks derived from melting of crustal material. Heat for such a melting may have been supplied by the previous mantle-derived mafic magmas that intruded the crust and were underplated at the mantle-crust transition zone. This model is documented by the stratigraphically dated Cambro–Ordovician volcanics of the Chantonnay, La Roche-sur-Yon, and Saint-Gilles Units. It can be advocated that the mafic and acidic rocks of the Montaigu Leptyno-Amphibolite Complex belong to the same magmatic event because they share the same magmatic features.

In contrast, a second and quite different magmatic geochemical composition is illustrated by the amphibolites of the Saint-Martin-des-Noyers and the eclogites of the Les Essarts Complex. These mafic rocks originated from a depleted source (Fig. 10b, and rare earth element data of the literature) of N-MORB composition contaminated by lithophile elements. These mafic rocks are not dated. However, it is worth noting that similar basaltic lavas, originated from mixing of a depleted source and an enriched source, constitute a thick volcanic pile at the top of the Chantonnay Basin sequences named "La Meilleraie Volcanic Formation" (see Section 2.1.2, Table 2) (Thiéblemont, 1988) (Fig. 10b, LMT1). This volcanic stack includes hybridized lavas that resemble some metabasites of the Saint-Martin-des-Noyers Unit (Fig. 10b, LMT2 and 3). The La Meilleraie Volcanic Formation is middle to upper Devonian in age. Based on identical petrological features, it is straightforward to postulate that the Saint-Martin-des-Noyers Unit was contemporaneous. In that case, the increasing contribution of the depleted source for the La Meilleraie Volcanic Formation, the Saint-Martin-des-Noyers Unit, and Les Essarts Complex is a distinct indication of lithosphere thinning and asthenosphere uprising during mid to late Devonian times, possibly leading to the opening of a marine basin.

### 4.2. Occitan magmatic activities

The magmatic activities in the Occitan Domain studied in this work are distributed in five volcanic phases (V1–V5) ranging from earliest Cambrian to early Ordovician times (Fig. 6) (disregarding the youngest activities).

The first phase (V1) is represented by the uppermost Ediacaran to lowermost Cambrian Rivernous Rhyolitic Complex. This complex located in the northern Montagne Noire parautochthon is correlated with the rhyodacitic lavas of the "Schistes X", an important stratigraphic unit of the Axial Zone dated to the latest Ediacaran time (Lescuyer and Cocherie, 1992). It can be also correlated with acidic lavas of the Canaveilles Group from the South Canigou Massif in the eastern Pyrenees. Age datings of these Pyrenean volcanics provide various results (U-Pb SHRIMP method in zircon; Cocherie et al., 2005) due to abundant inherited cores. A previous age of 581 Ma was selected by Cocherie et al. (2005) but was re-investigated by Castiñeiras et al. (2008) who retain the youngest age of 540 Ma. In addition, Castiñeiras et al. (2008) dated to

548.8 ± 8 Ma a metarhyolite of the neighbouring Roc de Frausa Massif (= Roc de France) and to 560 ± 11 Ma a similar rock of the Cap de Creus Massif. Nevertheless, new U-Pb geochronological data of Casas et al. (2015) from interbedded acidic rocks of the Canigou and Cap de Creus sequences give ages ranging between 577 and 558 Ma. The amount of inherited zircons is an important problem when interpreting isotopic data. Waiting for more straightforward geochronological analyses, we assume that the V1 volcanic phase took place at the Ediacaran—Cambrian boundary interval, its boundary horizon being dated at 542 Ma (Gradstein et al., 2004).

The significance of this acidic volcanic activity is not clear. Crustal melting should be the evident magmatic process. But, petrological data are too poor to decipher the geotectonic conditions of the magma genesis. A detailed structural and metamorphic analysis (Álvaro et al., 2014a), in order to test the possible onset of a Cadomian tectono-thermal effect, proved that the rhyolitic volcanics were deformed during a single and common deformation stage shared by the overlying Cambrian strata and presumably Variscan in age. In that part of the Montagne Noire, there was no important deformation event across the Ediacaran—Cambrian transition. Consequently, the V1 activity is not related to any late Cadomian or Pan-African orogenic event. It can only be said that a suspected extensional tectonic event occurred around 540 Ma in allowing outpouring of crustal melts possibly residual of a former and undetermined magmatic process.

The second phase (V2) occurred in the late early Cambrian. It began by massive outpouring of magnesian-rich saturated basalts of the Ensèges-Moulergues Volcanic Complexes in the northern Montagne Noire, and of the Saint-Bresson volcanic Complex in southern Cévennes. The uppermost basaltic lava flows are associated with rhyolitic breccia flows. The mafic lavas are poor in rare earth elements, fractionated in the light rare earth elements, and originated from a depleted mantle source. Meanwhile they are enriched in lithophile elements. This enrichment is attributed to crustal contamination by volatile transfer. Acidic lavas are peraluminous and display a crustal signature. The prevailing contribution of a depleted mantle source for the N-MORB-like basaltic magma implies asthenosphere melting and thinning of the continental lithosphere. However, the following Cambro—Ordovician sedimentary deposition did not tally with a marine basin. The mafic lavas are limited to high-magnesia cumulate facies having recorded crustal contamination. They include abundant partly melted sialic xenoliths. The associated acidic lavas could have resulted from crustal melting. One may assume that the magma was ponded during a long time inside a crustal reservoir. Any MORB-like fresh magma never reached the surface as a result of which, we conclude to the abortion of the rifting process.

The third latest early Cambrian phase (V3) is recorded in the eastern Lacaune Mountains of the northern Montagne Noire. Abundant olivine-basalt lava flows and sills are interbedded in the Série Noire Formation, a kerogenous black shale and limestone unit deposited in slope-related to deep basinal settings, and constitute the Saint-Méen Volcanic Complex. The basalt is saturated, moderately magnesian, REE-poor and weakly fractionated in the LREE, but enriched in lithophile elements. The magma source resembles that of the V2 basalts with a more important contribution of an enriched component of lithospheric mantle. An intra-crustal ponding is also inferred. Owing to the lithosphere contribution, the rifting process did not evolve. On the contrary, the mantle cooled down according to the decreasing involvement of the asthenosphere, the lack of crustal melting and the deepening of the sedimentary basin.

The fourth phase (V4) was the most dramatic volcanic event in the Occitan Domain occurring in the early Tremadocian with rising up of the basin floors and subaerial explosive and effusive abundant rhyolitic activities. This event supplied (1) the Larroque Volcanic

Formation, described as parautochthonous units in the Rouergue and allochthonous units in the Albigeois and northern Montagne Noire, (2) the Davejean acidic volcanic part in the Mouthoumet Massif, and (3) the Génis rhyolitic unit of the western Limousin area that is correlated with the Tremadocian rhyolitic activity of the Chantonnay and La Roche-sur-Yon basins, and of the Saint-Gilles nappe. This acidic magmatic output resulted in massive crustal melting requiring a rather important heat supply. Such a great thermal anomaly can only be explained by asthenospheric upwelling leading to lithospheric doming, continental break-up, and a decompressionally driven mantle melting. Magmatic products accumulated at the mantle-crust boundary and provided heat transfer for crustal melting (Hupert and Sparks, 1988).

The Tremadocian fifth phase (V5) is the logical complement of the V4 crustal melting event. Emptying of the rhyolitic crustal reservoirs caused collapses and sinking of basin floors. Once the removal of the intra-crustal barrier formed by the acidic magma was achieved, some parts of the underplated basic magma could ascent and reach the surface. This magmatism is depicted by flows and sills of the Peyrebrune Volcanic Complex and the Davejean Volcanic Complex basalts. Basaltic rocks are evolved, REE-rich, and LREE-fractionated. They display a typical initial rift tholeiite (IRT) magmatic signature indicating contributions of both asthenospheric and lithospheric mantle sources.

## 5. Northern Gondwana volcano-tectonic activity

Correlations are tempted between the volcano-tectonic activities of the South Armorican and Occitan domains and are extended to the Northern Gondwana Variscan Belt in the Iberian Zones of the western Ibero-Armorican Arc branch (Fig. 1).

### 5.1. From Cambrian extensional pulses to Tremadocian continental break-up

The latest Ediacaran to earliest Cambrian rhyolitic activities are distributed in the northern flank (Rivernous Volcanic Complex, V1 volcanic phase) and the Axial Zone (Schistes X) of the Montagne Noire, and also in the eastern Pyrenees (Canaveilles Group of the southern Canigou Massif). They are dated around 545 and 540 Ma. These rhyolitic activities are younger than those of northern Iberia, dated between 575 and 560 Ma (Rubio-Ordóñez et al., 2015), and attributed to the arc-related final stage of the Cadomian orogeny. They could be contemporaneous with those of the latest stage of the Ediacaran andesitic to rhyolitic Volcanic Chain of the Moroccan Anti-Atlas dated between 578 and 543 Ma (Gasquet et al., 2005; Pouclet et al., 2007), somewhat correlatable with the Bodonal acidic volcanics of the Ossa-Morena Rift (Sánchez-García et al., 2010; Álvaro et al., 2014b). As already reported for the Rivernous Rhyolitic Complex (Álvaro et al., 2014a), the Occitan earliest Cambrian acidic volcanics are not related to any Cadomian or Pan-African tectonic event; until now, they have no pertinent tectonic relationships.

The lower Cambrian mafic and acidic lavas (V2 volcanic phase) are localized in the southeastern tectonic slices of the northern Montagne Noire. Guérangé-Lozes and Burg (1990) suggested that the volcanic activity was initiated along former ENE—WSW trending fractures that controlled the following décollement of the thrust. Unfortunately, it is not possible to check if the present-day NE—SW elongated setting of the volcanic bodies parallel to the foliation of the metasedimentary formations corresponds or not to the initial volcanic fissural system. The tholeiitic depleted magmatic signature of these earliest lavas fits well with an intracontinental extensional fracturing of incipient rifting. However, the source enrichment of the following lavas implying renewal

contribution of the lithospheric source component (V3 volcanic phase) attests for a decreasing activity of any rifting process.

The lower Cambrian sequences are not well constrained in the South Armorican Domain. The middle Cambrian to Furongian basaltic activities of the Cholet and Chantonnay basins displaying a continental tholeiitic magmatic signature have similarities with the Engastine Complex of the Thiviers-Payzac Basin of West-Limousin, but there are no clear equivalents in the Occitan Domain. It is concluded that, except for a limited part of the Occitan Domain where incipient rifting took place (Ensèges Volcanic Complex), the Cambrian volcano-tectonic activity was limited to intracontinental fracturing and outpouring of continental tholeiites and secondary felsic lavas.

The more conspicuous correlative is the widespread early Tremadocian acidic subaerial volcanism. This crustal-originated massive melting was associated with a major continental break-up. From northwest to southeast, the Tremadocian rhyolitic activities are distributed in autochthonous and allochthonous terrains originated from various sedimentary basins. Occurrences of these volcanics are located in the Fig. 22, as well as the lower Ordovician orthogneisses.

The more accurate dating is available in the Vendean area. The parautochthonous La Chapelle-Hermier rhyolites of the La Roche-sur-Yon Basin (472–486 Ma) are contemporaneous with those of the Saint-Gilles and Mareuil nappes (477–486 Ma) and the Chantonnay Basin (470–485 Ma). Structural features attest that the nappes recorded a westward transport (Burg, 1981; Brun and Burg, 1982; Burg et al., 1987; Béchennec et al., 2008; Lahondère et al., 2009). The closest eastern possible source for the thrust material is the Intermediate Structural Zone (Fig. 2), where orthogneiss bodies could be regarded as magmatic chambers of the volcanics, namely Les Essarts orthogneiss dated at 483 ± 4 Ma and the Mervent orthogneiss dated at 486 + 15/−11 Ma (see Section 2.1.3). To the northeast, poorly dated rhyolites of the Cholet Basin may be allotted to the same Tremadocian volcanic event. To the northwest, Tremadocian orthogneiss is recognized in the Champtoceaux Complex (485 ± 11 Ma; Paquette et al., 1984; and 481 + 6/−5 Ma; Ballèvre et al., 2002). Thanks to the restoration of the ductile strain of the regional deformation in a simple-shear model, Gumiaux et al. (2004a) demonstrated that the Champtoceaux Complex was the continuation of the Les Essarts Complex and thus, their orthogneisses originated from the same fracture. In the south of Brittany, the Tremadocian magmatic activity is marked out by the Belle-Île – La Vilaine continuation of the rhyolite-bearing nappe of Saint-Gilles (Ballèvre et al., 2012), the orthogneisses of Lanvaux (478 ± 18 Ma; Janjou et al., 1998), Moëlan (485 ± 6 Ma; Calvez, 1976), Loc'h (483 ± 3 Ma; Béchennec et al., 1999), Cosquer and Lanmeur (497 ± 11 Ma and 498 ± 12 Ma; Guerrot et al., 1997), the metarhyolites of Merrien (481 ± 11 Ma; Guerrot et al., 1997), and the orthogneiss (480 ± 8 Ma; Paquette et al., 1985) of the eclogite-bearing basic-ultrabasic complex of Baie d'Audierne.

Taking into account the distribution of the rhyolites and related orthogneisses, there are supporting evidences that the rhyolitic activity of the South Armorican Domain outpoured from a fracture swarm, though the present-day location of the fracture zone is depending on the thrust displacements and the shear zone motions. However, there are strong evidences that the late Variscan shear zones reworked such a previous fracture system.

To the southeast, the continuation of the structural pattern from South Armorica to Massif Central below the sedimentary cover of the Seuil du Poitou is done in the structural map of Rolin and Colchen (2001a) interpreting geophysical and bore hole data. Using this map, we draw a sketch map of the South-Armorican and Occitan Cambro–Devonian basins in the Fig. 23. The fracture zone of the Mervent orthogneiss, the southernmost branch of the South-Armorican Shear Zone, is prolonged until the NW–SE dextral Parthenay Shear Zone (PSZ). Similarly, the MSSZ joins the PSZ, in setting

up the eastern border of the lens-shaped Chantonnay Basin. After a 120 km southeast offset along the PSZ, the fracture system renews along the Estivaux Fault (EsF) bordering the Thiviers-Payzac Basin with orthogneiss elongated bodies dated to the early and mid-Ordovician, and with the Genis Tremadocian rhyolites (Guillot et al., 1977; Roig et al., 1996; Melleton et al., 2010). Farther to the southeast, the La Bessenoits klippe of eclogite-bearing leptyno-amphibolite complex includes an orthogneiss dated to 481 ± 1 Ma (Paquette et al., 1995). The similar Levezou Complex includes a leptynite dated to 480 Ma (Pin and Lancelot, 1982). Lastly, a thick nappe stack of rhyolite extended from the Rouergue and Albigeois region to the northern Montagne Noire. This is the Larroque Volcanic Complex correlated with the dated early Tremadocian Vendean rhyolites. Fig. 23 clearly illustrates the wide setting of the Tremadocian rhyolitic activities and there is no doubt that the Tremadocian rhyolitic fracture system of the Occitan Domain is the continuation of the South Armorican one. Another distinct, though less important, rhyolitic activity was also recorded in the Mouthoumet Massif.

All these volcanoes pertain to a "Tremadocian Volcanic Chain" emplaced along the north Gondwanan basins. Most of these basins are parautochthonous. The Occitan basins were moderately thrust to the south or south-west. The Saint-Gilles and cognate basins were thrust to the west. The upper allochthonous position of the northern basins is due to late orogenic northward backthrusting.

### 5.2. The Iberian link: toward a Tremadocian tectono-magmatic correlation

There is an extensive body of literature on the correlatives between the South Armorican-Occitan and Iberian branches of the Variscan Arc based on their structural, lithological and petrological salient features (synthesis in Ballèvre et al., 2014). We already approached the chronostratigraphic and petrological equivalence between Tremadocian South Armorican-Occitan and Iberian metarhyolites (Figs. 8b and 17). The Tremadocian magmatic activity of associated orthogneisses and metarhyolites from the Iberian Domain is illustrated in Fig. 24. The question is: which are the lithostructural relationships between the two branches of the Ibero-Armorican Arc? Discriminating Tremadocian rhyolitic-granitic magmatic complexes could provide appropriate guides for connecting both branches.

In Fig. 22, the suspected location of Iberia is drawn for the Carboniferous–Permian time assuming: (1) a 250 km right lateral offset along the North-Pyrenean fault system (Raymond, 1987); and (2) a 35° clockwise rotation for cancelling the Gulf of Biscay (or Gulf of Gascogne) opening (Perroud and Bonhommet, 1981; García-Mondéjar, 1996; Sibuet et al., 2004). The Iberian lower Ordovician magmatic formations dominated by acidic volcanics are widely distributed into four magmatic complexes or systems at sites #1, 2, 3, and 4. The first magmatic site is located in the Cantabrian Zone and in the easternmost side of the West Asturian-Leonese Zone (#1a and #1b). It is limited to few sills and beds of rhyolitic lavas and volcaniclastics from the upper Barrios Formation at the base of the "Armorican Quartzite" where it is dated to 477.5 ± 0.9 Ma (early Floian), and in the upper part of the lower Tremadocian Borrachón Formation (Gutiérrez-Alonso et al., 2007; Álvaro et al., 2008). The second site is the Ollo de Sapo Formation located on eastern side of the Central Iberian Zone and consisting of acidic volcanic and volcanosedimentary rocks interbedded at the base of the lower Ordovician platform-facies sediments (Valverde-Vaquero and Dunning, 2000; Montero et al., 2007, 2009; Díez Montes et al., 2010; Talavera et al., 2013). The formation extents from the Cantabrian coast to the Hiendelaencina region, in the easternmost part of the Central Iberian Zone, and includes orthogneiss bodies of Guadarrama and Miranda do Douro (Bea et al., 2006; Zeck et al.,
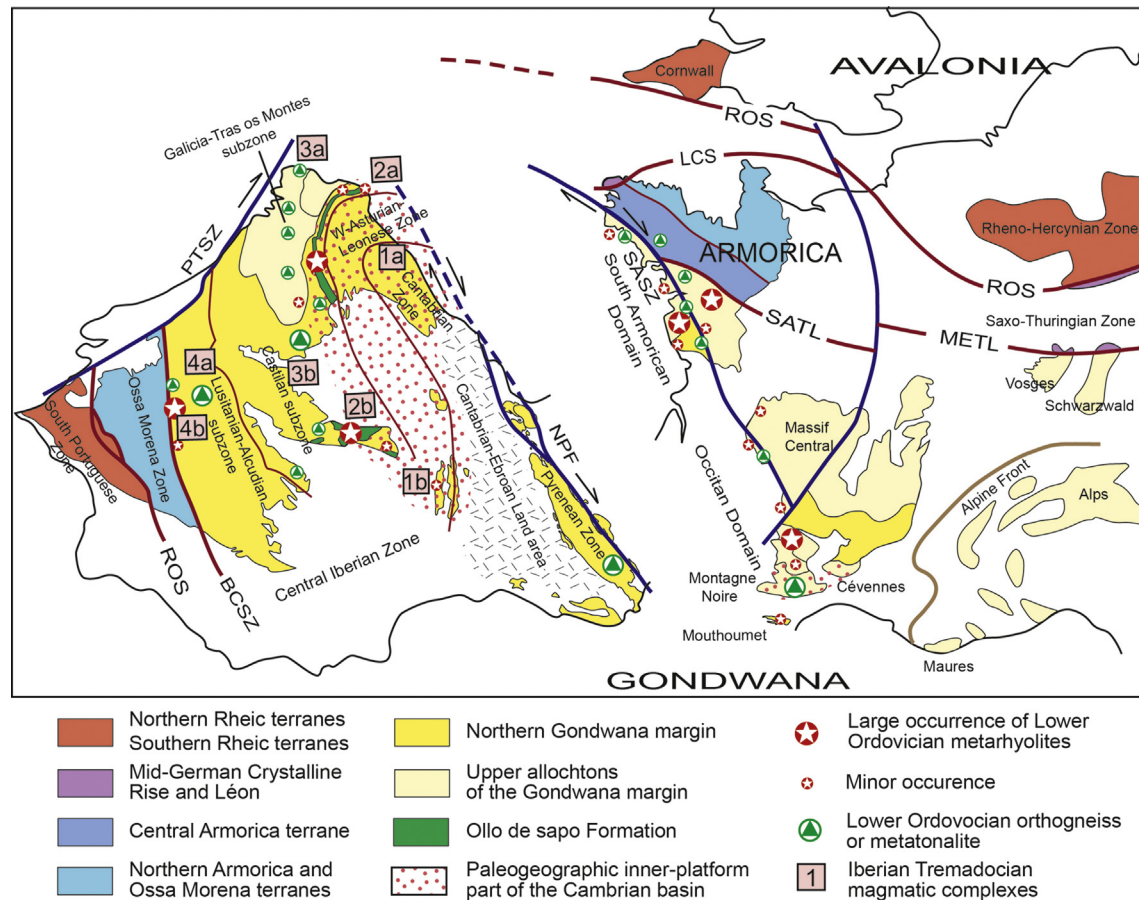
**ARTICLE IN PRESS**



**Figure 22.** Sketch map of the westernmost Variscan realm. The Iberian branch of the Ibero-Armorican Arc is drawn in its Late Carboniferous position assuming a 250 km right-lateral motion along the northern Pyrenees fault system (Raymond, 1987) and a 35° clockwise rotation for closing the Gulf of Biscay (Perroud and Bonhommet, 1981; García-Mondéjar, 1996; Sibuet et al., 2004). The lower Ordovician metarhyolites and related orthogneisses are pointed out in the South Armorican and Occitan domains, where they are disposed along a tectonic lineament, and in the Iberian Domain, where they are located along four elongated tectono-magmatic systems: 1a-b, 2a-b, 3a-b, 4a-b (see text). ROS, Rheic Ocean Suture; LCS, Le Conquet Suture; SATL, South Armorican Tectonic Line; METL, Medio-European Tectonic Line; SASZ, South Armorican Shear Zone; PTSZ, Porto-Tomar Shear Zone; BCSZ, Badajoz-Cordoba Shear Zone; NPF, North Pyrenean Fault.

2007) (#2a and #2b). The total length of this belt reaches ca. 570 km, with a large and subcontinuous outcrop of the Sanabria northwestern section of 28 km in width, and a thickness of ca. 2000 m. The formation is folded in a complex anticlinorium structure overlying orthogneissic domes. Reverse faults and recumbent folds developed above the doming core, but the whole complex remains autochthonous and is interpreted as a succession of volcanic domes of dacites and rhyolites. The granitic core is considered as the subvolcanic magmatic reservoir. The third site gathers the Rio Baio, Mora and Saldanha volcanic complexes in the Galicia-Tras os Montes subzone, and associated orthogneisses extended in the Castillan subzone (Valverde-Vaquero et al., 2005; Talavera et al., 2008, 2013; Bea et al., 2009; Andonaegui et al., 2012; Días da Silva et al., 2014) (#3a and #3b). The felsic lavas are interbedded in a thrust sheet between the autochthonous Ollo de Sapo antiform and the Ordenes, Cabo Ortegal, and Morais Massif upper thrusts. They are located in the Schistose Domain of Central Iberian Zone and consist of a lower mafic and acidic suite and of an upper acidic volcaniclastic ensemble. The fourth site includes the Urra Rhyolitic Formation in western margin of the Lusitanian-Alcudian subzone of Central Iberian Zone and the tonalite belt of the Central Extremadure batholith (Solá et al., 2005, 2008; Antunes et al., 2009; Neiva et al., 2009; Rubio-Ordóñez et al., 2012) (#4a and #4b). The Urra Rhyolitic Formation comprises a lower prophyritic unit ca. 200 m thick and an upper volcaniclastic unit ca. 500 m thick. The associated plutons are calc-alkaline granites and related

diorites and gabbros. The volcanosedimentary sequence is overlain by the "Armorican Quartzite Formation".

Age datings of the Furongian to early Ordovician magmatic activity limited to the more accurate U-Pb zircon or monazite data are plotted in Fig. 23, also with a distinction between rhyolitic volcanic products and genetically related granitic plutons suspected to belong to magmatic reservoirs of the volcanic counterparts. Ages of rhyolites of the Vendean area (Chantonnay, La Chapelle-Hermier, Saint-Gilles and Mareuil-sur-Lay) sharing the same petrological patterns are not very different to those of the Ollo de Sapo and Guadarrama, taking into account bracketed errors. An earliest Tremadocian age is recorded. Few accurate ages are available for the Mora-Saldanha and Urra volcanics. The Urra site seems to be older and of late Furongian age. But, the Urra volcanic sequence is overlain by the "Armorican Quartzite Formation" that is dated to early Floian (Gutiérrez-Alonso et al., 2007). The associated plutons to volcanics, as demonstrated in the Ollo de Sapo antiform (Díez Montes et al., 2010), are of similar ages. Indeed, ash-fall tuff beds related to the Ollo de Sapo eruptive activity are dated to 477 Ma (4 samples, Gutiérrez-Alonso et al., 2016). One may note that the Pyrenean orthogneisses are clearly younger and belong to a distinct magmatic event.

In the South Armorican Domain, assuming that the Les Essarts Complex orthogneisses are the endogenous sources of Saint-Gilles rhyolitic nappes, there are close likenesses with the Ollo de Sapo magmatic and structural system (#2, Fig. 22) in term of high amounts of magmatic supply and extensive tectonic line. Differences are
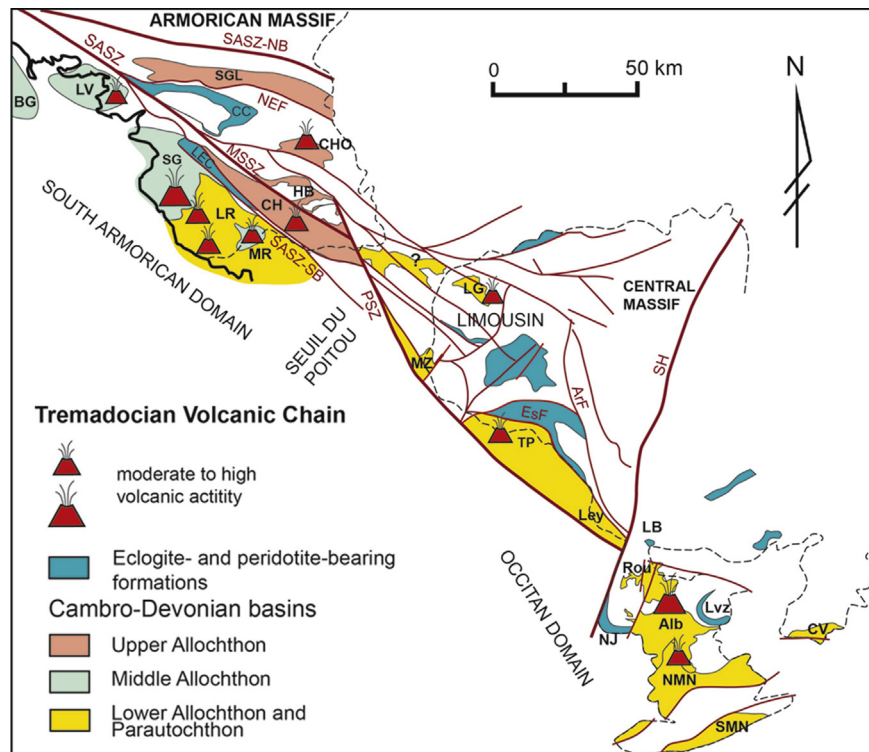
**Figure 23.** Sketch map of the early Palaeozoic basins of the North Gondwana margin from South Armorican to Occitan domains. Basins: Alb, Albigeois; BG, Belle-Île —Groix; CH, Chantonnay; Cho, Cholet; CV, Cévennes; HB, Haut-Bocage; LB, La Roche-sur-Yon; Ley, Leyme; LG, La Gartempe; LV, La Vilaine; MR, Mareuil-sur-Lay; Mz, Mazerolles; NMN, North Montagne Noire; Rou, Rouergue; SG, Saint-Gilles; SGL, Saint-Georges-sur-Loire; SMN, South Montagne Noire; TP, Thiviers-Payzac. Eclogite- and peridotite-bearing formations: CC, Champtoceaux; LB, La Bessenoits; Lvz, Lévézou; NJ, Najac. Faults: ArF, Argentat Fault; EsF, Estivaux Fault; SASZ, South Armorican Shear Zone; NB, northern branch; SB, southern branch; MSSZ, Montaigu-Secondigny Shear Zone; PSZ, Parthenay Shear Zone; SH, Sillon Houiller. Strike-slip motions are estimated to 120 km along the Parthenay Shear Zone, and 80 km along the South Armorican Shear Zone.

explained by much more severe shearing compression and strike slip motion for the Vendean nappe rhyolite leading to décollement of the volcanic cover, while the Ollo de Sapo Formation shows limited thrusting. In the Occitan Domain, owing to its high volume of metarhyolitic flows, the Larroque Volcanic Formation (Figs. 4 and 5), of similar stratigraphic age and petrological significance, is equivalent to the Ollo de Sapo tectono-volcanic system.

It is concluded that a *Tremadocian Tectonic Belt* extended from South Armorican and Occitan domains to Iberian Zones in a swarm of fractures well developed in the Iberian branch, but compressed in the SAOD due to severe thrust and right-lateral shearing. In the South Armorican Domain, this fracture system was reworked along the southern branches of the South Armorican Shear Zone (Figs. 2 and 23). The other fracture zones with their rhyolitic products are manifest in the La Roche-sur-Yon, Chantonnay and Cholet basins (Figs. 2—4). In the Occitan Domain, the reworking of fracture zones which supplied the Larroque Rhyolitic Formation (Fig. 5) precludes accurate location of the initial fracture system.

### 5.3. The question of the propagation of the Tremadocian Tectonic Belt

The Tremadocian Tectonic Belt of the Vendean Intermediate Structural Zone was the source of westward thrust Saint-Gilles — Belle-Île volcanic and sedimentary sequences (Fig. 2). Indeed, eclogites have been exhumed in this structural zone and are suspected to originate from a subducted oceanic crust. Can we infer that the Tremadocian breaking evolved from a continental rift to an ocean basin? In the South Armorican Domain, Tremadocian subaerial rhyolitic lavas are overlain by quartz-rich conglomerates and sandstones belonging to the widespread siliciclastic platform of the

"Armorican Quartzite" facies, a common detrital witness of a syn-rift stage, particularly in the Chantonnay Basin (Fig. 3). Into rifted basins, these coarse deposits were fining upward to shales before being disconformably overlain by the uppermost Ordovician and Silurian shales after a middle—upper Ordovician gap, suggesting a post-rift stage. In the Occitan Domain, the same siliciclastic platform was established, although its sandstone-dominated lithostratigraphic units do not use the classical "Armorican Quartzite" nomenclature. In the Albigeois-northern Montagne Noire area, the lower Ordovician overlying clayey sediments are interbedded with basaltic lavas displaying a salient Initial Rift Tholeiite-enriched magmatic signature (IRT, V5 phase, Fig. 6). However, this volcanic activity ended with the mid Ordovician land emersion, finally constrained by the onset of the Sardic phase (Álvaro et al., 2016). Consequently, the Tremadocian continental break-up was not immediately followed by a marine basin opening. The IRTs were generated during the Tremadocian asthenosphere upwelling and were stored below rhyolitic reservoirs, the high volume of which constituted a barrier for the ascent of deep mafic magmas. After the emptying of the acidic magma chambers and the collapse of the magmatic domes, residual mafic magmas were able to reach the surface. Indeed, where the volume of rhyolitic magma is low, both acidic and mafic magmas reached the surface together, as in the western part of the La Roche-sur-Yon Basin, indicating that these magmas were generated during the same geotectonic event (Fig. 4).

After the Sardic phase and a transpressive-transtensive modification of the Rheic Ocean opening patterns (Helbing and Tiepolo, 2005), also interpreted as the collision of Gondwana with the Qaidam arc and the accretion of the Qilian block (Von Raumer and Stampfli, 2008; Von Raumer et al., 2013, 2015), the previous framework of tectonic troughs was reactivated. Local troughs were
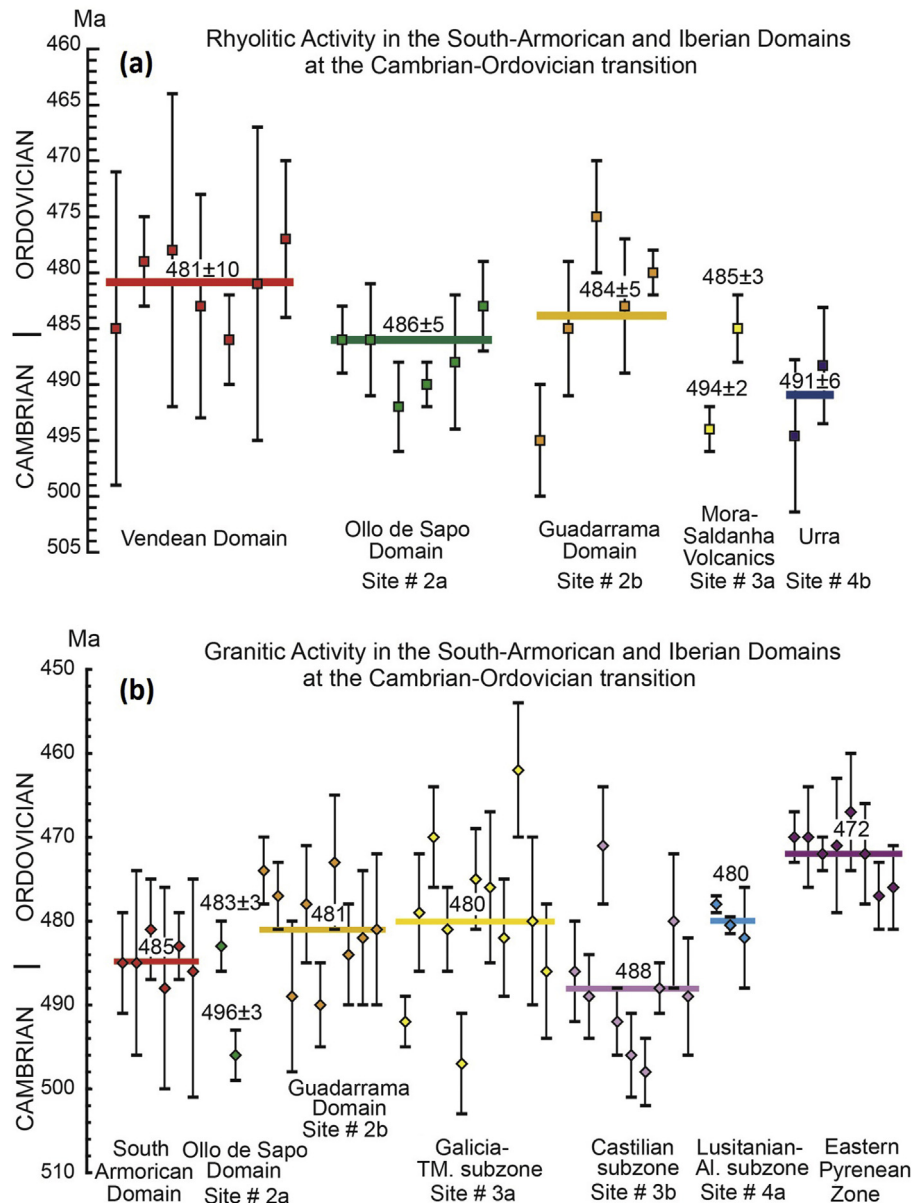
**Figure 24.** Timing of the rhyolitic (a) and granitic (b) activity in the South Armorican, Occitan and Iberian tectono-magmatic lineaments across the Cambrian–Ordovician transition. Age dating from the literature. References in the text.

opened and their palaeoreliefs finally sealed by Silurian and Devonian transgressive deposits (Álvaro et al., 2016). The extensional strain focused along the former Tremadocian Tectonic Belt and an incipient oceanization was reached, as proved by the eclogite remnants. Some eclogites show an N-MORB composition and originated from a depleted mantle, but others display E-MORB, IAT, IRT, and CT geochemical signatures implying contribution of both depleted and enriched mantle sources (Bernard-Griffiths and Jahn, 1981; Bernard-Griffiths and Cornichet, 1985; Paquette et al., 1985; Piboule and Briand, 1985; Berger et al., 2010). These features are consistent with a continent-ocean transition zone and narrow oceanic basins. Similarly, the metabasites of the Île-de-Groix nappe display two contrasting magmatic series mixing transitional tholeiites (E-MORB type) and alkali-basalts originated from unenriched or moderately enriched mantle sources, though isotopically depleted (Bernard-Griffiths et al., 1986; El Korh et al., 2013). Such magmatic features are indicative of both ocean-floor and continental margin. Ages of the eclogites are poorly constrained owing to

discordant interpretations of the various U-Pb zircon ages as inheritance, magmatic crystallization or post-magmatic and metamorphic processes. First isotopic data advocated mid Silurian to early Devonian ages for the high-pressure eclogite facies metamorphism (Peucat et al., 1982; Paquette et al., 1985; Berger et al., 2010). More accurate analyses combining Sm-Nd, Rb-Sr and $^{40}Ar/^{39}Ar$ methods support a late Devonian age (ca. 390 and 360 Ma) for two eclogite units of the Champtoceaux Complex (Bosse et al., 2000). The high-pressure event of the eclogites from the Montagne-Noire Axial Zone is dated at 358 Ma (Faure et al., 2014). Nevertheless, the eclogites may have different sources and different ages. The eclogites of Les Essarts, Champtoceaux and Audierne complexes are usually allotted to an ocean floor subducted until to about 50–60 km in depth (13 kbars) (Godard, 1988, 2001a, 2010; Lucks et al., 2002). This hypothesis is supported by seismic imaging showing a suspected slab that subducted northward below the South Armorican margin (Bitri et al., 2001, 2003, 2010; Judenherc et al., 2003; Gumiaux et al., 2004b). It is thus admitted that an

oceanic crust existed in the Champtoceaux-Les Essarts Siluro–Devonian structural zone and in its prolongation to the western Limousin (Berger et al., 2006, 2010). In the Vendean area, the Chantonnay Basin infill ended with under-water flowing of basaltic lavas of the La Meilleraie Volcanic Formation above a middle–upper Devonian sedimentary terrigenous sequence (Fig. 3). The volcanic rocks consist of transitional tholeiites originated from two mixed depleted and moderately enriched mantle sources (Thiéblemont, 1988) (see Sections 2.1.2. and 4.1.). Geochemical and unpublished Rb/Sr and Nd/Sm isotopic analyses (Thiéblemont, pers. comm. 2014) proved that the La Meilleraie magmatic sources are similar to those of the Les Essarts eclogites that constituted the floor of the neighbouring marine basin drifted from the former Champtoceaux-Les Essarts Ordovician fracture zone. It has also been shown that the western edge of this basin is rimed by the Saint-Martin-des-Noyers metabasites displaying more or less depleted geochemical signatures similar to those of the La Meilleraie metabasalts and the eclogites (Section 3.1.5). These metabasites can thus be attributed to the southwestern margin of the basin whilst the eclogites constituted the basin floor during Devonian times. It is noteworthy that the Devonian La Meilleraie lavas are devoid of severe deformation and were only weakly metamorphosed. The late Devonian convergent compressive strain strictly focused along the oceanic drifted basin because of its thinned and hot lithospheric substratum. The late subduction of the oceanic basin, marked out by the high-pressure metamorphism of oceanic crust (eclogites) and sedimentary cover (blueschists) could be dated around 365–358 Ma (Bosse et al., 2000, 2005). Finally, throughout the South Armorican and Occitan domains, the Silurian–Devonian extensional basin pattern partly reworked the Tremadocian break-up system. Replacing this area in the plate-tectonic reconstruction of the Gondwana margin by Von Raumer and Stampfli (2008), Stampfli et al. (2013), and Von Raumer et al. (2013), the extensional basin inherited from the Tremadocian rifting would be a part of the Palaeotethys as segments of rift structures which are distinctively located south of the propagating eastern branch of the Rheic Ocean (Linnemann et al., 2008).

In the Iberian branch of Ibero-Armorican Arc, the Ollo de Sapo Domain was the site of the above-reported Tremadocian tectonic episode but not of the Siluro–Devonian one. Eclogites are located in the Malpica-Tui Unit, and in the Cabo Ortegal, Órdenes, Bragança and Morais upper allochthonous complexes. The Malpica-Tui Unit emplaced in the lower allochthon that represents a distal part of the Gondwana continental margin (Martínez Catalán et al., 1996). The complexes are suspected to derive from the Rheic Ocean (Martínez Catalán et al., 2009). In that case, they are equivalent to the eclogite-bearing Léon terrains of Brittany (Cabanis and Godard, 1987; Faure et al., 2010). This assumption questions the setting of the Rheic Ocean between Iberia and Armorica and in northwestern Iberia, either east (Martínez Catalán et al., 2009) or west (Simancas et al., 2009) of the northwesternmost Schistose Domain autochthon and its Malpica-Tui Unit lower allochthon. The eastern location is supported by the assumed existence of a volcanic arc according to the suspected calc-alkaline composition of mafic Cambrian magmatic rocks (Andonaegui et al., 2002, 2012, 2016). However, the composition of these rocks is consistent with MORB-like olivine-tholeiites with moderate crustal assimilation, but clearly differs from calc-alkaline arc-related basalts. This composition should agree with the pull-apart basin model proposed by Arenas et al. (2014). By contrast, these mafic rocks are similar to Cambrian lavas of the Montagne Noire (i.e. V2 and V3 volcanic phases). Alternatively, the Iberian allochthonous eclogite-bearing formations may have originated from the continuation of the Audierne area that was reactivated during the Siluro–Devonian opening of South Armorican marine basin. The Malpica-Tui eclogites are considered as equivalent to Champtoceaux-Cellier eclogites (Ballèvre et al., 2009, 2014). In this framework, the thrust sheets of the northwest Iberian allochthonous units would be a remnant of a marine basin that extended from the South Armorican Basin, and not of the Rheic Ocean. This last interpretation is in a good agreement with the model of Ribeiro et al. (2007). For these authors, the allochthonous units resulted from obduction of the western Palaeotethys that is the South-Armorican Ocean. This assumption is also proposed as an alternative model by Ballèvre et al. (2014). Indeed, at the time of the Tremadocian continental break-up episode, the Rheic Ocean was diachronously spreading all along the western edge of Iberian and Armorican domains between Gondwana and Avalonia as shown in the Fig. 25. However, the southwestward propagation (in present coordinates) of the suspected South-Armorican Ocean remains questionable. In the Moroccan High Atlas and Anti-Atlas, any large Tremadocian rhyolitic activity is absent. The rift mainly opened in the earliest Cambrian (Pouclet et al., 2008; Álvaro et al., 2014b) and is related to
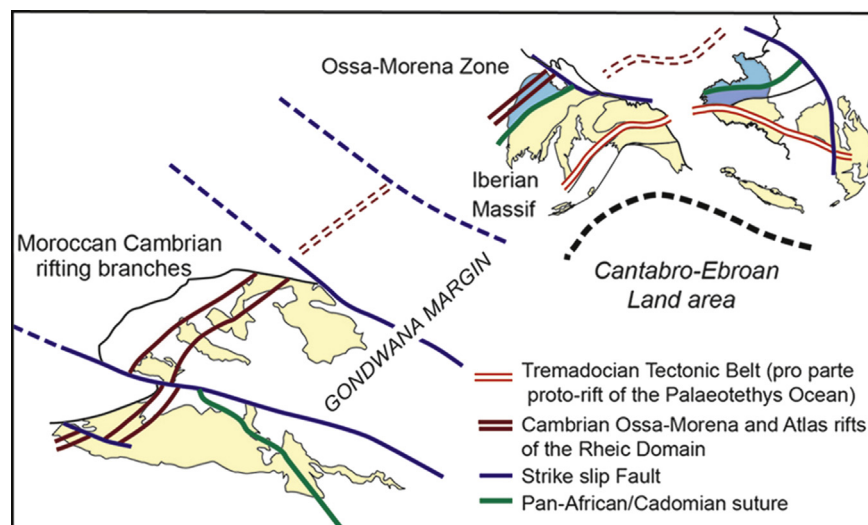


**Figure 25.** Sketch of the northwestern Gondwana margin with setting of the Cambrian to Tremadocian geodynamic structures at the rifting stage of the Rheic Ocean. The Tremadocian Tectonic Belt extended from Occitan and South Armorican domains to the Central Iberian Zone in the North Gondwana continental margin. It provided a suite of rhyolitic magmatic events with, particularly, the volcanic supereruptions of the Larroque, Saint-Gilles, and Ollo de Sapo volcanic formations. Some parts of this system constituted the protorift of the Siluro–Devonian Palaeotethys Ocean.

the Rheic Ocean (Simancas et al., 2009). It extended into the Ossa-Morena Zone in the mid Cambrian (Sánchez-García et al., 2003, 2010; Etxebarria et al., 2006; Sarrionandia et al., 2012), and reached the northern Armorica in the early Ordovician (Faure et al., 2010), as well as the Saxo-Thuringian Zone (Linnemann et al., 2004, 2008; Stampfli et al., 2013). In the following time, the Rheic Ocean evolved to drifting (Sánchez-García et al., 2003) while the extensional tectonic regime ran out in the continental margin.

## 6. Conclusions

The geological background and tectonostratigraphic patterns of the South Armorican and Occitan domains are revised in order to conduct a petrographical and geochemical study of the Cambrian–lower Ordovician volcanic formations.

Across the Precambrian–Cambrian transition, a rhyolitic activity is recorded in the southern part of the Occitan Domain and in the Pyrenean Domain. In the lack of pre-Variscan deformational process, this magmatic activity cannot be allotted to the Cadomian or Pan-African orogeny and its significance remains abstruse. In the late early Cambrian, the first basaltic activity consists of continental tholeiites having some trace element patterns of N-MORBs. The contribution of the asthenospheric mantle suggests a lithospheric thinning and incipient rifting. However, the cumulate features of the lavas, their crustal contamination and the abundance of associated partly melted sialic xenoliths show that the magma was stored during a long time span into a crustal reservoir. Any MORB-like fresh magma never reached the surface. In the middle Cambrian to Furongian, lava flows and sills of continental tholeiites are interbedded in black shales and limestones (Occitan Domain) or turbidities (South Armorican Domain). It could indicate an evolving condition of crustal extension to a drifting state. Instead, the magmatic source of the lavas shows an increasing contribution of an enriched component of the lithospheric mantle and a decreasing involvement of the depleted asthenosphere. Deepening of the sedimentary basin is due to cooling conditions with the cessation of active rifting process. A dramatic change took place in the early Tremadocian with uplifting of the basin floors and important sub-aerial rhyolitic activities in all the sedimentary basins which built the "Tremadocian Volcanic Chain". Two major rhyolitic formations are emphasized, the La Sauzaie and Larroque Volcanic formations which are correlated with the notorious Ollo de Sapo Formation in the Iberian Peninsula. The acidic subaerial volcanics are overlain by coarse siliciclastic detrital sequences, pointing to a rifting process and erosion of rift soulders in the Floian time. Subsequent post-rift deposition of shales with interbedded extension-related tholeiites in deepening basins testifies to increasing subsidence and drifting process.

We postulate that a major continental break-up, the "Tremadocian Tectonic Belt", was initiated by tectonic thinning of the lithosphere and upwelling of the asthenosphere. Mantle-derived mafic magmas intruded the crust and were underplated at the mantle-crust transition zone. This hot material provided heat for melting the crust which supplied the rhyolitic volcanism of the volcanic chain. After emptying of the rhyolitic crustal reservoirs, underlying mafic magmas could ascent and reach the surface.

An attempt is done to continue the Tremadocian Tectonic Belt from South Armorica to Iberia. The extensional process was developed in the Occitan to Iberian continental Cadomian margin while the Rheic Ocean was spreading along this margin in separating the Avalonian and Cadomian terranes. This process was interrupted in the mid-to-late Ordovician times and renewed in the Silurian. Then, the oceanization took place along the inherited fracture zone of the Tremadocian Tectonic Belt that acted as a lithospheric plate margin and focused all the driving forces. Indeed,

the Tremadocian fracture network guided the opening of the Siluro–Devonian Massif Central–South Armorican Ocean that evolved to part of the Palaeotethys Ocean.

## References

Alabouvette, B., 1984. Notice explicative, Carte géol. France (1/50 000), feuille Lodève (989). Bureau de Recherches Géologiques et Minières, Orléans, 52 p (in French).

Alabouvette, B., 1988. Notice explicative, Carte géol. France (1/50 000), feuille Le Vigan (937). Bureau de Recherches Géologiques et Minières, Orléans, 68 p (in French).

Alsac, C., 1991. Etude pétrographique des roches volcaniques du mont Merdellou (monts de l'Est de Lacaune). Rap. Bureau de Recherches Géologiques et Minières, 91GEOPHG, 62 p (in French).

Alsac, C., Cabanis, B., Guérangé-Lozes, J., Béziat, D., 1987. Caractères magmatiques du volcanisme basique ordovicien de la nappe de Saint-Salvi-de-Carcavès dans l'Albigeois cristallin (Tarn-Aveyron, France). Comptes Rendus de l'Académie des Sciences, Paris 305, 1199–1205 (in French with English abstract).

Álvaro, J.J., Vizcaïno, D., 1999. Biostratigraphic significance and environmental setting of the trace fossil *Psammichnites* in the Lower Cambrian of the Montagne Noire, France. Bulletin de la Societe Geologique de France 170, 821–828 (in French with English abstract).

Álvaro, J.J., Vizcaïno, D., Chauvel, J.J., Courjault-Radé, P., Dabard, M.P., Debrenne, F., Feist, R., Pillola, G.L., Vennin, E., 1998. Nouveau découpage stratigraphique des séries cambriennes des nappes de Pardailhan et du Minervois (versant sud de la Montagne Noire, France). Geologie de la France 2 (1998), 3–12 (in French with English abstract).

Álvaro, J.J., Ezzouhairi, H., Ribeiro, M.L., Ramos, J.F., Solá, A.R., 2008. Early Ordovician volcanism of the Iberian Chains (NE Spain) and its influence on preservation of shell concentrations. Bulletin de la Societe Geologique de France 179, 569–581.

Álvaro, J.J., Monceret, E., Monceret, S., Verraes, G., Vizcaïno, D., 2010. Stratigraphic record and palaeogeographic context of the Cambrian Epoch 2 subtropical carbonate platforms and their basinal counterparts in SW Europe, West Gondwana. Bulletin of Geosciences 85, 573–584.

Álvaro, J.J., Bauluz, B., Clausen, S., Devaere, L., Gil Imaz, A., Monceret, E., Vizcaïno, D., 2014a. Stratigraphic review of the Cambrian–Lower Ordovician volcanosedimentary complexes from the northern Montagne Noire, France. Stratigraphy 11, 83–96.

Álvaro, J.J., Bellido, F., Gasquet, D., Pereira, M.F., Quesada, C., Sánchez-Garcia, T., 2014b. Diachronism in the late Neoproterozoic–Cambrian arc-rift transition of North Gondwana: a comparison of Morocco and the Iberian Ossa-Morena. Journal of African Earth Sciences 98, 113–132.

Álvaro, J.J., Colmenar, J., Monceret, E., Pouclet, A., Vizcaïno, D., 2016. Late Ordovician (post–Sardic) rifting branches in the North Gondwanan Montagne Noire and Mouthoumet massifs of southern France. Tectonophysics. http://dx.doi.org/10.1016/j.tecto.2015.11.031.

Andonaegui, P., González del Tánago, J., Arenas, R., Abati, J., Martínez Catalán, J.R., Peinado, M., Díaz García, F., 2002. Tectonic setting of the Monte Castelo gabbro (Ordenes Complex, northwestern Iberian Massif): evidence for an arc-related terrane in the hanging wall of the Variscan suture. In: Martínez Catalán, J.R., Hatcher Jr., R.D., Arenas, R., Díaz García, F. (Eds.), Variscan–Appalachian Dynamics: The Building of the Late Palaeozoic Basement, Geological Society of America Special Papers, vol. 364, pp. 37–56.

Andonaegui, P., Castiñeiras, P., González Cuadra, P., Arenas, R., Sánchez Martínez, S., Abati, J., Díaz García, F., Martínez Catalán, J.R., 2012. The Corredoiras orthogneiss (NW Iberian Massif): geochemistry and geochronology of the Paleozoic magmatic suite developed in a peri-Gondwanan arc. Lithos 128–131, 84–99.

Andonaegui, P., Sánchez Martínez, S., Castiñeiras, P., Abati, J., Arenas, R., 2016. Reconstructing subduction polarity through the geochemistry of mafic rocks in a Cambrian magmatic arc along the Gondwana margin (Órdenes Complex, NW Iberian Massif). International Journal of Earth Sciences 105 (3), 713–725.

Antunes, I.M.H.R., Neiva, A.M.R., Silva, M.M.V.G., Corfu, F., 2009. The genesis of I- and S-type granitoid rocks of the Early Ordovician Oledo pluton, Central Iberian Zone (central Portugal). Lithos 111, 168–185.

Arenas, R., Díez Fernández, R., Sánchez Martínez, S., Gerdes, A., Fernández-Suárez, J., Albert, R., 2014. Two-stage collision: exploring the birth of Pangea in the Variscan terranes. Gondwana Research 25-2, 756–763.

Audren, C., Jégouzo, P., Barbaroux, L., 1975. Notice explicative, Carte géol. France (1/50 000), feuille La Roche-Bernard (449). Bureau de Recherches Géologiques et Minières, Orléans, 41 p (in French with English abstract).

Augier, R., Choulet, F., Faure, M., Turillot, P., 2015. A turning-point in the evolution of the Variscan orogen: the ca. 325 Ma regional partial-melting event of the coastal South Armorican domain (South Brittany and Vendée, France). Bulletin de la Société géologique de France 186 (2–3), 63–91.

Ballèvre, M., Capdevila, R., Guerrot, C., Peucat, J.-J., 2002. Discovery of an alkaline orthogneiss in the eclogite-bearing Cellier Unit (Champtoceaux Complex, Armorican Massif): a new witness of the Ordovician rifting. Comptes Rendus Geoscience 334, 303–311.

Ballèvre, M., Bosse, V., Ducassou, C., Pitra, P., 2009. Palaeozoic history of the Armorican Massif: models for the tectonic evolution of the suture zones. Comptes Rendus Geoscience 341, 174–201.

Ballèvre, M., Fourcade, S., Capdevila, R., Peucat, J.-J., Cocherie, A., Mark Fanning, C., 2012. Ordovician felsic volcanism in the Southern Armorican Massif (Variscan belt, France): implications fro the breakup of Gondwana. Gondwana Research 21, 1019–1036.

Ballèvre, M., Martínez Catalán, J.R., López-Carmona, A., Pitra, P., Abati, J., Díez Fernández, R., Ducassou, C., Arenas, R., Bosse, V., Castiñeiras, P., Fernández-Suárez, J., Gómez Barreiro, J., Paquette, J.-L., Peucat, J.-J., Poujol, M., Ruffet, G., Sánchez Martínez, S., 2014. Correlation of the nappe stack in the Ibero-Armorican arc across the Bay of Biscaye: a joint French-Spanish project. In: Schulmann, K., Martínez Catalán, J.R., Lardeaux, J.M., Janoušek, V., Oggiano, G. (Eds.), The Variscan Orogeny: Extent, Timescale and the Formation of the European Crust, Geological Society, London, Special Publications, vol. 405.

Bea, F., Montero, P., Talavera, C., Zinger, T., 2006. A revised Ordovician age for the Miranda do Douro orthogneiss, Portugal. Zircon U-Pb ion-microprobe and La-ICPMS dating. Geologica Acta 4 (3), 395–401.

Bea, F., Pesquera, A., Montero, P., Torres-Ruiz, J., Gil-Crespo, P.P., 2009. Tourmaline $^{40}Ar/^{39}Ar$ chronology of tourmaline-rich rocks from Central Iberia dates the main Variscan deformation phases. Geologica Acta 7 (4), 399–412.

Béchennec, F., Hallégouët, B., Thiéblemont, D., 1999. Notice explicative, Carte géol. France (1/50 000), feuille Quimper (346). Bureau de Recherches Géologiques et Minières, Orléans, 120 p (in French).

Béchennec, F., Chèvremont, P., Stussi, J.M., Thiéblemont, D., 2008. Notice explicative, Carte géol. France (1/50 000), feuille Le Poiré-sur-Vie (561). Bureau de Recherches Géologiques et Minières, Orléans, 180 p. Carte géologique par Béchennec, F., Chèvremont, P., Schuster, M., Lacquement, F. (2008) (in French).

Béchennec, F., Chèvremont, P., Bouton, P., Karnay, G., Stussi, J.M., Thiéblemont, D., 2010. Notice explicative, Carte géol. France (1/50 000), feuille Luçon (585). Bureau de Recherches Géologiques et Minières, Orléans, 188 p. Carte géologique par Béchennec, F., Chèvremont, P., Karnay, G., Grabenstaetter, L., Bouton, P. (2010) (in French).

Berger, G.M., Alabouvette, B., Bessière, G., Bilotte, M., Crochet, B., Dubar, M., Marchal, J.P., Tambareau, Y., Viallatte, J., Viallard, P., 1997. Notice explicative, Carte géol. France (1/50 000), feuille Tuchan (1078). Bureau de Recherches Géologiques et Minières, Orléans, 113 p. Carte géologique par Berger, G.M., Bessière, G., Bilotte, M., Viallard, P. (1997) (in French).

Berger, J., Féménias, O., Mercier, J.C.C., Demaiffe, D., 2006. A Variscan slow-spreading ridge (MOR–LHOT) in Limousin (French Massif Central): magmatic evolution and tectonic setting inferred from mineral chemistry. Mining Magazine 70, 175–185.

Berger, J., Féménias, O., Ohnenstetter, D., Bruguier, O., Plissart, G., Mercier, J.-C., Demaiffe, D., 2010. New occurrence of UHP eclogites in Limousin (French Massif Central): age, tectonic setting and fluid-rock interactions. Lithos 118, 365–382.

Bergeron, J., 1888. Note sur les roches éruptives de la Montagne Noire. Bulletin de la Société géologique de France (sér. 3) 17, 54–63 (in French).

Bernard-Griffiths, J., Jahn, B.M., 1981. REE geochemistry of eclogites and associated rocks from Sauviat-sur-Vige, Massif Central, France. Lithos 14, 263–274.

Bernard-Griffiths, J., Cornichet, J., 1985. Origin of eclogites from South Brittany, France: a Sm-Nd isotopic and REE study. Chemical Geology 52, 185–201.

Bernard-Griffiths, J., Carpenter, M.S.N., Peucat, J.J., Jahn, B.M., 1986. Geochemical and isotopic characteristics of blueschist facies rocks from the Ile de Groix, Armorican Massif (north-west France). Lithos 19, 235–253.

Bessière, G., Schulze, H., 1984. Le Massif de Mouthoumet (Aude, France): nouvelle définition des unités structurales et essai d'une reconstruction paléo-géographique. Bulletin de la Société géologique de France 26, 885–894 (in French).

Bessière, G., Baudelot, S., 1988. Le Paléozoïque inférieur du massif de Mouthoumet (Aude, France) replacé dans le cadre du domaine sud–Varisque: révision et conséquences. Comptes Rendus de l'Académie des Sciences, Paris (sér 2) 307, 771–777 (in French).

Bessière, G., Bilotte, M., Crochet, B., Peybernès, B., Tambereau, Y., Villatte, J., 1989. Notice explicative, Carte géol. France (1/50 000), feuille Quillan (1077). Bureau de Recherches Géologiques et Minières, Orléans, 98 p. Carte géologique par Crochet, B., Vialatte, J., Tambareau, Y., Bilotte, M., Bousquet, J.P., Kuhfuss, A., Bouillin, J.P., Gélard, J.P., Bessière, G., Paris, J.P. (1989) (in French).

Béziat, D., Bruchon, I., Joron, J.L., Monchoux, P., 1992. Caractères magmatiques des volcanites du Cambrien des Monts de l'ouest de Lacaune (versant nord de la Montagne Noire). Comptes Rendus de l'Académie des Sciences, Paris 314, 475–481 (in French).

Béziat, D., Joron, J.L., Monchoux, P., 1993. Spessartites in the Montagne Noire, France: mineralogical and geochemical data, 5, 879–891.

Bitri, A., Brun, J.-P., Truffert, C., Guennoc, P., 2001. Deep seismic imaging of the Cadomian thrust wedge of Northern Brittany. Tectonophysics 331 (1–2), 65–80.

Bitri, A., Ballèvre, M., Brun, J.P., Chantraine, J., Gapais, D., Guennoc, P., Gumiaux, C., Truffert, C., 2003. Seismic imaging of the Hercynian collision zone in the south-eastern Armorican Massif (Armor 2 project/Géofrance 3D Program). Comptes Rendus Geoscience 335, 969–979.

Bitri, A., Brun, J.-P., Gapais, D., Cagnard, F., Gumiaux, C., Chantraine, J., Martelet, G., Truffert, C., 2010. Deep reflection seismic imaging of the internal zone of the

South Armorican Hercynian belt (western France) (ARMOR 2/Géofrance 3D Program). Comptes Rendus Geoscience 342, 448–452.

Bogdanoff, S., Donnot, M., Ellenberger, F., 1984. Notice explicative, Carte géol. France (1/50 000), feuille Bédarieux (988). Bureau de Recherches Géologiques et Minières, Orléans, 105 p (in French).

Bosse, V., Féraud, G., Ruffet, G., Ballèvre, M., Peucat, J.-J., de Jong, K., 2000. Late Devonian subduction and early-orogenic exhumation of eclogite-facies rocks from the Champtoceaux Complex (Variscan belt, France). Geological Journal 35, 297–325.

Bosse, V., Féraud, G., Ballèvre, M., Peucat, J.-J., Corsini, M., 2005. Rb-Sr and $^{40}Ar/^{39}Ar$ ages in blueschists from Ile de Groix (Armorican Massif, France): implications for closure mechanisms in isotope systems. Chemical Geology 220, 21–45.

Bouton, P., Branger, P., 2007. Notice explicative, Carte géol. France (1/50 000), feuille Coulonges-sur-l'Autize (587). Bureau de Recherches Géologiques et Minières, Orléans, 132 p. Carte géologique par Bouton, P., Branger, P. (2007) (in French).

Boyer, C., 1974. Volcanismes acides paléozoïques dans le massif armoricain. Ph.D. thesis. Univ. Orsay, 384 p (in French).

Brun, J.P., Burg, J.P., 1982. Combined thrusting and wrenching in the Ibero-Armorican arc: a corner effect during continental collision. Earth and Planetary Science Letters 61, 319–332.

Burg, J.P., 1981. Tectonique tangentielle hercynienne en Vendée littorale: signification des linéations E-W dans les porphyroïdes à foliation horizontale. Comptes Rendus de l'Académie des Sciences, Paris 293 (II), 849–854 (in French).

Burg, J.P., Bale, P., Brun, J.P., Giradeau, J., 1987. Stretching lineation and transport direction in the Ibero-Armorican arc during the Siluro-Devonian collision. Geodynamica Acta 1 (1), 71–87.

Cabanis, B., Godard, G., 1987. Les éclogites du pays de Léon (Nord-Ouest du Massif armoricain): étude pétrologique et géochimique; implications géodynamiques. Bulletin de la Société géologique de France (sér. 8) 3 (6), 1133–1142 (in French).

Cabanis, B., Thiéblemont, D., 1988. La discrimination des tholéiites continentales et des basaltes arrière-arc. Proposition d'un nouveau diagramme, le triangle Th-3xTb-2xTa. Bulletin de la Société géologique de France (sér. 8) 4 (6), 927–935 (in French).

Cagnard, F., Gapais, D., Brun, J.P., Gumiaux, C., Van den Driessche, J., 2004. Late pervasive crustal-scale extension in the south Armorican Hercynian belt (Vendée, France). Journal of Structural Geology 26, 435–449.

Calvez, J.Y., 1976. Comportement des systèmes uranium-plomb et rubidium-strontium dans les orthogneiss d'Icart et de Moëlan (Massif Armoricain). Ph.D. thesis. Univ. Rennes, 74 p (in French).

Cannat, M., Bouchez, J.-L., 1986. Linéations N-S et E-W en Vendée littorale (Massif armoricain). Episodes tangentiels successifs éo–hercyniens en France occidentale. Bulletin de la Société géologique de France (sér. 8) 2 (2), 299–310 (in French).

Cartier, C., Faure, M., 2004. The Saint-Georges-sur-Loire olistostromes, a key zone to understand the Gondwana-Armorica boundary in the Variscan belt (Southern Brittany, France). International Journal of Earth Sciences 93, 945–958.

Cartier, C., Faure, M., Lardeux, H., 2001. The Hercynian Orogeny in the South Armorican Massif (Saint-Georges-sur-Loire Unit, Ligerian Domain, France): rifting and welding of continental stripes. Terra Nova 13, 143–149.

Casas, J.M., Navidad, M., Castiñeiras, P., Liesa, M., Aguilar, C., Carreras, J., Hofmann, M., Gärtner, A., Linnemann, U., 2015. The Late Neoproterozoic magmatism in the Ediacaran series of the Eastern Pyrenees: new ages and isotope geochemistry. International Journal of Earth Sciences 104, 909–925.

Castiñeiras, P., Navidad, M., Liesa, M., Carreras, J., Casas, J.M., 2008. U-Pb zircon ages (SHRIMP) for Cadomina and Early Ordovician magmatism in the Eastern Pyrenees: new insights into the pre–Variscan evolution of the northern Gondwana margin. Tectonophysics 461, 228–239.

Cavet, P., Gruet, M., Pillet, J., 1966. Sur la présence de Cambrien à *Paradoxides* à Cléré-sur-Layon (Maine-et-Loire), dans le Nord-Est du Bocage vendéen (Massif armoricain). Comptes Rendus de l'Académie des Sciences, Paris (sér. D) 263, 1685–1688 (in French).

Cocchio, A.M., 1982. Donnés nouvelles sur les acritarches du Trémadoc et de l'Arénig dans le Massif de Mouthoumet (Corbières, France). Revue de Micro-paléontologie 25, 26–39 (in French).

Cocherie, A., Albarède, F., 2001. An improved U-Th-Pb age calculation for electron probe dating of monazite. Geochimica et Cosmochimica Acta 65, 450–452.

Cocherie, A., Baudin, T., Autran, A., Guerra, C., Fanning, C.M., Laumonier, B., 2005. U–Pb zircon (ID–TIMS and SHRIMP) evidence for the early Ordovician intrusion of metagranites in the late Proterozoic Canaveilles Group of the Pyrenees and the Montagne Noire (France). Bulletin de la Société géologique de France 176, 269–282.

Cohen, H., Tormo, N., 2006. Lithostratigraphie du Groupe de Barroubio dans l'unité de Mélagues (Versant Nord de la Montagne Noire, France). Bulletin de la Société d'étude et de Sciences Naturelles de Béziers 21 (62), 16–25 (in French).

Colchen, M., Poncet, D., 1989. Présence, dans la série paléozoïque de Brétignolles-sur-Mer (Vendée, sud du massif armoricain), d'une formation à blocs et olistolites d'âge dinantien. Conséquences géodynamiques. Comptes Rendus de l'Académie des Sciences 309 (Série II), 1503–1507 (in French).

Comble, C., De Wever, P., Ters, M., Weyant, M., 1985. Découverte de Conodontes et de Radiolaires d'âge Tournaisien dans les schistes bariolés de Brétignolles-sur-Mer (Vendée). Comptes Rendus de l'Académie des Sciences, Paris 300, 899–904 (in French).

Cornet, C., 1980. Genèse structurale des Corbières. Bulletin de la Société géologique de France (sér. 7) 22, 179–184 (in French).

Courtessole, R., 1973. Le Cambrien moyen de la Montagne Noire. Biostratigraphie. Imprimerie d'Oc, Montpellier, 248 p (in French).

Debrenne, F., Courjault-Radé, P., 1986. Découverte de faunules d'Achéocyathes dans l'Est des monts de Lacaune, flanc nord de la Montagne Noire. Interprétations

biostratigraphiques. Bulletin de la Société géologique de France (sér. 8) 2 (2), 285–292 (in French).

Debrenne, F., Orgeval, J.J., Verraes, G., 1976. Présence d'Archéocyathes dans le substratum carbonaté de la mine des Malines (Gard, France). Comptes Rendus sommaires de la Société géologique de France 6, 259–261 (in French).

Deflandre, G., Ters, M., 1966. Sur la présence d'Acritarches ordoviciens dans les schistes subardoisiers de la région de la Mothe-Achard (Vendée). Extension du Silurien en Vendée littorale. Comptes Rendus de l'Académie des Sciences, Paris 262, 237–240 (in French).

Deflandre, G., Ters, M., 1970. Présence de microplancton silurien fixant l'âge des ampelites associées aux phtanites de Brétignolles (Vendée). Comptes Rendus de l'Académie des Sciences, Paris 270, 2162–2166 (in French).

Demange, M., Guérangé-Lozes, J., Guérangé, B., 1995. Notice explicative, Carte géol. France (1/50 000), feuille Lacaune (987). Bureau de Recherches Géologiques et Minières, Orléans, 153 p. Carte géologique par Demange, M., Guérangé-Lozes, J., Guérangé, B. (1996) (in French).

Devaere, L., Clausen, S., Steiner, M., Álvaro, J.J., Vachard, D., 2013. Chronostratigraphic and palaeogeographic significance of an early Cambrian microfauna from the Heraultia Limestone, northern Montagne Noire, France. Palaeontologia Electronica, 16.2.17A, 91 p.

Días da Silva, I., Valverde-Vaquero, P., González Clavijo, E., Díez-Montes, A., Martínez Catalán, J.R., 2014. Structural and stratigraphical significance of U-Pb ages from the Mora and Sardanha volcanic complex (NE Portugal, Iberian Variscides). In: Schulman, K., Martínez Catalán, J.R., Lardeaux, J.M., Janousek, V., Oggiano, G. (Eds.), The Variscan Orogeny: Extent, Timescale and the Formation of European Crust, Geological Society, London, Special Publications, vol. 405, pp. 115–135.

Díez Montes, A., Martínez Catalán, J.R., Bellido Mulas, F., 2010. Role of the Ollo de Sapo massive felsic volcanism in the Early Ordovician dynamics of northern Gondwana. Gondwana Research 17, 363–376.

Diot, H., Féménias, O., Moreau, C., Gaufriau, A., Roy, C., Karnay, G., 2007. Notice explicative, Carte géol. France (1/50 000), feuille Fontenay-le-Comte (586). Bureau de Recherches Géologiques et Minières, Orléans, 96 p. Carte géologique par Moreau, C., Femenias, O., Diot, H., Karnay, G. (2007) (in French).

Diot, H., Féménias, O., Gaufriau, A., Lebret, P., Paquet, F., 2015. Notice explicative, Carte géol. France (1/25 000), feuille Ile d'Yeu (559). Bureau de Recherches Géologiques et Minières, Orléans (in French).

Donnot, M., Guérangé, B., 1978. Le synclinorium cambrien de Brusque. Implications stratigraphiques et structurales dans les Monts de l'Est de Lacaune (Tarn, Aveyron, Hérault). Versant nord de la Montagne Noire. Bulletin du Bureau de Recherches Géologiques et Minières 4, 333–363 (in French).

Ducassou, C., Poujol, M., Hallot, E., Bruguier, O., Ballèvre, M., 2011. Petrology and age of the high-K calc-alkaline Mésanger magmatism (Armorican massif, France): implications for the dextral displacement along the Nort-sur-Erdre Fault. Bulletin de la Société géologique de France 182 (6), 467–477.

Durand, B., Gagny, C., 1966. Observations sur le mode de gisement et les conditions de mise en place des coulées volcaniques spilitisées de Peyrebrune (région de Réalmont), Tarn/France. Geologische Rundschau 55, 329–341 (in French).

El Korh, A., Schmidt, S.Th, Vennemann, T., Ballèvre, M., 2013. Trace element and isotopic fingerprints in HP-LT metamorphic rocks as a result of fluid-rock interactions (Ile de Groix, France). Gondwana Research 23 (3), 880–900.

Etxebarria, M., Chalot-Prat, F., Apraiz, A., Eguiluz, L., 2006. Birth of a volcanic passive margin in Cambrian time: rift paleogeography of the Ossa-Morena Zone, SW Spain. Precambrian Research 147, 366–383.

Faure, M., Leloix, C., Roig, J.Y., 1997. L'évolution polycyclique de la chaîne hercynienne. Bulletin de la Société géologique de France 168, 695–705 (in French).

Faure, M., Bé Mézème, E., Duguet, M., Cartier, C., Talbot, J.-Y., 2005. Paleozoic tectonic evolution of medio-europa from the example of the massif central and massif armoricain. Journal of the Visual Explorer 19 (5), 26.

Faure, M., Be Mezeme, E., Cocherie, A., Rossi, P., Chemenda, A., Boutelier, D., 2008. Devonian geodynamic evolution of the Variscan Belt, insights from the French Massif Central and Massif Armoricain. Tectonics 27 (2), TC2005.

Faure, M., Sommers, C., Melleton, J., Cocherie, A., Lautout, O., 2010. The Léon Domain (French Massif Armoricain): a westward extension of the Mid-German Crystalline Rise? Structural and geochronological insights. International Journal of Earth Sciences 99, 65–91. http://dx.doi.org/10.1007/s00531-008-0360-x.

Faure, M., Cocherie, A., Gaché, J., Esnault, C., Guerrot, C., Rossi, P., Wei, L., Qiuli, L., 2014. Middle carboniferous intracontinental subduction in the Outer zone of the variscan Belt (Montagne noire axial zone, French Massif Central): multimethod geochronological approach of polyphase metamorphism. In: Schulmann, K., Martínez Catalán, J.R., Lardeaux, J.M., Janousek, V., Oggiano, G. (Eds.), The Variscan Orogeny: Extent, Timescale and the Formation of the European Crust, Geological Society, London, Special Publications, vol. 405, pp. 289–311.

Floc'h, J.-P., Joubert, J.M., Constans, J., Maurin, G., 1993. Notice explicative, carte géol. France (1/50 000), feuille Bellac (639). Bureau de Recherches Géologiques et Minières, Orléans, 78 p (in French).

Fournier-Vinas, C., Débat, P., 1970. Présence de micro-organismes dans les terrains métamorphiques précambriens (schistes X) de l'Ouest de la Montagne Noire. Bulletin de la Société géologique de France 12, 351–355 (in French).

Frost, B.R., Barnes, C.G., Collins, W.J., Arculus, R.J., Ellis, D.J., Frost, C.D., 2001. A geochemical classification for granitic rocks. Journal of Petrology 42, 2033–2048.

Gachet, G., 1983. Volcanisme cambrien des unités de Brusque et du Merdellou (monts de l'Est de Lacaune). Approches pétrographiques et structurales. Ph.D. thesis. Claude Bernard Univ., Lyon, 133 p (in French).

García-Mondéjar, J., 1996. Plate reconstruction of the Bay of Biscay. Geology 24, 635–638.

Gasquet, D., Levresse, G., Cheilletz, A., Azizi-Samir, M.R., Mouttaqi, A., 2005. Contribution to a geodynamic reconstruction of the Anti-Atlas (Morocco) during Pan-African times with the emphasis on inversion tectonics and metallogenic activity in the Precambrian-Cambrian transition. Precambrian Research 140, 157–182.

Godard, G., 1981. Lambeaux probables d'une croûte océanique subductée : les éclogites de Vendée (Massif Armoricain, France). Ph.D. thesis. Univ. Nantes, France, 153 p (in French).

Godard, G., 1983. Dispersion tectonique des éclogites de Vendée lors d'une collision continent-continent. Bull. Mineral 106, 719–722 (in French).

Godard, G., 1988. Petrology of some eclogites in the Hercynides: the eclogites from the southern Armorican massif, France. In: Smith, D.C. (Ed.), Eclogites and Eclogites-facies Rocks. Elsevier, Amsterdam, pp. 451–519.

Godard, G., 2001a. The Les Essarts eclogite-bearing metamorphic Complex (Vendée, southern Armorican Massif, France): Pre–Variscan terrains in the Hercynian belt? Géologie de la France 2001 (1/2), 19–51.

Godard, G., 2001b. Eclogites and their geodynamic interpretation: a history. Journal of Geodynamics 32, 165–203.

Godard, G., 2010. Two orogenic cycles recorded in eclogites-facies gneiss from the southern Armorican Massif (France). European Journal of Mineralogy 21, 1173–1190.

Godard, G., Bouton, P., Poncet, D., 2010. Notice explicative, carte géol. France (1/50 000), feuille Montaigu (536). Bureau de Recherches Géologiques et Minières, Orléans, 171 p. Carte géologique par Godard, G., Bouton, P., Poncet, D., Carlier, G., Chevalier, M. (2007) (in French).

Goujou, J.C., Debrand-Passard, S., Hantzpergue, P., Lebret, P., 1994. Notice explicative, carte géol. France (1/50 000), feuille Les Sables d'Olonne-Longeville (584). Bureau de Recherches Géologiques et Minières, Orléans, 95 p (in French).

Gradstein, F.M., Ogg, J.G., Smith, A.G., Bleeker, W., Lourens, L.J., 2004. A new geological time scale, with special reference to Precambrian and Neogene. Episodes 27, 83–100.

Guérangé-Lozes, J., 1987. Les nappes varisques de l'Albigeois cristallin. Lithostratigraphie, volcanisme et déformations. Doc. Bureau de Recherches Géologiques et Minières 135, 1–257 (in French).

Guérangé-Lozes, J., Burg, J.P., 1990. Les nappes varisques du Sud-Ouest du Massif Central. Géologie de la France 3 (4), 71–106 (in French).

Guérangé-Lozes, J., Guérangé, B., 1991. Notice explicative, Carte géol. France (1/50 000), feuille Camarès (961). Bureau de Recherches Géologiques et Minières, Orléans, 84 p. Carte géologique par Donnot, M., Lefavrais, A., Lablanche, G., Greber, C., Rouchy, J.M., Prian, J.P. (1990) (in French).

Guérangé-Lozes, J., Mouline, M.P., 1998. Notice explicative, Carte géol. France (1/50 000), feuille Carmaux (933). Bureau de Recherches Géologiques et Minières, Orléans, 65 p. Carte géologique par Guérangé-Lozes, J., Mouline, M.P. (1998) (in French).

Guérangé-Lozes, J., Alabouvette, B., 1999. Notice explicative, Carte géol. France (1/50 000), feuille Saint-Sernin-sur-Rance (960). Bureau de Recherches Géologiques et Minières, Orléans, 84 p. Carte géologique par Guérangé-Lozes, J., Alabouvette, B. et al. (1999) (in French).

Guérangé-Lozes, J., Guérangé, B., Mouline, M.P., Delsahut, B., 1996. Notice explicative, Carte géol. France (1/50 000), feuille Réalmont (959). Bureau de Recherches Géologiques et Minières, Orléans, 78 p. Carte géologique par Guérangé-Lozes et al. (1996) (in French).

Guerrot, C., Béchennec, F., Thiéblemont, D., 1997. Le magmatisme paléozoïque de la partie nord-ouest du domaine sud-armoricain: données géochronologiques nouvelles. Comptes Rendus de l'Académie des Sciences, Paris (sér. 2a) 324, 977–984 (in French).

Guillot, P.L., Boyer, C., Tegyey, M., 1977. Grès de Thiviers, ardoises d'Allassac, quartzites de Payzac: un complexe volcano-détritique rhyo-dacitique dans la série métamorphique du Bas-Limousin (Massif Central français). Bulletin du Bureau de Recherches Géologiques et Minières 1 (3), 189–208 (in French).

Guillot, P.L., Lefavrais-Raymond, A., Astruc, J.G., Bonjoly, D., 1989. Notice explicative, carte géol. France (1/50 000), feuille La Capelle Marival (834). Bureau de Recherches Géologiques et Minières, Orléans, 67 p (in French).

Guillot, P.L., Astruc, J.G., Feix, I., Humbert, L., Lefavrais-Henri, M., Lefavrais-Raymond, A., Michard, A., Monier, G., Roubichou, P., 1992. Notice explicative, carte géol. France (1/50 000), feuille Saint-Céré (810). Bureau de Recherches Géologiques et Minières, Orléans, 76 p (in French).

Guineberteau, B., 1986. Le massif granitique de Mortagne-sur-Sèvre (Vendée) : structure, gravimétrie, mise en place: distribution de U-Th-K. Géologie et Géochimie de l'Uranium 11, 218 (in French).

Guiraud, M., Burg, J.P., Powell, R., 1987. Evidence for a Variscan suture zone in the Vendée, France: a petrological study of blueschist facies rocks from Bois de Cené. Journal of Metamorphic Geology 5, 225–237.

Gumiaux, C., Gapais, D., Brun, J.P., Chantraine, J., Ruffet, G., 2004a. Tectonic history of the Hercynian Armorican Shear belt (Brittany, France). Geodinamica Acta 17, 289–307.

Gumiaux, C., Judenherc, S., Brun, J.P., Gapais, D., Granet, M., Poupinet, G., 2004b. Restoration of lithosphere-scale wrenching from integrated structural and tomographic data (Hercynian belt of western France). Geology 32, 333–336.

Gutiérrez-Alonso, G., Fernández-Suárez, J., Gutiérrez-Marco, J.C., Corfu, F., Murphy, J.B., Suárez, M., 2007. U-Pb depositional age for the upper Barrios Formation (Armorican Quartzite facies) in the Cantabrian zone of Iberia: Implications for stratigraphic correlation and paleogeography. In: Linnemann, U., Nance, R.D., Kraft, P., Zulauf, G. (Eds.), The Evolution of the Rheic Ocean: From Avalonian–Cadomian active margin to Alleghenian–Variscan collision, Geological Society of America Special Paper, vol. 423, pp. 287–296.

Gutiérrez-Alonso, G., Gutiérrez-Marco, J.C., Fernández-Suárez, J., Bernárdez, E., Corfu, F., 2016. Was there a super-eruption on the Gondwana coast 477 Ma ago? Tectonophysics. http://dx.doi.org/10.1016/j.tecto.2015.12.012.

Helbing, H., Tiepolo, M., 2005. Age determinations of Ordovician magmatism in NE Sardinia and its bearing on Variscan basement evolution. Journal of the Geological Society London 162, 689–700.

Henderson, P., 1984. General geochemical properties and abundances of the rare earth elements. In: Henderson, P. (Ed.), Rare Earth Element Geochemistry, Developments in Geochemistry, vol. 2. Elsevier, Amsterdam, pp. 1–32.

Holm, P.E., 1985. The geochemical fingerprints of different tectono-magmatic environments using hygromagmatophile element abundance of tholeiitic basalts and basaltic andesites. Chemical Geology 51, 303–323.

Hupert, H.E., Sparks, R.S.J., 1988. The generation of granitic magma by intrusion of basalt into continental crust. Journal of Petroleum 29, 599–624.

Iglesias, M., Brun, J.P., 1976. Signification des variations et anomalies de la déformation de la chaîne hercynienne (les séries cristallophylliennes de la Vendée littorale, Massif armoricain). Bulletin de la Société géologique de France (sér. 7) 18 (6), 1443–1452 (in French).

Janjou, D., Lardeux, H., Chantraine, J., Callier, L., Etienne, H., 1998. Notice explicative, Carte géol. France (1/50 000), feuille Segré (422). Bureau de Recherches Géologiques et Minières, Orléans, 68 p (in French).

Judenherc, S., Granet, M., Brun, J.-P., Poupinet, G., 2003. The Hercynian collision in the Armorican Massif: evidence of different lithospheric domain inferred from seismic tomography and anisotropy. Bulletin de la Société géologique de France 174, 45–57.

Klein, C., Trichet, J., 1968. Sur les blaviérites normandes et mancelles. Comptes Rendus de l'Académie des Sciences, Paris (sér. D) 267, 2268–2271 (in French).

Lahondère, D., Chèvremont, P., Béchennec, F., Bouton, P., Godard, G., Stussi, J.M., 2009. Notice explicative, Carte géol. France (1/50 000), feuille Palluau (535). Bureau de Recherches Géologiques et Minières, Orléans, 173 p. Carte géologique par Lahondère, D., Chèvremont, P., Godard, G., Bouton, P., Béchennec, F., Rebay, G., Santarelli, N., Viaud, J.-M. (2009) (in French).

Lapparent de, J., 1909. Etude comparative de quelques porphyroïdes françaises (Thesis Univ. Paris). Bulletin de la Société française de Minéralogie 32, 174–304 (in French).

Ledru, P., Autran, A., Santallier, D., 1994. Lithostratigraphy of Variscan terranes in the French Massif Central: a basis for paleogeographical reconstruction. In: Keppie, J.D. (Ed.), Pre–Mesozoic Geology in France and Related Areas. Springer, Berlin, pp. 276–288.

Le Métour, J., Bernard-Griffiths, J., 1979. Age (limite Ordovicien–Silurien) de mise en place du massif hypovolcanique de Thouars (Massif Vendéen). Implications géologiques. Bulletin du Bureau de Recherches Géologiques et Minières (sér. 2) 1 (4), 365–371 (in French).

Lescuyer, J.-L., Cocherie, A., 1992. Datation sur monozircons des métadacites de Sériès: arguments pour un âge protérozoïque terminal des "schistes X" de la Montagne Noire (Massif central français). Comptes Rendus de l'Académie des Sciences, Paris (sér. 2) 314, 1071–1077 (in French).

Linnemann, U., McNaughton, N.J., Romer, R.L., Gehmlich, M., Drost, K., Tonk, C., 2004. West African provenance for Saxo-Thuringia (Bohemian Massif): did Armorica ever leave pre-Pangean Gondwana? – U/Pb-SHRIMP zircon evidence and the Nd-isotopic record. International Journal of Earth Sciences 93, 683–705.

Linnemann, U., Pereira, F., Jeffries, T.E., Drost, K., Gerdes, A., 2008. The Cadomian Orogeny and the opening of the Rheic Ocean: the diachrony of geotectonic processes constrained by LA-ICP-MS U-Pb zircon dating (Ossa-Morena and Saxo-Thuringian Zones, Iberian and Bohemian Massifs). Tectonophysics 461, 21–43.

Linnen, R.L., Keppler, H., 2002. Melt composition control of Zr/Hf fractionation in magmatic processes. Geochimica et Cosmochimica Acta 66 (18), 3293–3301.

Lucks, H., Schulz, B., Audren, C., Triboulet, C., 2002. Variscan pressure-temperature evolution of garnet pyroxenites and amphibolites in the Baie d'Audierne metamorphic series, Brittany (France). In: Martínez-Catalán, J.R., Hatcher Jr., R.D., Arenas, J.R., Díaz García, F. (Eds.), Variscan–Appalachian Dynamics: The building of the Late Paleozoic Basement, Geol. Soc. Am., Spec. Pap, vol. 364, pp. 89–103.

Marignac, C., Leroy, J., Macaudière, J., Pichavant, M., Weisbrod, A., 1980. Evolution tectonométamorphique d'un segment de l'orogène hercynien: les Cévennes méridionales, Massif Central français. Comptes Rendus de l'Académie des Sciences, Paris (sér. D) 291, 605–608 (in French).

Marini, F., 1987. Clinopyroxènes reliques dans les métabasites paleozoïques de l'Albigeois: indicateurs d'un volcanisme transitionnel tholéitique en distension (formation des "Schistes et roches vertes", Tarn, âge ordovicien probable). Comptes Rendus de l'Académie des Sciences, Paris (sér. 2) 304, 29–34 (in French).

Marini, F., 1988. "Phase" sarde et distension ordovicienne du domaine sud–varisque, effets de point chaud? Une hypothèse fondée sur les données nouvelles du volcanisme albigeois. Comptes Rendus de l'Académie des Sciences, Paris (sér. 2) 306, 443–450 (in French).

Martínez Catalán, J.R., Arenas, R., Díaz García, F., Rubio Pascual, F.J., Abati, J., Marquínez, J., 1996. Variscan exhumation of a subducted Paleozoic continental margin: the basal units of the Ordones Complex, Galicia, NW Spain. Tectonics 15, 106–121.

Martínez Catalán, J.R., Arenas, R., Abati, J., Sánchez Martínez, S., Díaz García, F., Fernández Suárez, J., González Cuadra, P., Castiñeiras, P., Gómez Barreiro, J., Díez Montes, A., González Clavijo, E., Rubio Pascual, F.J., Andonaegui, P., Jeffries, T.E., Alcock, J.E., Díez Fernández, R., Lopez Carmona, A., 2009. A rootless suture and the loss of the roots of a mountain chain: the Variscan belt of NW Iberia. Comptes Rendus Geoscience 341, 114–126.

Melleton, J., Cocherie, A., Faure, M., Rossi, P., 2010. Precambrian protoliths and Early Paleozoic magmatism in the French Massif Central: U-Pb data and the North Gondwana connection in the west European Variscan belt. Gondwana Research 17, 13–25.

Montero, P., Bea, F., González-Lodeiro, F.G., Talavera, C., Whitehouse, M.J., 2007. Zircon ages of the metavolcanic rocks and metagranites of the Ollo de Sapo Domain in central Spain: implications for the Neoproterozoic and Early Palaeozoic evolution of Iberia. Geological Magazine 114, 963–976.

Montero, P., Talavera, C., Bea, F., González-Lodeiro, F.G., Whitehouse, M.J., 2009. Zircon geochronology of the Ollo de Sapo Formation and the age of the Cambro–Ordovician rifting in Iberia. Journal of Geology 117, 174–191.

Montigny, R., Allègre, C.J., 1974. A la recherche des océans perdus: les éclogites de Vendée, témoins métamorphisés d'une ancienne croûte océanique. Comptes Rendus de l'Académie des Sciences, Paris (sér. D) 279, 543–545 (in French).

Munier-Chalmas, E., 1881-82. Sur une roche nouvelle (Blaviérite) des environs de Changé près de Laval. Bulletin de La Societe D'Etudes Scientifiques D'Angers 11–12, 360–363 (in French).

Murphy, J.B., Gutiérrez-Alonso, G., Nance, R.D., Fernández-Suárez, J., Keppie, J.D., Quesada, C., Strachan, R.A., Dostal, J., 2006. Origin of the Rheic Ocean: rifting along a Neoproterozoic suture? Geology 34, 325–328.

Nance, R.D., Murphy, J.B., Strachan, R.A., Keppie, J.D., Gutiérrez-Alonso, G., Fernández-Suárez, J., Quesada, C., Linnemann, U., D'Lemos, R., Pisarevsky, S.A., 2008. Neoproterozoic–early Paleozoic tectonostratigraphy and palaeogeography of the peri-Gondwanan terranes: Amazonian v. West African connection. In: Ennih, N., Liégeois, J.P. (Eds.), The Boundaries of the West African Craton, Geological Society, London, Special Publications, vol. 297, pp. 345–383.

Nance, R.D., Gutiérrez-Alonso, G., Keppie, J.D., Linnemann, U., Murphy, J.B., Quesada, C., Strachan, R.A., Woodcock, N.H., 2010. Evolution of the Rheic Ocean. Gondwana Research 17, 194–222.

Neiva, A.M.R., Williams, I.S., Ramos, J.M.F., Gomes, M.E.P., Silva, M.M.V.G., Antunes, I.M.H.R., 2009. Geochemical and isotopic constraints on the petrogenesis of Early Ordovician granodiorite and Variscan two-micas granites from the Gouveia area, central Portugal. Lithos 111, 186–202.

Ortenzi, A., 1986. Proposition d'un modèle paléogéographique des Cévennes méridionales au Cambrien. Corrélations avec la Montagne Noire. Comptes Rendus de l'Académie des Sciences, Paris (sér. 2) 303, 1029–1034 (in French).

Paquette, J.L., Marchand, J., Peucat, J.-J., 1984. Absence de tectonique cadomienne dans le complexe de Champtoceaux (Bretagne méridionale)? Comparaison des systèmes Rb-Sr et U-Pb d'un métagranite. Bulletin de la Société géologique de France (sér. 7) 26, 907–912 (in French).

Paquette, J.L., Peucat, J.-J., Bernard-Griffiths, J., Marchand, J., 1985. Evidence for old Precambrian relics shown by U-Pb zircon dating of eclogites and associated rocks in the Hercynian belt of South Brittany, France. Chemical Geology: Isotope Geoscience Section 52, 203–216.

Paquette, J.-L., Monchoux, P., Couturier, M., 1995. Geochemical and isotopic study of a norite-eclogite transition in the European Variscan belt: Implications for U-Pb zircon systematics in metabasic rocks. Geochimica et Cosmochimica Acta 59, 1611–1622.

Patiño-Duce, A.E., Johnson, A.D., 1991. Phase equilibria and melt productivity in the pelite system: implications for the origin of peraluminous granitoids and aluminous granulites. Contributions to Mineralogy and Petrology 107, 202–218.

Patiño-Duce, A.E., Beard, J.S., 1995. Dehydration-melting of biotite gneiss and quartz-amphibolite from 3 to 15 kbar. Journal of Petrology 36 (3), 707–738.

Perroud, H., Bonhommet, N., 1981. Paleomagnetism of the ibero-armoricain arc and the Hercynian orogeny in Western Europe. Nature 292 (5822), 445–448.

Peucat, J.J., Vidal, Ph, Godard, G., Postaire, B., 1982. Precambrian U-Pb zircon ages in eclogites and garnet pyroxenites from South Brittany (France): an old oceanic crust in the West European Hercynian belt? Earth and Planetary Science Letters 60, 70–78.

Pfänder, J.A., Münker, C., Stracke, A., Mezger, K., 2007. Nb/Ta and Zr/Hf in ocean island basalts – implications for crust-mantle differentiation and the fate of niobium. Earth and Planetary Science Letters 254, 158–172.

Piboule, M., Briand, B., 1985. Geochemistry of eclogites and associated rocks of the southeastern area of the Fench Massif Central: origin of the protoliths. Chemical Geology 50, 189–199.

Pin, C., Lancelot, J.-R., 1982. U-Pb dating of an Early Paleozoic bimodal magmatism in the French Massif Central and of its further metamorphic evolution. Contributions to Mineralogy and Petrology 79, 1–12.

Pin, C., Marini, F., 1993. Early Ordovician continental break-up in Variscan Europe: Nd–Sr isotope and trace element evidence from bimodal igneous associations of the Southern Massif central, France. Lithos 29, 177–196.

Poncet, D., Bouton, P., 2010. Notice explicative, Carte géol. France (1/50 000), feuille Moncoutant (564). Bureau de Recherches Géologiques et Minières, Orléans, 116p. Carte géologique par Poncet, D., Bouton, P. (2010) (in French).

Pouclet, A., Lee, J.S., Vidal, P., Cousens, B., Bellon, H., 1995. Cretaceous to Cenozoic volcanism in South Korea and in the Sea of Japan: magmatic constraints on the opening of the back-arc basin. In: Smellie, J.L. (Ed.), Volcanism Associated with Extension at Consuming Plate Margins, Geological Society, London, Special Publications, vol. 81, pp. 169–191.

Pouclet, A., Aarab, A., Fekkak, A., Benharref, M., 2007. Geodynamic evolution of the northwestern Paleo-Gondwana margin in the Moroccan Atlas at the Precambrian–Cambrian boundary. In: Linneman, U., Nance, R.D., Kraft, P., Zulauf, G. (Eds.), The Evolution of the Rheic Ocean: From Avalonian–Cadomian Active Margin to Alleghenian–Variscan Collision, Geological Society of America Special Papers, vol. 423, pp. 27–60.

Pouclet, A., Ouazzani, H., Fekkak, A., 2008. The Cambrian volcanosedimentary formations of the westernmost High Atlas (Morocco): their place in the

geodynamic evolution of the West African Paleo-Gondwana northern margin. In: Ennih, N., Liégeois, J.-P. (Eds.), The Boundaries of the West African Craton, Geological Society, London, Special Publications, vol. 297, pp. 303–327.

Prian, J.P., 1980. Ph.D. thesis. Les phosphorites cambriennes du versant septentrional de la Montagne noire, au sud du basin permien de Camarès (Aveyron), vol. VI. Univ. Paris, 407 p (in French).

Putirka, K.D., 1999. Clinopyroxene + liquid equilibria to 100 kbar and 2450 K. Contributions to Mineralogy and Petrology 135, 151–163.

Putirka, K., 2008. Thermometers and barometers for volcanic systems. In: Putirka, K., Tepley, F. (Eds.), Minerals, Inclusions and Volcanic Processes. Review in Mineralogy and Geochemistry. The Mineralogical Society of America, vol. 69, pp. 61–120.

Putirka, K.D., Mikaelian, H., Rhyerson, F., Shaw, H., 2003. New clonopyroxene-liquid thermobarometers for mafic, evolved, and volatile-bearing lava compositions, with applications to lavas from Thibet and the Snake River Plain, Idaho. American Mineralogist 88, 1542–1554.

Putirka, K.D., Perfit, M., Ryerson, F.J., Jackson, M.G., 2007. Ambient and excess mantle temperatures, olivine thermometry, and active vs. passive upwelling. Chemical Geology 241, 177–206.

Quesada, C., 1991. Geological constraints on the Paleozoic tectonic evolution of tectonostratigraphic terranes in the Iberian Massif. Tectonophysics 185, 225–245.

Raymond, D., 1987. Le Dévonien et le Carbonifère inférieur du sud-ouest de la France (Pyrénées, Massif du Mouthoumet, Montagne Noire): sédimentation dans un basin flexural en bordure sud de la chaîne de collision varisque. Geologische Rundschau 76/3, 795–803.

Ribeiro, A., Munhá, J., Dias, R., Mateus, A., Peirera, E., Ribeiro, L., Fonseca, P., Araújo, A., Oliveira, T., Romão, J., Chaminé, H., Coke, C., Pedro, J., 2007. Geodynamic evolution of the SW Europe Variscides. Tectonics 26, 1–24.

Roger, F., Respaut, J.-P., Brunel, M., Matte, P., Paquette, J.-L., 2004. Première datation U-Pb des orthogneiss oeillés de la zone axiale de la Montagne Noire (Sud du Massif central): nouveaux témoins du magmatisme ordovicien dans la chaîne Varisque. Comptes Rendus Geoscience 336, 19–28.

Roig, J.-Y., Faure, M., Ledru, P., 1996. Polyphase wrench tectonics in the southern French Massif Central. Kinematic inferences from pre- and syn-kinematic granitoids. Geologische Rundschau 85, 138–153.

Rolin, P., Colchen, M., 2001a. Carte structurale du socle varisque Vendée-Seuil du Poitou-Limousin. Géologie de la France 1–2, 3–6 (in French).

Rolin, P., Colchen, M., 2001b. Les cisaillements hercyniens de la Vendée au Limousin. Géologie de la France 1–2, 87–116 (in French).

Rolin, P., Audru, J.-C., Bouroullec, I., Wyns, R., Thiéblemont, D., Cocherie, A., Guerrot, C., Courtois, N., Bernard, E., 2000. Notice explicative, Garte géol. France (1/50 000), feuille Les Herbiers (537). Bureau de Recherches Géologiques et Minières, Orléans, 117 p (in French).

Rubio Ordóñez, A., Valverde-Vaquero, P., Corretge, L.G., Cuesta-Fernández, A., Gallastegui, G., Fernández-González, M., Gerdes, A., 2012. An early ordovician tonalitic-granodioritic belt along the Schistose-Greywacke domain of the Central Iberian Zone (Iberian Massif, Variscan Belt). Geological Magazine 149, 1–13.

Rubio-Ordóñez, A., Gutiérrez-Alonso, G., Valverde-Vaquero, P., Cuesta, A., Gallastegui, G., Gerdes, A., Cárdenes, V., 2015. Arc-related Ediacaran magmatism along the northern margin of Gondwana: geochronology and isotopic geochemistry from northern Iberia. Gondwana Research 27, 216–227.

Rudnick, R.L., Gao, S., 2004. Composition of the Continental crust. In: Holland, H.D., Turekian, K.K. (Eds.), Treatise on Geochemistry, vol. 3. Elsevier, Amsterdam, pp. 1–64.

Sánchez-García, T., Bellido, F., Quesada, C., 2003. Geodynamic setting and geochemical signatures of Cambrian–Ordovician rift-related igneous rocks (Ossa-Morena Zone, SW Iberia). Tectonophysics 365, 233–255.

Sánchez-García, T., Bellido, F., Pereira, M.F., Chichorro, M., Quesada, C., Pin, Ch, Silva, J.B., 2010. Rift-related volcanism predating the birth of the Rheic Ocean (Ossa-Morena Zone, SW Iberia). Gondwana Research 17, 392–407.

Santallier, D., Floc'h, J.-P., 1989. Tectonique tangentielle et décrochements ductiles dévono–carbonifères superposés dans la region de Bellac (nord-ouest du Massif Central français). Comptes Rendus de l'Académie des Sciences, Paris 309, 1419–1424 (in French).

Sarrionandia, F., Carracedo-Sánchez, M., Eguiluz, L., Abalos, B., Rodríguez, J., Pin, C., Gil Ibarguchi, J.I., 2012. Cambrian rift-related magmatism in the Ossa-Morena Zone (Iberian Massif): geochemical and geophysical evidence of Gondwana break-up. Tectonophysics 570–571, 135–150.

Sassier, C., Boulvais, P., Gapais, D., Capdevila, R., Diot, H., 2006. From granitoid to kyanite-bearing micaschist during fluid-assisted shearing (Ile d'Yeu, France). International Journal of Earth Sciences 95, 2–18.

Sibuet, J.C., Srivastava, S.P., Sparkman, W., 2004. Pyrenean orogeny and plate kinematics. Journal of Geophysical Research 109, B08104.

Simancas, J.F., Azor, A., Martínez-Poyatos, D., Tahiri, A., El Hadi, H., González-Lodeiro, F., Pérez-Estaún, Carbonell, R., 2009. Tectonic relationships of Southwest Iberia with the allochthons of Northwest Iberia and the Moroccan Variscides. Comptes Rendus Geoscience 341, 103–113.

Solá, A.R., Montero, P., Ribeiro, M.L., Neiva, A.M.R., Zinger, T., Bea, F., 2005. Pb/Pb age of the Carrascal Massif, central Portugal. Geochimica et Cosmochimica Acta 69 (10 Suppl. 1, Goldschmidt Conf. Abstr.), A856.

Solá, A.R., Pereira, M.F., Williams, I.S., Ribeiro, M.L., Neiva, A.M.R., Montero, M., Bea, F., Zinger, T., 2008. New insights from U-Pb zircon dating of early ordovician magmatism on the northern gondwana margin: the urra formation (SW Iberian Massif, Portugal). Tectonophysics 461, 114–129.

Stampfli, G.M., Hochard, C., Vérard, C., Wilhem, C., von Raumer, J., 2013. The formation of Pangea. Tectonophysics 593, 1–19.

Sun, S.S., McDonough, W.H., 1989. Chemical and isotopic systematic of oceanic basalts: implications for mantle composition and processes. In: Saunders, A.D., Norry, M.J. (Eds.), Magmatism in the Ocean Basins, Geological Society, London, Special Publications, vol. 42, pp. 313–345.

Talavera, C., Bea, F., Montero, P., Whitehouse, M., 2008. A revised Ordovician age for the Sisargas orthogneiss, Galicia (Spain). Zircon U-Pb ion-microprobe and LA-ICPMS dating. Geodinamica Acta 6 (4), 313–317.

Talavera, C., Montero, P., Bea, F., González Lodeiro, F., Whitehouse, M., 2013. U-Pb zircon geochronology of the Cambro–Ordovician metagranites and metavolcanic rocks of central and NW Iberia. International Journal of Earth Sciences 102, 1–23.

Ters, M., 1970. Découverte d'un gisement de Graptolithes du Silurien (Wenlock) dans la "série de Brétignolles" (Vendée). Comptes Rendus de l'Académie des Sciences, Paris 271, 1060–1062 (in French).

Ters, M., Viaud, J.M., 1983. Notice explicative, Carte géol. France (1/50 000), feuille Challans (534). Bureau de Recherches Géologiques et Minières, Orléans, 99 p (in French).

Ters, M., Viaud, J.M., 1987. Notice explicative, Carte géol. France (1/50 000), feuille Saint-Gilles-Croix-de-Vie (560). Bureau de Recherches Géologiques et Minières, Orléans, 135 p (in French).

Thiéblemont, D., 1988. Le magmatisme paléozoïque en Vendée. Apport de la géochimie des éléments traces et de la pétrologie du métamorphisme à la comprehension du développement orogénique varisque. Doc. Bureau de Recherches Géologiques et Minières, Orléans, France 157, 1–365 (in French).

Thiéblemont, D., Cabanis, B., Le Métour, J., 1987a. Etude géochimique d'un magmatisme de distension intracontinentale: la série bimodale ordovico–silurienne du Choletais (Massif vendéen). Géologie de la France 1987 (1), 65–76 (in French).

Thiéblemont, D., Cabanis, B., Wyns, R., Treuil, M., 1987b. Etude géochimique (majeurs et traces) de la formation amphibolitique de Saint-Martin des Noyers (complexe cristallophyllien des Essarts, Vendée). Mise en évidence d'un paléo-arc insulaire dans la partie interne de l'orogène varisque. Bulletin de la Société géologique de France (sér. 8) 3 (2), 371–378 (in French).

Thiéblemont, D., Guerrot, C., Le Métour, J., Jézéquel, P., 2001. Le complexe de Cholet-Thouars: un ensemble volcano-plutonique cambrien moyen au sein du bloc précambrien des Mauges. Géologie de la France 1 (2), 7–17 (in French).

Thoral, M., 1935. Contribution à l'étude géologique des Monts de Lacaune et des terrains cambriens et ordoviciens de la Montagne Noire. Bull. Carte géol. France 38 (192), 320. Librairie Polytechnique Ch. Béranger, Paris (in French).

Tormo, N., 2002. La formation de Coulouma (Cambrien Moyen) de l'unité de Mélagues. Lithostratigraphie, biostratigraphie et aperçu paléogéographique. Bulletin de la Société d'étude et de Sciences Naturelles de Béziers 19, 47–104.

Tormo, N., 2003. Contribution à la connaissance paléontologique de l'unité de Mélagues. Lithostratigraphie, biostratigraphie, paléogéographie. Bulletin de la Société d'étude et de Sciences Naturelles de Béziers 20, 16–30.

Turillot, P., 2010. Fusion crustale et évolution tardi-orogénique du Domaine Sud Armoricain. Ph.D. thesis. Univ. Orléans, 366 p (in French).

Turillot, P., Augier, R., Monié, P., Faure, M., 2011. Late Orogenic exhumation of the Variscan high-grade units (South Armorican Domain, western France), combined structural and $^{40}$Ar/$^{39}$Ar constraints. Tectonics 30, TC5007.

Valverde-Vaquero, P., Dunning, G.R., 2000. New U–Pb ages for Early Ordovician magmatism in central Spain. Journal of the Geological Society of London 157, 15–26.

Valverde-Vaquero, P., Marcos, A., Farias, P., Gallastegui, G., 2005. U-Pb dating of Ordovician felsic volcanism in the Schistose domain of the Galicia-Trás-os-Montes zone near Cabo Ortegal (NW Spain). Geologica Acta 3, 27–37.

Verraes, G., 1979. Contribution à l'étude de la province métallogénique sous-cévenole: les gîtes Pb-Zn de Montdardier, la Sanguinède et 102, district des Malines (Gard), France. Mém. Centr. Etudes Recherches Géologiques Hydrologiques Montpellier 17, 1–269 (in French).

Vizcaïno, D., Álvaro, J.J., 2001. The Cambrian and Lower Ordovician of the southern Montagne Noire: a synthesis for the beginning of the new century. Société géologique du Nord (2e sér) 8, 185–242.

Vizcaïno, D., Álvaro, J.J., 2003. Adequacy of the Lower Ordovician trilobite record in the southern Montagne Noire (France): biases for biodiversity documentation. Transactions of the Royal Society of Edinburgh Earth Sciences 93, 1–9.

Von Raumer, J.F., Stampfli, G.M., 2008. The birth of the Rheic Ocean – early Palaeozoic subsidence patterns and tectonic plate scenarios. Tectonophysics 461, 9–20.

Von Raumer, J.F., Bussy, F., Schaltegger, U., Schulz, B., Stampfli, G.M., 2013. Pre–Mesozoic Alpine basements – their place in the European Paleozoic framework. GSA Bulletin 125, 89–108.

Von Raumer, J.F., Stampfli, G.M., Arenas, R., Sánchez Martínez, S., 2015. Ediacaran to Cambrian oceanic rocks of the Gondwana margin and their tectonic interpretation. International Journal of Earth Sciences 104, 1107–1121.

Weaver, B.L., Tarney, J., 1984. Major and trace element composition of the continental lithosphere. Physics and Chemistry of the Earth 15, 39–68.

Workman, R.K., Hart, S.R., 2005. Major and trace element composition of the depleted MORB mantle (DMM). Earth and Planetary Science Letters 231, 53–72.

Wyns, R., Lablanche, G., Lefavrais-Raymond, A., 1988. Notice explicative, Carte géol. France (1/50 000), feuille Chantonnay (563). Bureau de Recherches Géologiques et Minières, Orléans, 76 p (in French).

Zang, W., Fyfe, W.S., 1995. Chloritization of the hydrothermally altered bedrock at the Igarapé Bahia gold deposit, Carajas, Brazil. Mineralium Deposita 30, 30–38.

Zeck, H.P., Whitehouse, M.J., Ugidos, J.M., 2007. 496±3 Ma zircon ion microprobe age for pre–Hercynian granite, Central Iberian Zone, NE Portugal (earlier claimed 618±9 Ma). Geological Magazine 144, 21–31.